# NORTH FLORIDA SOUTHEAST GEORGIA (NFSEG) GROUNDWATER FLOW MODEL CONCEPTUALIZATION

by

Douglas Durden, Tim Cera, and Nathan Johnson

for

NFSEG Technical Team

April 23, 2013

# TABLE OF CONTENTS

## LIST OF FIGURES

LIST OF TABLES

# NFSEG MODEL CONCEPTUALIZATION

## OVERVIEW

The model conceptualization is a detailed plan for representing the groundwater flow system. Topics for consideration include the extent of the model domain, the model lateral boundary conditions, model layering, representation of surface-water bodies and processes, such as evapotranspiration, representation of pumping, and model calibration.

The NFSEG groundwater flow model will be developed in stages, starting with the development of a preliminary steady-state groundwater flow model. This model will be calibrated manually and then subjected to testing for determination of its ability to respond adequately to differing stress conditions. Responses of concern include, at minimum, the ability to converge (general model stability) and runtime. Changes in stress conditions will likely include changes in pumping scenarios and represented climatic conditions. If the model is deemed adequate in its responses, then it will be subjected to additional calibration using the inverse modeling software PEST (Doherty, 2010) to obtain the best global model calibration. As the model development, testing and calibration processes proceed, revisions to certain aspects of the model conceptualization proposed herein may be necessary. The types of changes might include replacement of the solver routine, simplification of the model-layering scheme, reduction in the extent of the model domain, and changes in the grid design. The representation of surface-water features may require additional simplification as well.

Once steady-state calibration is completed, a transient version of the NFSEG groundwater flow model will be constructed using the finalized steady-state version of the model as a starting point. The transient version of the NFSEG groundwater flow model will be constructed around monthly stress periods. It will be calibrated both manually and through use of PEST. The NFSEG regional groundwater flow model will be developed in accordance with the planned U.S. Geological Survey (USGS) system-wide groundwater flow model of the Floridan aquifer system, which will be part of a Floridan aquifer system groundwater availability study (http://fl.water.usgs.gov/FASWAM/ ). A more detailed description of the NFSEG regional groundwater flow model conceptualization follows.

# HYDROGEOLOGIC CONCEPTUALIZATION

## Recap of FAS/SECPAS Conceptualization

The report to the NFSEG Technical Team on data availability (i.e., the NFSEG DAR) within the proposed domain of the NFSEG regional groundwater flow model provides descriptions of the Floridan aquifer system (FAS) and Southeastern Coastal Plain Aquifer System (SECPAS) and their degree of interaction. To summarize a portion of that description herein, the FAS is comprised generally of an upper aquifer, the Upper Floridan aquifer, that is separated from a lower aquifer, the Lower Floridan aquifer, by an intervening semiconfining unit referred to as the middle semiconfining unit. The FAS is overlain by a regionally extensive semiconfining unit called the intermediate aquifer system (IAS) or intermediate confining unit. The IAS is overlain, in turn, by a generally unconfined aquifer system called the surficial aquifer system (SAS). The SECPAS is comprised of several regionally mapped aquifers, including, from top to bottom, the Pearl River Aquifer, the Chattahoochee River Aquifer, and the Black Warrior River Aquifer separated by regionally extensive, intervening semiconfining units (Figure 1).

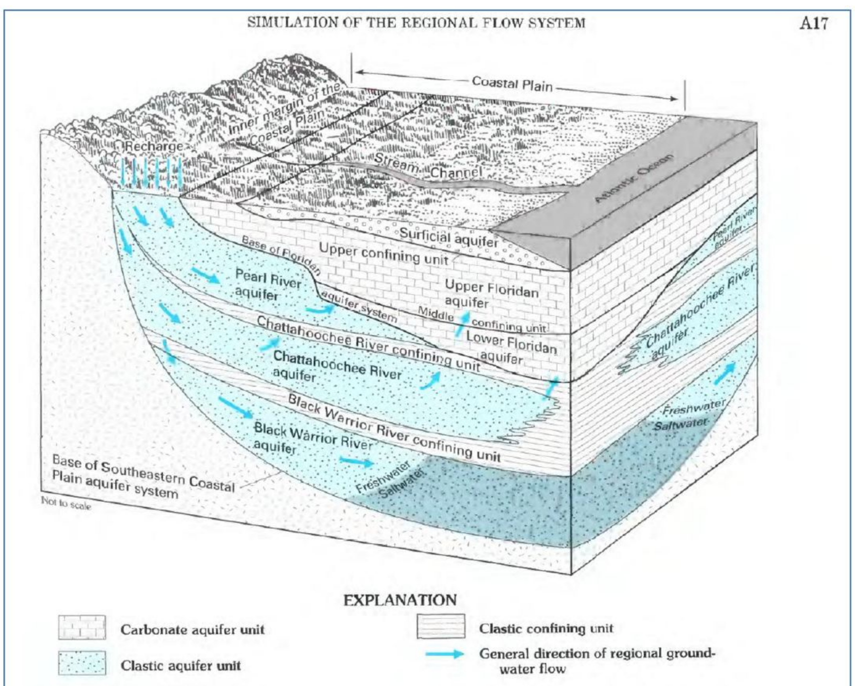

FIGURE 10.—Relation between hydrogeologic framework and simulated flow directions along a hypothetical dip section through Georgia (modified from Barker, 1986).

**Figure 1. Hydrogeologic Relation between the Floridan Aquifer System and the Southeastern Coastal Plain Aquifer System along a Hypothetical Dip Section in Georgia.**

The clastic rocks of the SECPAS grade by facies change both laterally and vertically into the carbonate rocks of the FAS in western South Carolina, south Georgia, and southeastern Alabama (Barker & Pernik, 1994). Although leakage between the FAS and SECPAS occurs, the amounts represent a relatively small proportion of the total flux moving through the FAS (Barker & Pernik, 1994).

## Investigation of Degree of Interaction Between the FAS and the SECPAS

The Pearl River aquifer is the SECPAS equivalent of the Lower Floridan aquifer, and, as a result, the two aquifers are in direct hydraulic connection at their boundaries (i.e., not separated by a semiconfining unit). Interaction between the two lowermost regional SECPAS aquifers and the FAS occurs via diffuse upward leakage across semiconfining units. The level of interaction between the two lowermost regional SECPAS aquifers and the FAS is therefore likely to be considerably less than the level of interaction between the Pearl River Aquifer and the FAS. In view of this, a proposal was made in the NFSEG DAR to limit representation of the SECPAS in the NFSEG regional groundwater flow model to representation of the Pearl River aquifer only, and, furthermore, to represent the Pearl River aquifer as part of the same model layer as the Lower Floridan aquifer. As stated in the NFSEG DAR, this approach has been used in previous regional model representations of the FAS in southeast Georgia and Northeast Florida (e.g., Krause & Randolph (1989) and Payne *et al.* (2005)).

Since the submittal of the NFSEG DAR, the author has performed additional investigation concerning the degree of interaction between the portion of the SECPAS beneath the Pearl River aquifer and the overlying Pearl River and Lower Floridan aquifers. The investigation involved mass-balance analysis of aquifer layer 3 of the Georgia EPD regional groundwater flow model (CDM, Inc., 2011). Layer 3 of the Georgia EPD regional groundwater flow model is used to represent the Pearl River/Lower Floridan aquifers (Table 1). The domain of the Georgia EPD regional groundwater flow model covers most of the proposed NFSEG model domain (Figure 2), and most of the vertical extent of the SECPAS is represented actively in the Georgia EPD regional groundwater flow model (Table 1). Thus, the Georgia EPD regional groundwater flow model can be used to investigate relative flux rates between the FAS and lower portions of the SECPAS, and this was the approach used herein.

The results of the investigation show that of the total flux into and out of layer 3 of the Georgia EPD regional groundwater flow model, only about 4 percent of the total was inflow through the bottom (i.e., derived from the portion of the SECPAS below the Pearl River aquifer). Outflow through the bottom of layer 3 from the Pearl River/Lower Floridan aquifer into the Upper Chattahoochee River aquifer accounted for about 5 percent of the total flux through layer 3 (Table 2). A plot of the distribution of the exchange rates shows that although some locally high rates of exchange occur, these are limited to relatively small portions of the proposed model domain (Figure 2).

In view of the aforementioned results, two potential approaches may be applied in regards to the representation of the SECPAS in the NFSEG regional groundwater flow model. In the first approach, the SECPAS below the Pearl River aquifer would be omitted from the NFSEG regional groundwater flow model entirely. In this case, the exchange rate between the two systems would be approximated as 0 inches/year both in the calibration period(s) and in any predictive simulations. This approach would tend to result in predictive drawdowns that are somewhat overestimated. Hence, this approach would be conservative in regards to estimation of impacts due to pumping effects. This approach is simpler, so it is preferred. It will be applied at least through the development of the steady-state version of the model but likely throughout the model-development process.

In the second approach, the Georgia EPD regional groundwater flow model would be used to calculate the rate of exchange between Pearl River/Lower Floridan aquifer and the Upper Chattahoochee River Aquifer, and the resulting leakage rates would be applied directly to the NFSEG regional groundwater flow model as specified flux. This approach would be conservative in predictive simulations in that it would tend to result in overestimated predictive drawdown amounts, as with the first approach. The advantage lies in the improved representation of the SECPAS in the NFSEG model calibration process. Simulations could also be performed using constant-head assignments to represent the upper Chattahoochee River aquifer in the areas of higher leakage rates. The head values and vertical hydraulic conductivity estimates of the Chattahoochee River confining unit could be obtained from the Georgia EPD regional groundwater flow model. This approach would tend to result in underestimated predictive drawdowns, so, together, the two sets of results would be expected to bracket the actual drawdown. Given that the leakage rates in question are generally only a small proportion of the amount of flux moving through the Pearl River/Lower Floridan aquifer, except in relatively small and isolated areas, it is expected that the range of the resulting drawdowns would be relatively small. Furthermore, the Florida portion of the NFSEG regional model domain would likely be impacted to only a negligible degree given the distance of the higher-leakage areas from the Florida-Georgia state line (Figure 2).

The first approach, discussed above, will be the primary approach used in the steady-state model development. The second approach will be used in the testing/sensitivity phase of the model development. Any decision to change the model from the preferred setup will be made in light of the testing/sensitivity-analysis results.

**Table 1. Georgia EPD Regional Groundwater Flow Model Layering Scheme.**

| Hydrogeologic Unit-- Subregional Designations | Hydrogeologic Unit-- Regional Designation | Model Layer* |
|---|---|---|
| Surficial Aquifer/Brunswick Aquifer Confining Unit/Brunswick Aquifer | Surficial Aquifer | 1 (Constant-Head) |
| Upper Floridan/Barnwell Aquifer | Upper Floridan Aquifer | 2 |
| Claiborne/Gordon/Lower Floridan Aquifer | Pearl River/Lower Floridan Aquifer | 3 |
| Clayton-Dublin Aquifers | Chattahoochee River Aquifer (Upper) | 4 |
| Providence Sand-Peedee Aquifers | Chattahoochee River Aquifer (Middle) | 5 |
| Eutaw-Midville Aquifer | Chattahoochee River Aquifer (Lower) | 6 |
| Upper Atkinson-Upper Tuscaloosa Aquifers | Black Warrior River Aquifer (Upper) | 7 |
| ***Semiconfining units represented with leakance (i.e., VCONT) specifications** | | |

**Table 2. Summary of Water Budget of the Georgia EPD Regional Groundwater Flow Model Layer 3 (i.e., Pearl River/Lower Floridan aquifer).**

| Flow Type | Overall Water Budget | | | |
|---|---|---|---|---|
| | Inflows (MGD) | Outflows (MGD) | Percent Total Inflows | Percent Total Outflows |
| Top | 359.72 | 297.09 | 17.7 | 14.7 |
| Bottom | 80.77 | 105.73 | 4.0 | 5.2 |
| Wells | 0.00 | 211.41 | 0.0 | 10.4 |
| Surface Water | 0.00 | 0.00 | 0.0 | 0.0 |
| Lateral Flux | 0.00 | 0.00 | 0.0 | 0.0 |
| Rivers | 571.27 | 1,412.70 | 28.2 | 69.7 |
| Springs | 0.00 | 0.00 | 0.0 | 0.0 |
| Recharge | 1,015.16 | 0.00 | 50.1 | 0.0 |
| ET | 0.00 | 0.00 | 0.0 | 0.0 |
| Totals: | 2,026.92 | 2,026.93 | 100.0 | 100.0 |

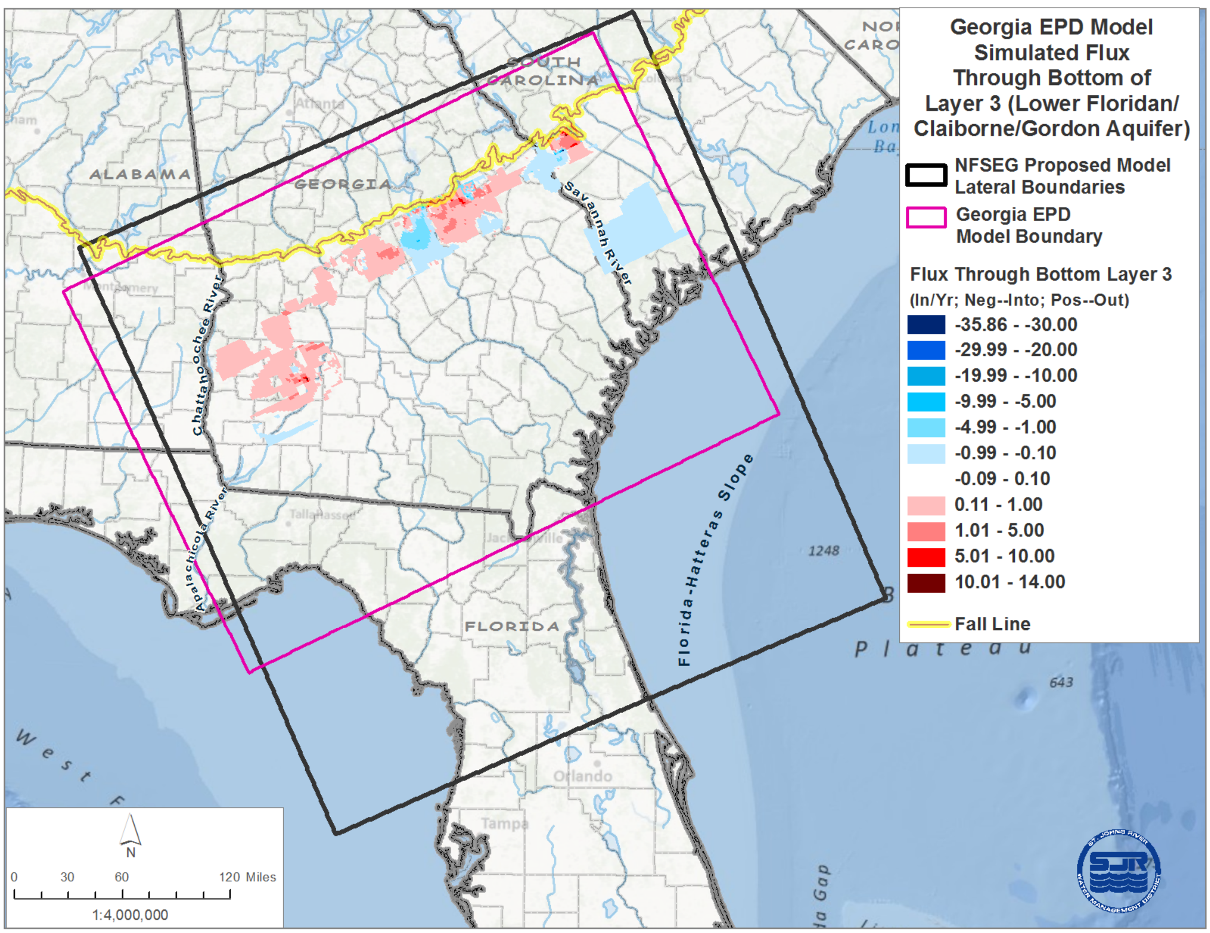


**Figure 2. Georgia EPD and Proposed NFSEG Model Lateral Boundaries with Georgia EPD Model-Derived Flux between the Upper Chattahoochee River Aquifer and FAS Superimposed.**

# MODEL CONCEPTUAL FRAMEWORK

## Proposed Lateral Extent

The proposed lateral extent of the NFSEG regional groundwater flow model was outlined in the NFSEG DAR, and, for the most part, the lateral extent as outlined there is still current. The proposal for use of the Apalachicola/Chattahoochee Rivers as the line of demarcation of the western lateral model boundary has been changed, however. In the present approach, the western lateral boundary will follow the National Hydrography Data (NHD) set flowline (http://nhd.usgs.gov/) of the Ochlockonee River for a short distance. It will then deviate from the NHD flowline of the Ochlockonee River to follow a groundwater streamline, as inferred from the 2010 estimated potentiometric surface of the Upper Floridan aquifer (Kinnaman & Dixon, 2011), to Lake Seminole at the junction of Alabama, Georgia, and Florida. From there, it will trace along the NHD flowline of Spring Creek, a relatively small tributary to the Apalachicola River located between the Chattahoochee and Flint Rivers. Based on the shape of the Upper Floridan aquifer potentiometric surface along its NHD flowline, Spring Creek appears to be in good connection with the FAS.

The use of the new location will result in a significant reduction in the size of the model domain without affecting the quality of simulations in areas of primary interest. The northeastern lateral boundary of the model domain in South Carolina has been moved to the southwest of its initial position (i.e., towards Savannah, Georgia) for similar reasons. The lateral boundary locations and the reasoning behind them are discussed in greater detail in the section of the present report entitled “Proposed Model Lateral Boundary Conditions,” which follows.

Areas that are west of the western lateral boundary will be inactive in the model domain. Areas that are seaward of the freshwater discharge zone off the coast of the Gulf of Mexico will be inactive as well. The outcrop regions of the SECPAS, which lie north of the pinch-out of the Upper Floridan aquifer and south of the Fall Line, will also be inactive. Areas seaward of the onset of the Florida-Hatteras slope in the Atlantic Ocean will be inactive, consistent with the approach of Payne *et al.* (2005).

As discussed in the NFSEG DAR, the size of the model extent is designed to minimize the potential for lateral boundary-constraint issues and also to include all significant pumping centers. Significant pumping centers in this regard are those implicated in contributing significantly to drawdown impacts in areas of critical concern.

## Proposed Model Layering Scheme

The proposed model-layering scheme is consistent with that outlined in the NFSEG DAR (Figure 3). The reader is hereby cautioned that use of the Gulf Trough as a zone of demarcation of the Lower Floridan aquifer and the Pearl River aquifer is approximate. The actual hydrostratigraphy to be incorporated into the model will be much more detailed in this regard and based on the results of an ongoing revision of the work of Miller (1986) being conducted jointly by the SJRWMD and USGS (L. Williams *et al.*, In Progress).

| Downdip of Gulf Trough | | | | Updip of Gulf Trough | | | |
|---|---|---|---|---|---|---|---|
| Series | Hydrogeologic Unit | | Model Layer | Series | Hydrogeologic Unit | | Model Layer |
| Post-Miocene | Surficial Aquifer System | | Layer 1[1] | Post-Miocene | Surficial Aquifer System[1] | | Layer 1[1] |
| Miocene | Intermediate Aquifer System/Intermediate Confining Unit | | Layer 2[1] | Miocene | Intermediate Aquifer System/Intermediate Confining Unit[1] | | Layer 2[1] |
| Oligocene | Upper Floridan Aquifer | Floridan Aquifer System | Layer 3[1] | Oligocene | Upper Floridan Aquifer | | Layer3[1] |
| Upper Eocene | Upper Floridan Aquifer | Floridan Aquifer System | Layer 3[1] | Upper Eocene | Pearl River Aquifer Confining Unit | Southeastern Coastal Plain Aquifer System | Layer 4[1] |
| Middle Eocene | Middle Semiconfining Unit; East: Lower Permeability; West: Higher Permeability or part of the transmissive system | Floridan Aquifer System | Layer 4[1] | Middle Eocene | Pearl River Aquifer | Southeastern Coastal Plain Aquifer System | Layer 5 |
| Middle Eocene | Lower Floridan Aquifer (Upper Zone) | Floridan Aquifer System | Layer 5[1] | Middle Eocene | Pearl River Aquifer | Southeastern Coastal Plain Aquifer System | Layer 5 |
| Lower Eocene | Lower Semiconfining Unit | Floridan Aquifer System | Layer 6[1] | Lower Eocene | Pearl River Aquifer | Southeastern Coastal Plain Aquifer System | Layer 5 |
| Lower Eocene / Paleocene | Lower Floridan Aquifer (Fernandina Permeable Zone) | Floridan Aquifer System | Layer 7[1] | Paleocene | Chattahoochee River Aquifer Confining Unit | Southeastern Coastal Plain Aquifer System | Layer 6[2] |
| Upper Cretaceous | Sub-Floridan Confining Unit | | Inactive | Upper Cretaceous | Chattahoochee River Aquifer | Southeastern Coastal Plain Aquifer System | Layer 7[2]<br>Inactive |

[1] Layer will be inactive where corresponding hydrogeologic layer is not represented. [2] Layer will be inactive updip of the Gulf Trough.

**Figure 3. Proposed Model Layering Scheme.**

## Proposed Model Grid Cell Dimensions

The dimensions of the model grid cells will be 2,500 feet (ft) by 2,500 ft. The grid cells will be nested within those of the U.S. Geological Survey (USGS) system-wide groundwater flow model of the Floridan aquifer system (http://fl.water.usgs.gov/FASWAM/). The model grid of the NFSEG regional groundwater flow model will be uniform throughout the model domain. Grid-cell dimensions of 2,500 ft by 2,500 ft are adequately small given the large size of the proposed model domain and the regional character of the model. Grid uniformity will lend towards simplicity of design and will help to minimize numerical complications.

### Proposed Model Lateral Boundary Conditions

An important objective in the specification of the lateral boundary conditions of the NFSEG regional groundwater flow model is simplicity of design and application. To this end, no-flow lateral boundary conditions will be used to the greatest possible extent, as such boundaries preclude the need to specify source heads or fluxes (Figure 4; Figure 5; and Figure 6).

The lateral boundaries of all semiconfining units (i.e., model layers 2, 4, and 6) will be represented as no-flow. This is because flow within semiconfining units is predominately in the vertical direction.

The lateral boundary conditions of the SAS (model layer 1) will also be no-flow. This is because groundwater flow within the surficial aquifer is primarily local in nature. Therefore, horizontal flux near the lateral boundaries of model layer 1 will tend to be insignificant from a regional standpoint. In many, if not most, cases, the lateral boundaries of model layer 1 will represent either the line of pinch-out of the SAS itself or, along the Atlantic coast, the line of pinch-out of the freshwater flow system within the surficial aquifer system. The no-flow condition is the preferred choice of lateral boundary condition in such instances.

The lower and lateral limits of freshwater flow within the portion of the model that represents the FAS will be defined by the estimated elevation of the 10,000 mg/l total-dissolved solids (TDS) surface. This boundary is expected to affect primarily the thickness and lateral limits of freshwater flow in the Lower Floridan aquifer, both the upper zone and Fernandina Permeable zone (model layers 5 and 7).

The Fernandina Permeable zone (model layer 7) is contained completely within the model domain. Therefore, the lateral boundaries of model layer 7 will represent lines of pinch-out, either of the Fernandina Permeable zone itself or of the freshwater flow system within the Fernandina permeable zone. Lines of pinch-out in model layer 7, as elsewhere, will be represented as no-flow boundaries.

The proposed model domain of the NFSEG regional groundwater flow model is oriented along southwest-northeast and northwest-southeast alignments. Hence, the model domain is comprised of a northwest-facing lateral boundary, a northeast-facing lateral boundary, a southeast-facing lateral boundary, and a southwest-facing lateral boundary (Figure 2). For simplicity, these will be referred to henceforth as the northern, eastern, southern, and western lateral boundaries, respectively. The type(s) of lateral boundary conditions to be assigned in each of these instances and the reasoning behind the specifications are discussed as follows.

Northern Boundary Lateral Boundary Condition

The northern lateral boundary of the model will represent the pinch-out of the Upper Floridan aquifer (model layer 3) and the consequent onset of the outcrop of the Pearl River aquifer (model layer 5; Figure 4). The pinch-out of the Upper Floridan aquifer will be represented by a no-flow lateral boundary condition.

The northern boundary of the portion of the Pearl River aquifer (model layer 5) to be represented within the model domain will be represented by GHB conditions. This lateral boundary will coincide with that of model layer 3 in terms of positioning. The source-head values assigned to the GHB conditions of model layer 5 along the northern boundary will be based on observations obtained from monitoring wells open to the Pearl River aquifer in the area. The portion of the Pearl River aquifer within the outcrop region will not be represented in the model (i.e., will be inactive; Figure 4).

Eastern Boundary Lateral Boundary Condition

The eastern lateral boundary represents the seaward limit of the FAS beneath the Atlantic Ocean and the limit of the model in South Carolina (Figure 4). Consistent with Payne *et al.* (2005), the onset of the Florida-Hatteras slope will be used as the approximate limit of the FAS beneath the Atlantic Ocean. This lateral boundary condition will be a no-flow boundary condition and will be applied to model layers 3 and 5. Available water-quality data will be used to approximate the seaward extent of fresh-water flow in the Lower Floridan aquifer (model layer 5). If fresh-water flow in the Lower Floridan aquifer (or Upper Floridan aquifer) appears to pinch out prior to the onset of the Florida-Hatteras slope, then the apparent pinch-out will be used to locate the no-flow lateral boundary condition either in model layer 3 or 5 or both. The water-quality data will be in the form of an elevation map of the 10,000 mg/l total-dissolved solids surface.. In the vicinity of the cone of depression centered on Savannah, Georgia, the eastern lateral boundary condition type will be changed to a GHB condition. This will enable the simulation of flux into the model domain in response to the influence of the cone of depression. Use of GHB lateral boundary conditions at this location, as opposed to a no-flow lateral boundary condition at a greater distance to the northeast, enables a significant reduction in size of the model domain. In the region up-gradient of the Savannah cone of depression, a groundwater streamline that intersects the line of pinch-out of the FAS will be used to demarcate the eastern lateral boundary. Along that portion of the eastern lateral boundary, therefore, a no-flow boundary condition will be prescribed (Figure 4).

Southern Boundary Lateral Boundary Condition

The southern lateral boundary will be defined primarily from streamlines, which are perpendicular in direction to the contours of the Upper Floridan aquifer potentiometric surface (Figure 4). The streamlines will be represented as no-flow boundary conditions. A relatively small portion of the southern lateral boundary condition will not be along a streamline, due to the configuration of the potentiometric surface in that area. The particular area is where the southern lateral boundary traverses the northern edge of the Green Swamp potentiometric high. This portion of the southern lateral boundary will be represented using GHB conditions to enable the simulation of flux that occurs across that boundary.

Placement of the southern lateral boundary condition just south of the southern Marion County, Florida, line is designed to position the southern lateral boundary an adequate distance south of critical areas within the model domain, including the area of the Keystone Heights high and the Lower Suwannee River. The southern lateral boundary will be placed south of the Rainbow and the majority of the Silver springs springsheds and south of a line of stagnation that runs through central Marion County and connects to streamlines to the east and west of it. These features, together with distance, will serve to insulate critical areas within the model domain from influences of the southern lateral boundary (Figure 4).

Western Boundary Lateral Boundary Condition

The western lateral boundary will represent the limit of freshwater flow in the FAS along the coast of the Gulf of Mexico and the limit of the model domain in the eastern Florida Panhandle. The Gulf coast within the model domain is primarily an area in which the Upper Floridan aquifer is unconfined. . Analysis by

Countryman & Stewart, 1997, suggests the boundary between freshwater and saline flow is located very near the coastline. This interpretation is consistent with other factors that lead to conditions in which groundwater can easily discharge from the Upper Floridan aquifer to the nearshore areas: The Upper Floridan aquifer in this area is unconfined, likely to have high transmissivity values, and groundwater levels near the coastline are just a few feet higher than mean sea level. Therefore, the location of this lateral boundary will be located in the offshore area close to the coastline. The western lateral boundary will be represented with GHB conditions. The source heads of the GHB conditions will be represented as the equivalent fresh-water head of sea level (Figure 4). Based on the fact that groundwater levels in the Upper Floridan aquifer along the coast are only a few feet above mean sea level, freshwater flow is not likely to be present in the Lower Floridan aquifer along the coast. In this case, the Lower Floridan aquifer will likely be inactive in this portion of the model domain.

In the Florida Panhandle, the western lateral boundary will be a no-flow boundary condition. Within the Florida portion of this boundary, the western lateral boundary will represent a groundwater stream line from the Gulf coast to Lake Seminole at the junction of Alabama, Georgia, and Florida. From that point to the line of pinch-out of the FAS, the western lateral boundary will trace along the NHD flowline of Spring Creek, the smallest of the three tributaries whose confluence forms the Apalachicola River. Based on the configuration of the FAS potentiometric surface along its length, Spring Creek, as its name implies, appears to be in good hydraulic connection with the FAS (Figure 4).

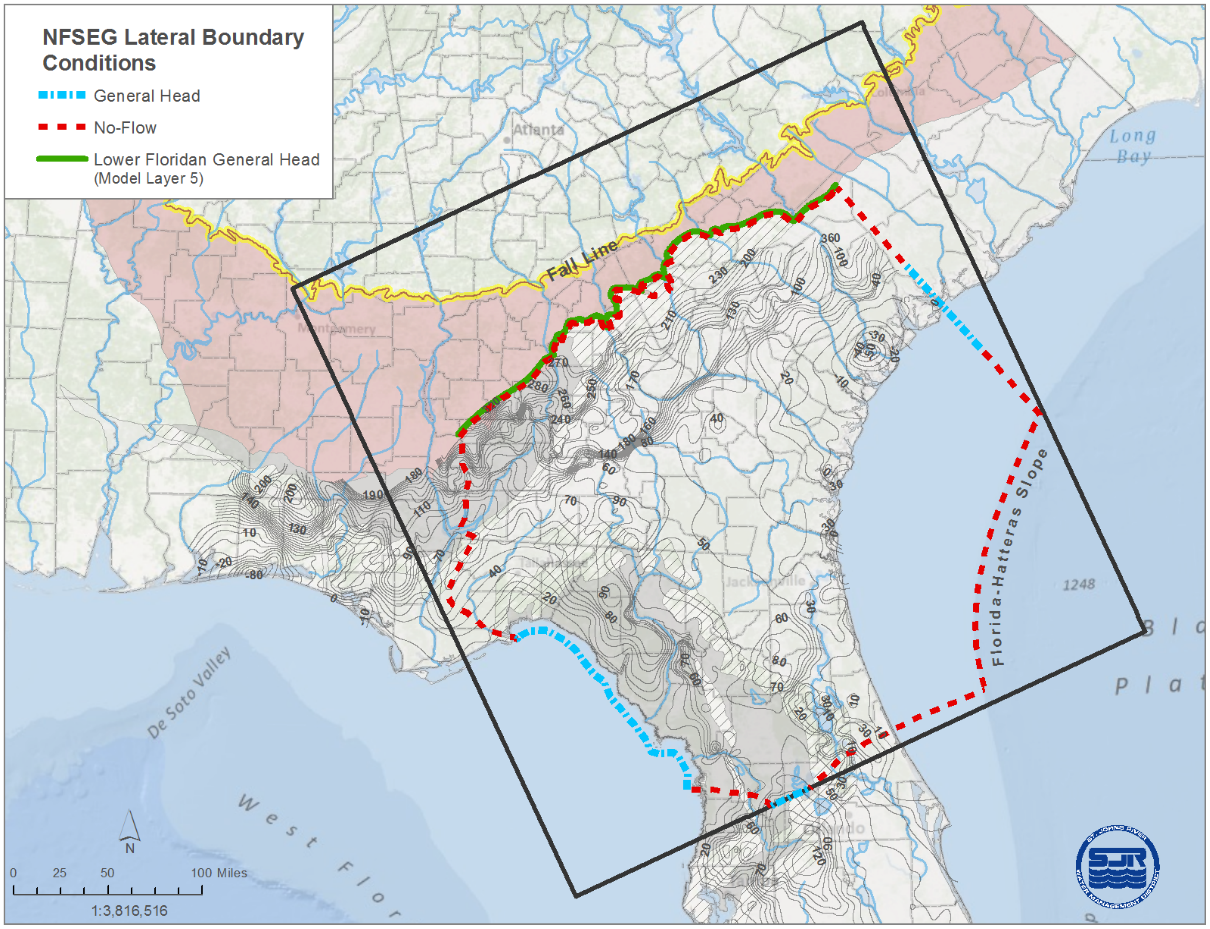


Figure 4. Proposed Lateral Boundary Condition Types and Locations.

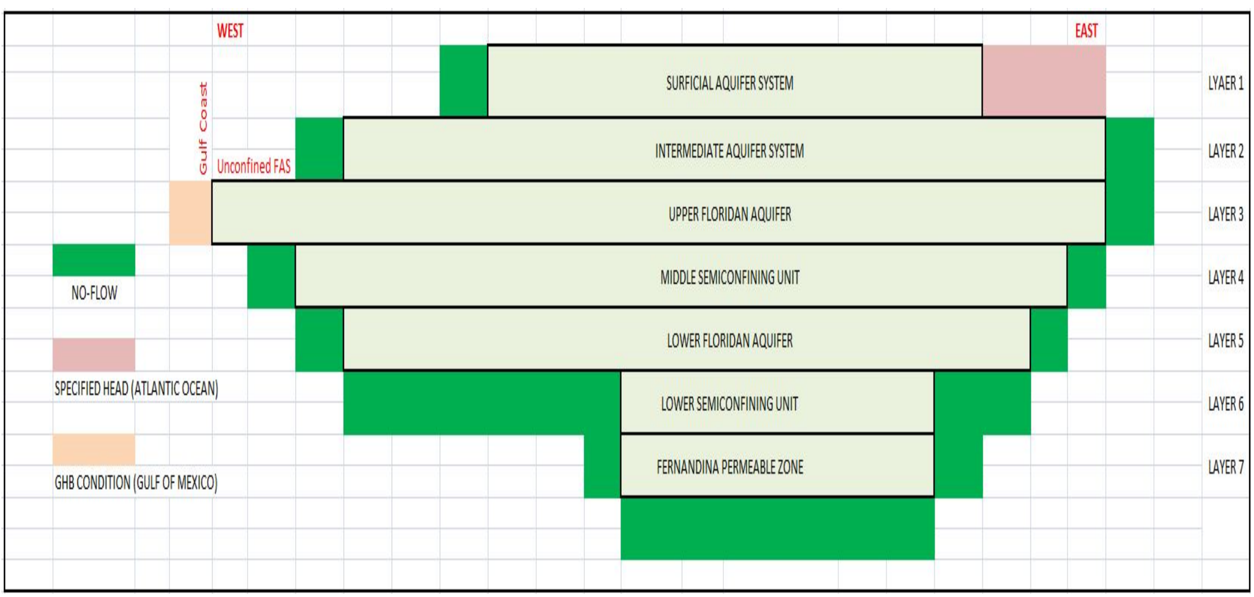


Figure 5. Generalized Model Layer and Lateral Boundary Condition Diagram (WEST-EAST).

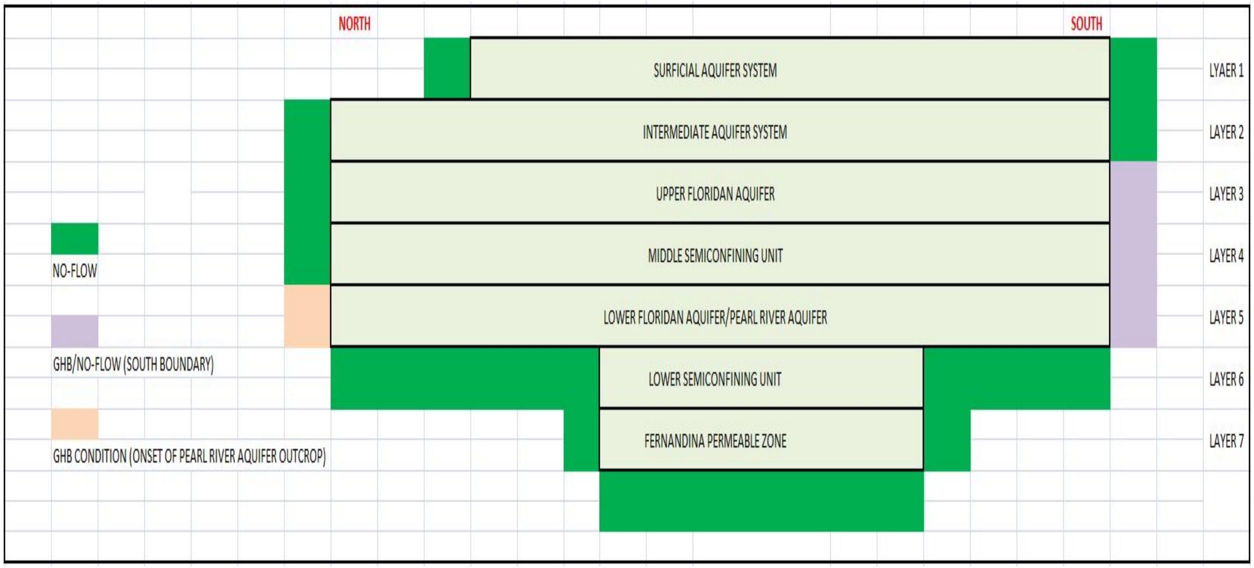


**Figure 6. Generalized Model Layer and Lateral Boundary Condition Diagram (NORTH-SOUTH).**

# GROUNDWATER LEVELS, 2000 THROUGH 2010

## General Discussion

Water-level trends are of interest because of the need to identify steady-state periods for calibration purposes. “Water-level trends” as used herein refers to regionally broad, long-term trends of either increasing, decreasing, or steady water levels. Long-term trends are associated with periods of months or years. Short-term fluctuations, by contrast, occur over periods of generally less than a month, frequently comprised of hours or days, as in, for instance, periods of pumping for crop freeze protection. Long-term trends can be representative of lasting changes or seasonal variations in climate and on-going or seasonal variations in well withdrawals that occur over relatively large areas. Hence, similar long-term trends can be observed in different hydrographs over relatively large areas of the Upper Floridan aquifer.

In order to identify major water-level trends within the potential model domain, 69 monitoring wells were selected for hydrograph review and analysis (Appendix A). The 69 wells are distributed throughout the potential model domain to afford a generalized overview of water-level trends within the area as a whole (Figure 7). Inspection of the 69 hydrographs indicates that water levels were generally steady in the period of 2000 through the first half of 2002. This steady period was followed by increases in water levels in the latter half of 2002 through early 2003. The increase in water levels was followed by a period of relatively stable water levels throughout most of 2003. Water levels declined and then recovered in 2004 and were generally stable in 2005. Water levels dropped precipitously from early 2006 into 2007. Water levels declined and then increased in 2008, but the increase was not as much as in 2003. Water levels held generally steady throughout 2009 into 2010. This description is, of course, generalized and therefore not entirely representative of every monitoring well (Appendix A).

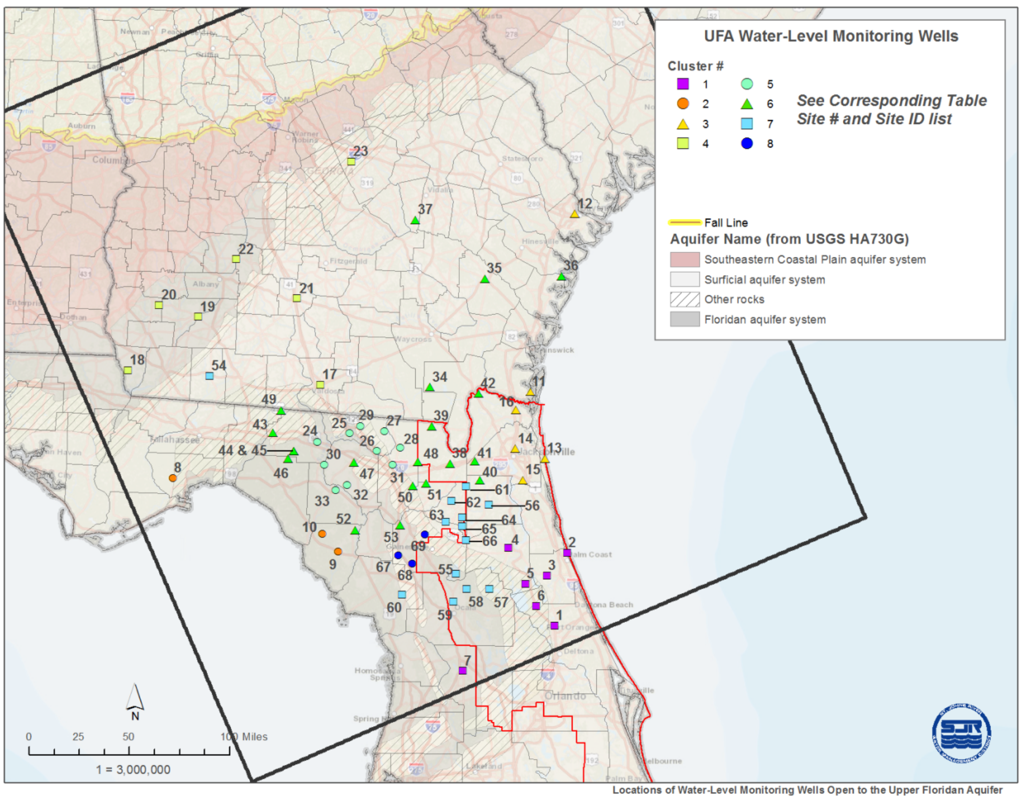


**Figure 7. Locations of Upper-Floridan-Aquifer Monitoring Wells from Which Hydrographs Were Obtained for Use in the Cluster and Principal-Component Analyses (See Table 3 for Well Names).**

**Table 3. Upper-Floridan-Aquifer Monitoring Wells from Which Hydrographs Were Obtained for Use in the Cluster and Principal-Component Analyses (See Figure 7 for Well Locations).**

| Cluster # | Site # | Site ID |
|---|---|---|
| 1 | 1 | FL290614081183301 |
| 1 | 2 | SJF-0200 |
| 1 | 3 | SJF-0353 |
| 1 | 4 | SJP-0123 |
| 1 | 5 | SJP-0705 |
| 1 | 6 | SJV-0531 |
| 1 | 7 | SW23115 |
| 2 | 8 | FL300740084293001 |
| 2 | 9 | SR-101210001 |
| 2 | 10 | SR-081132001 |
| 3 | 11 | GA304756081311101 |
| 3 | 12 | GA320530081085001 |
| 3 | 13 | SJD-0160 |
| 3 | 14 | SJD-0667 |
| 3 | 15 | SJD-1313 |
| 3 | 16 | SJN-0320 |
| 4 | 17 | GA304949083165301 |
| 4 | 18 | GA305356084534601 |
| 4 | 19 | GA311802084192302 |
| 4 | 20 | GA312232084391701 |
| 4 | 21 | GA312712082593301 |
| 4 | 22 | GA314330084005402 |
| 4 | 23 | GA322652083033001 |
| 5 | 24 | SR-011011002 |
| 5 | 25 | SR+011316001 |
| 5 | 26 | SR-011534001 |
| 5 | 27 | SR+011608001 |
| 5 | 28 | SR-011727001 |
| 5 | 29 | SR+021432001 |
| 5 | 30 | SR-031105006 |
| 5 | 31 | SR-031601003 |
| 5 | 32 | SR-041329001 |
| 5 | 33 | SR-051208001 |
| 6 | 34 | GA304942082213801 |
| 6 | 35 | GA313701081543501 |
| 6 | 36 | GA313823081154201 |
| 6 | 37 | GA320226082301101 |
| 6 | 38 | SJBA0054 |
| 6 | 39 | SJBA0057 |
| 6 | 40 | SJC-0583 |
| 6 | 41 | SJD-0254 |
| 6 | 42 | SJN-0221 |
| 6 | 43 | SR+010719001 |
| 6 | 44 | SR-020802001 |
| 6 | 45 | SR+020822002 |
| 6 | 46 | SR-020828001 |
| 6 | 47 | SR-021335001 |
| 6 | 48 | SR-021930001 |
| 6 | 49 | SR+030727001 |
| 6 | 50 | SR-041827002 |
| 6 | 51 | SR-041923001 |
| 6 | 52 | SR-081313005 |
| 6 | 53 | SR-081703001 |
| 7 | 54 | GA305235084125101 |
| 7 | 55 | SJA-0725 |
| 7 | 56 | SJC-0607 |
| 7 | 57 | SJM-0024 |
| 7 | 58 | SJM-0052 |
| 7 | 59 | SJM-0419 |
| 7 | 60 | SR-131736001 |
| 7 | 61 | SR-042236001 |
| 7 | 62 | SR-062102001 |
| 7 | 63 | SR-072132001 |
| 7 | 64 | SR-072215001 |
| 7 | 65 | SR-082202001 |
| 7 | 66 | SR-092307001 |
| 8 | 67 | SR-101722001 |
| 8 | 68 | SR-111811001 |
| 8 | 69 | SR-081926001 |

## Cluster and Principal-Component Analysis

Variations between hydrographs and fluctuations within hydrographs can make discernment of the dominant water-level trends within an overall region difficult. To address this problem, hierarchical cluster analysis and principal-component analysis were used in combination to resolve groups of hydrographs into a dominant pattern. This approach is both systematic and objective. All 69 previously discussed Upper-Floridan-aquifer hydrographs were included in the cluster and principle-component analyses (Appendix A).

Before being subjected to the principal-component analysis, the 69 hydrographs were first subjected to cluster analysis. Cluster analysis is a statistical analysis that groups hydrographs by degree of similarity. The Ward's method or Ward's "linkage" function was used to assess the degree of similarity between the hydrographs. The method selects for the minimum variance by minimizing the sum of squares using the least-squares method. Individual hydrographs were first standardized by subtracting the mean and dividing by the standard deviation to create unit well data on the same scale. Using the Ward's method on the standardized data selected for the degree of correlation instead of the degree of covariance. Correlation assesses the relative degree of variation similarity while covariance assesses the absolute distance between two data sets. Using covariance would tend to group wells of similar means together in the same cluster while correlation would group wells of similar relative variation in the same cluster.

The hierarchical clustering process starts with each well in its own cluster. At each step, two clusters that are the most correlated are combined into a single cluster. The process continues until the clustering is optimized based on scree values. The scree values are the distance that was bridged to join each cluster or, in other words, the difference between the sum of squares. The present analysis resulted in eight different clusters (Figure 7 and Table 3).

Once the 69 hydrographs were optimized into clusters, principle-component analysis was performed on the individual clusters to reduce the dimensionality of the clusters into a single signal. Principal-component analysis is a way to picture the signal of the well data with as few variables as possible. The first principal component is the linear combination of the standardized original variables that has the greatest possible variance. The first principle components explained at least 92% of the variation in the cases of all eight clusters. Therefore, in all cases, the first principle component was the only significant component and a good representation of the data. Hence, the first principle component was selected as being representative. The results of the cluster and principal-component analyses are shown in Figure 8 through Figure 15.

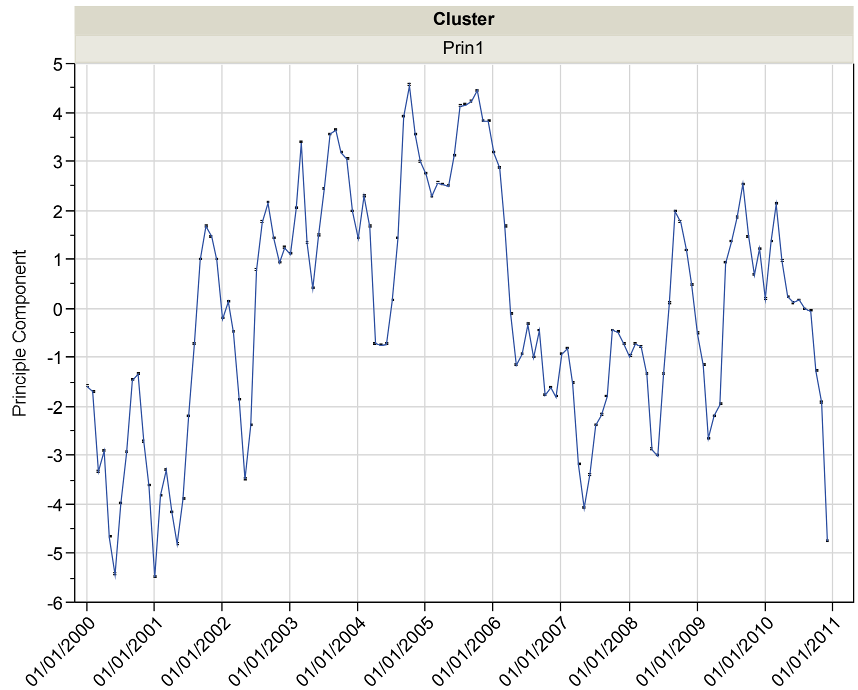


**Figure 8. Principal Component of Well Cluster 1 (See Figure 7 and Table 3 for Well Locations and Cluster Groupings).**

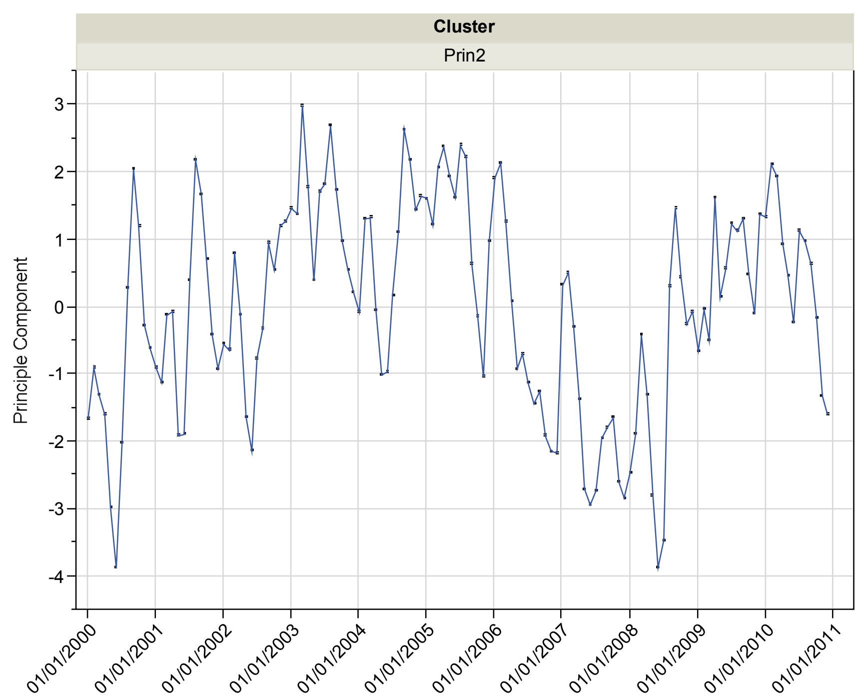


**Figure 9. Principal Component of Well Cluster 2 (See Figure 7 and Table 3 for Well Locations and Cluster Groupings).**

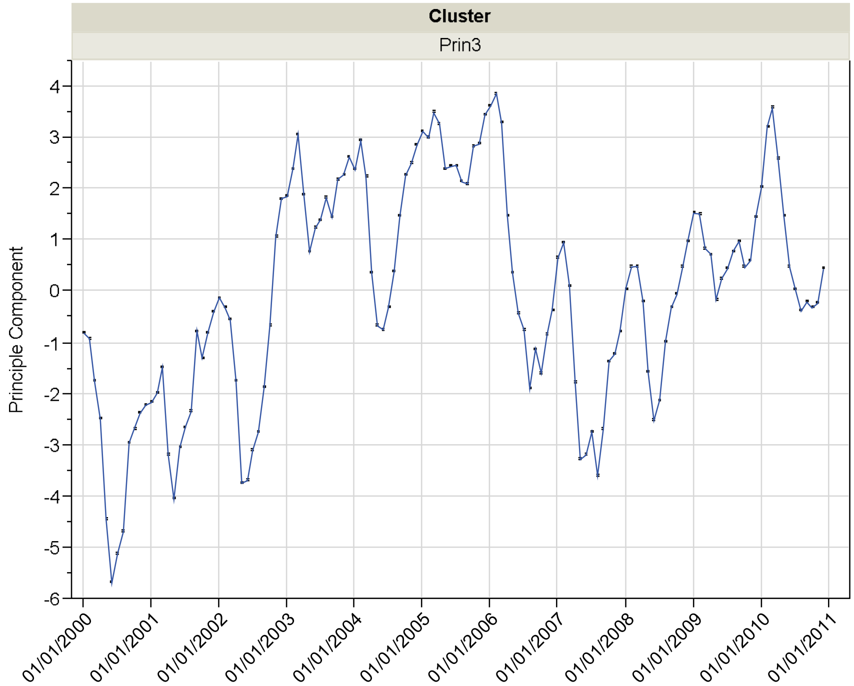


**Figure 10. Principal Component of Well Cluster 3 (See Figure 7 and Table 3 for Well Locations and Cluster Groupings).**

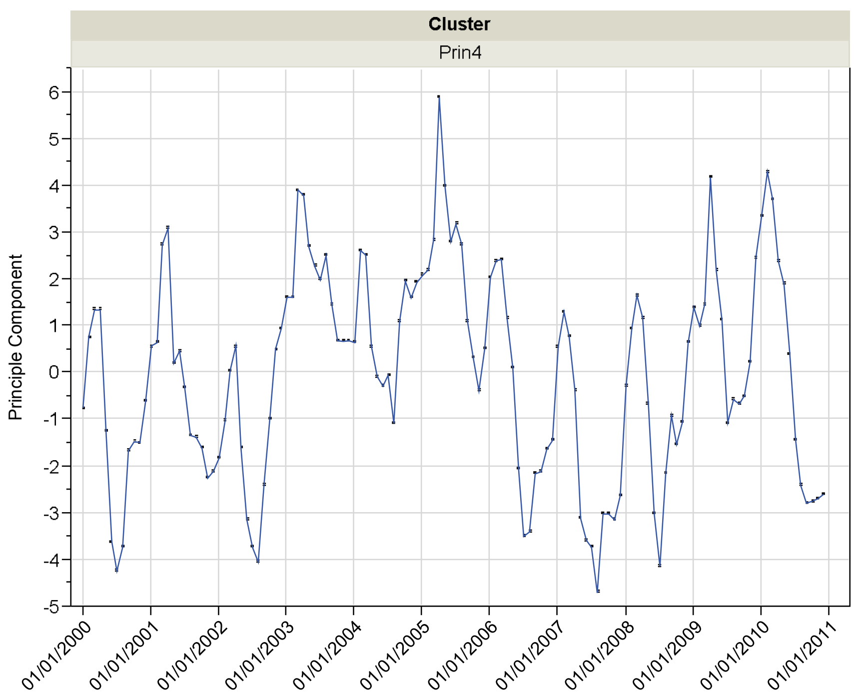


**Figure 11. Principal Component of Well Cluster 4 (See Figure 7 and Table 3 for Well Locations and Cluster Groupings).**

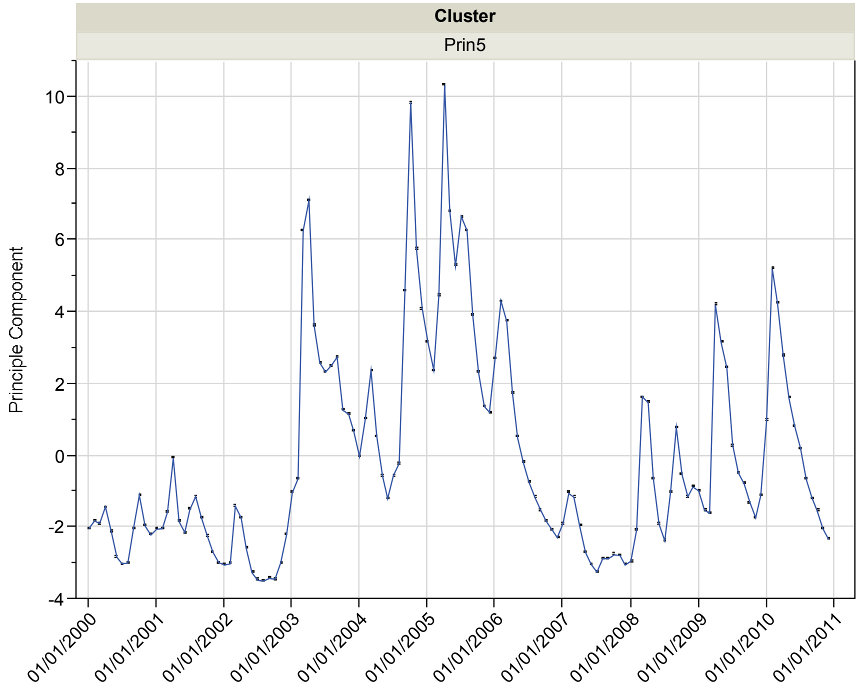


**Figure 12. Principal Component of Well Cluster 5 (See Figure 7 and Table 3 for Well Locations and Cluster Groupings).**

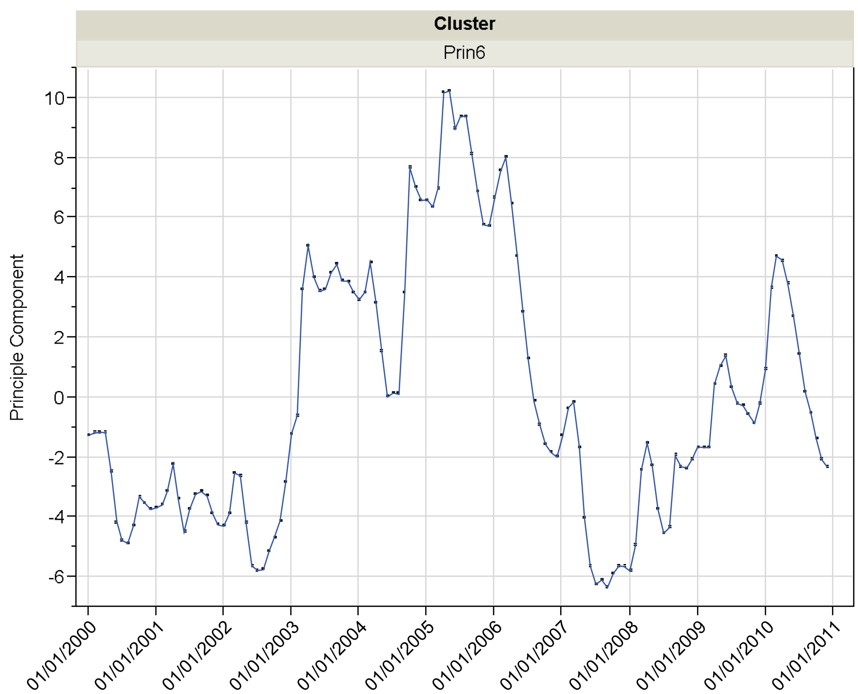


**Figure 13. Principal Component of Well Cluster 6 (See Figure 7 and Table 3 for Well Locations and Cluster Groupings).**

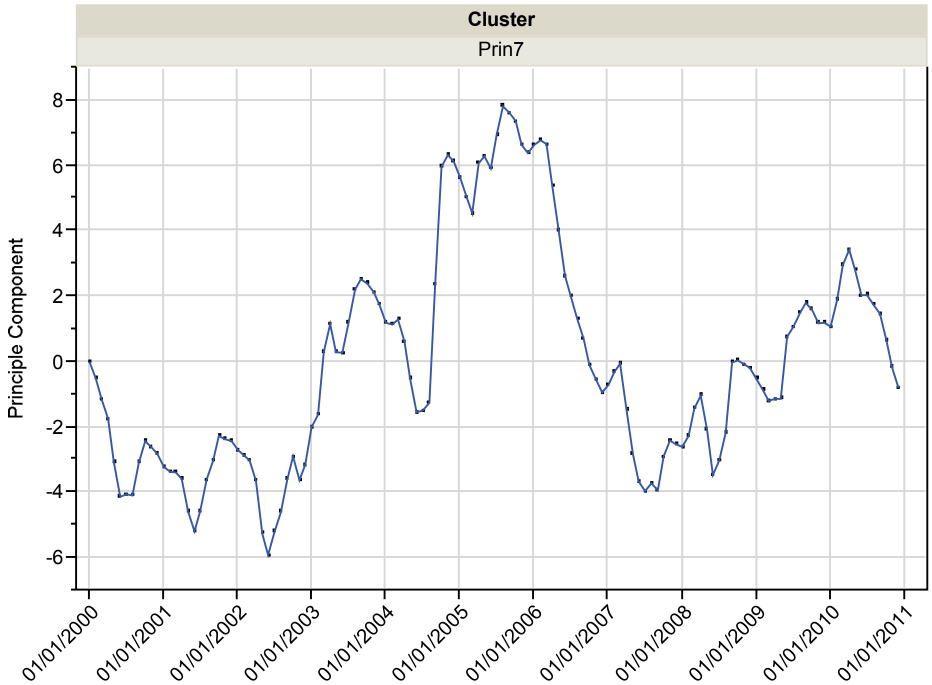


**Figure 14. Principal Component of Well Cluster 7 (See Figure 7 and Table 3 for Well Locations and Cluster Groupings).**

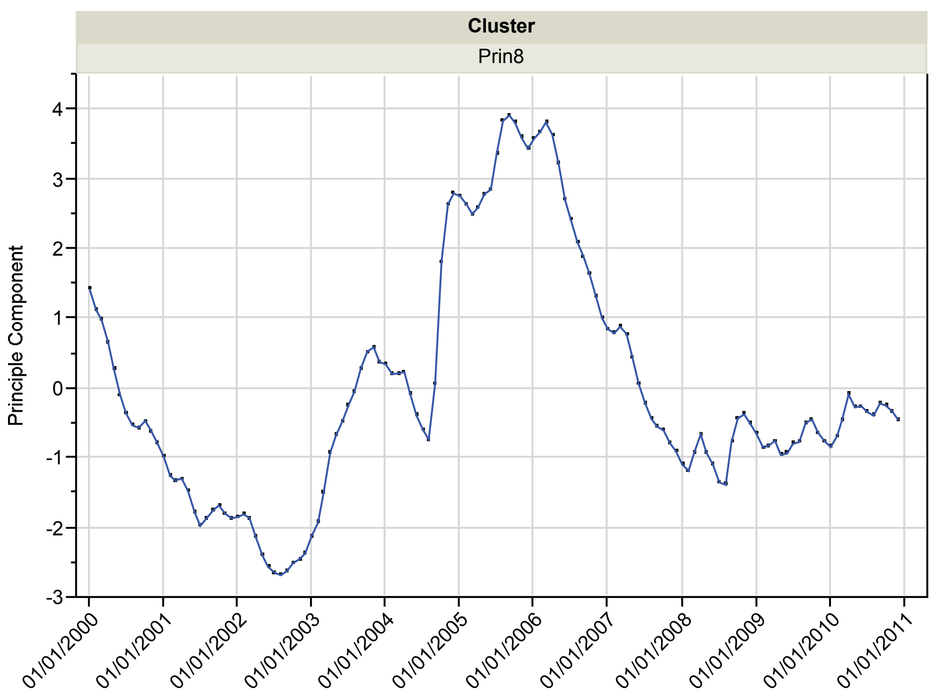


**Figure 15. Principal Component of Well Cluster 8 (See Figure 7 and Table 3 for Well Locations and Cluster Groupings).**

## Surficial-Aquifer Wells

Several surficial-aquifer hydrographs were also reviewed (Appendix B). These were not assessed in cluster and principal-component analyses. Nevertheless, inspection of these hydrographs indicates they are generally consistent with the analyses of the Upper Floridan-aquifer hydrographs (Figure 16).

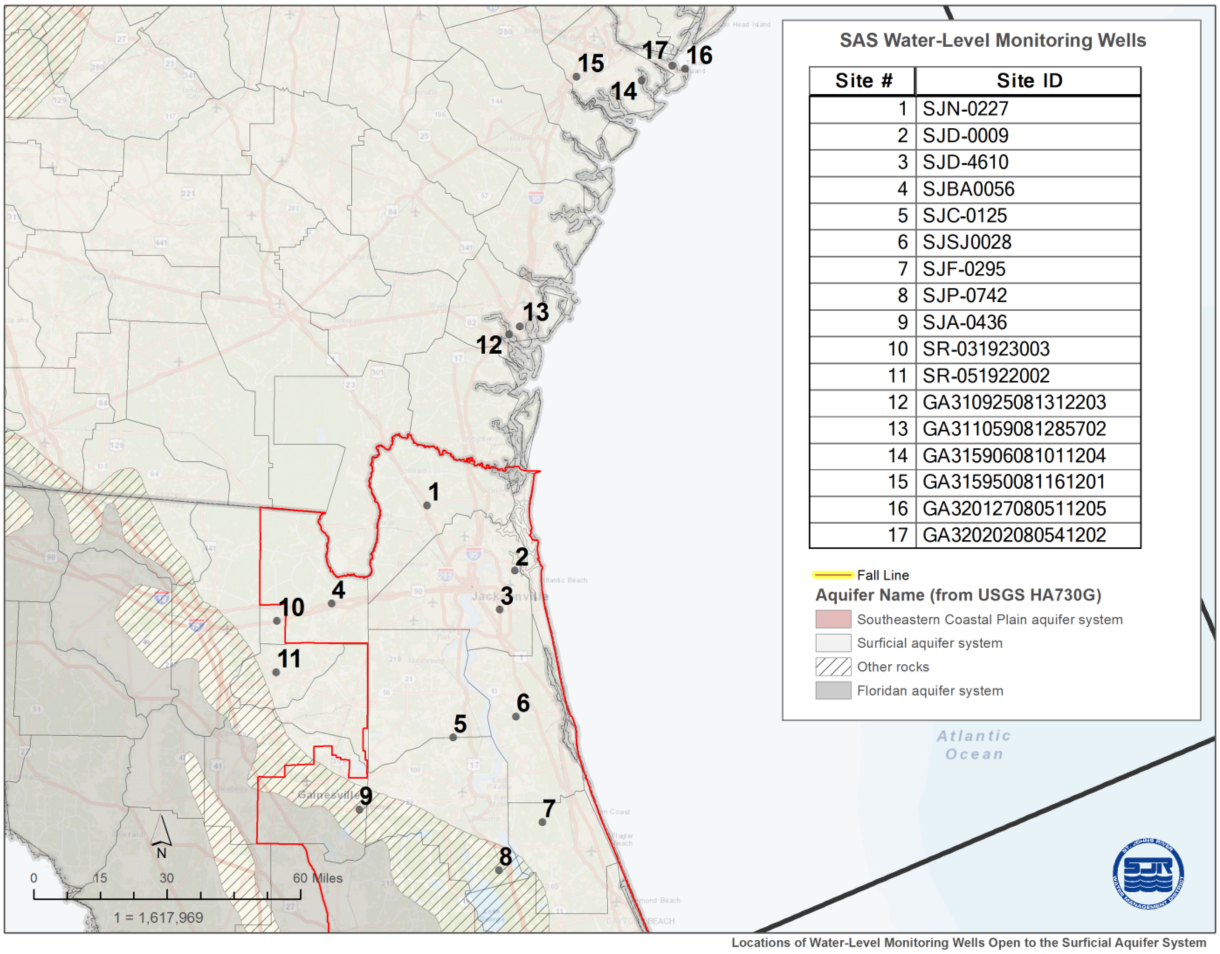


**Figure 16. Locations of Surficial-Aquifer Monitoring Wells from which Hydrographs were Obtained for Review.**

# RAINFALL, 2000 THROUGH 2010

Rainfall during calendar years in the period of 2000 through 2010 was characterized as being more or less average within the proposed model domain. This characterization was based on an analysis of both annual departures from respective annual long-term averages and monthly departures from the respective monthly long-term averages using data obtained from rainfall stations distributed throughout the area of interest (Figure 17 and Table 4).

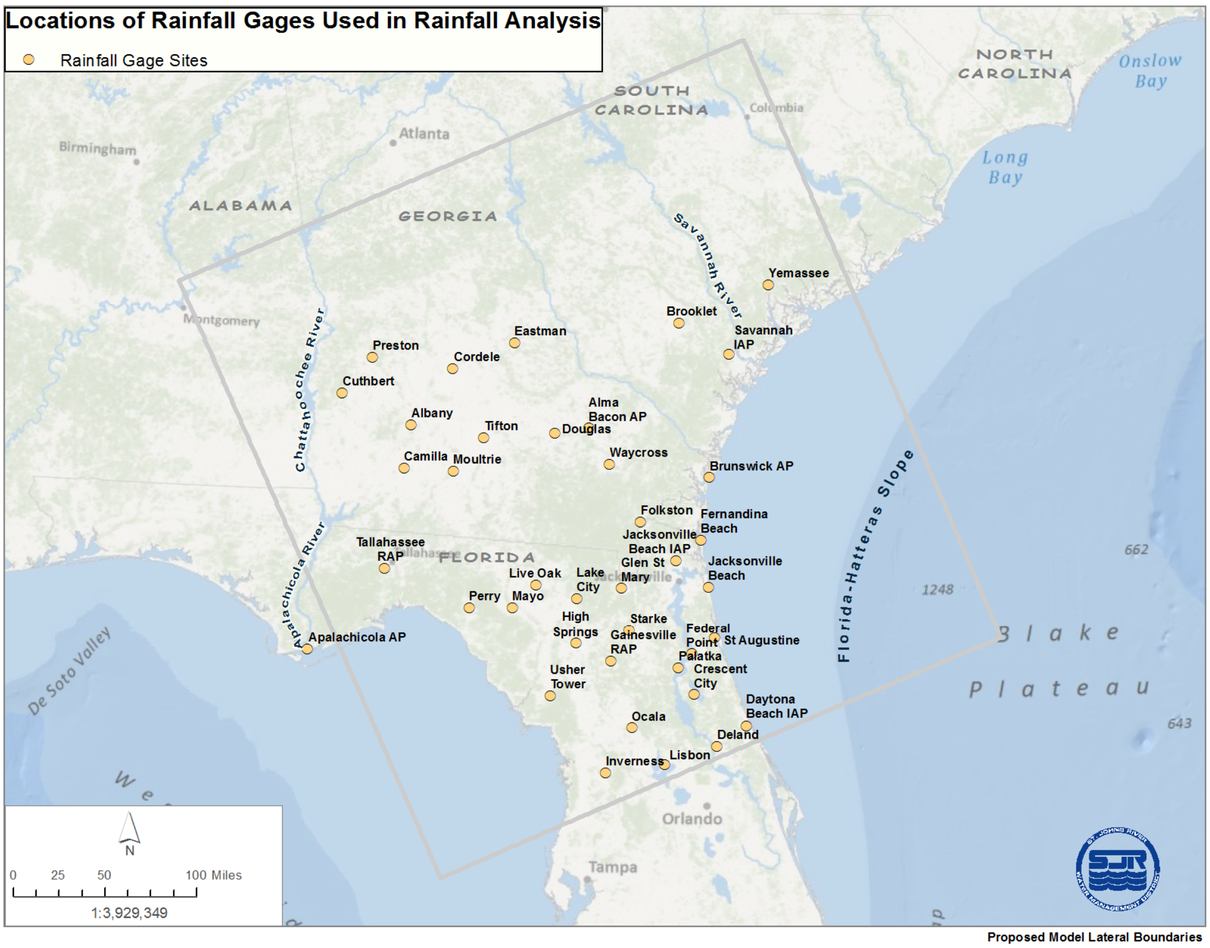


**Figure 17. Rainfall Stations Used in Rainfall Analysis.**

**Table 4. Rainfall Stations Used in Rainfall Analysis.**

| STATION | Name |
|---|---|
| GHCND:USC00090140 | ALBANY 3 SE GA US |
| GHCND:USW00013870 | ALMA BACON CO AIRPORT GA US |
| GHCND:USW00012832 | APALACHICOLA AIRPORT FL US |
| GHCND:USC00091266 | BROOKLET 1 W GA US |
| GHCND:USW00013878 | BRUNSWICK MALCOLM MCKINNON AIRPORT GA |
| GHCND:USC00091500 | CAMILLA 3 SE GA US |
| GHCND:USC00092266 | CORDELE GA US |
| GHCND:USC00081978 | CRESCENT CITY FL US |
| GHCND:USC00092450 | CUTHBERT GA US |
| GHCND:USW00012834 | DAYTONA BEACH INTERNATIONAL AIRPORT FL US |
| GHCND:USC00082229 | DELAND 1 SSE FL US |
| GHCND:USC00092783 | DOUGLAS GA US |
| GHCND:USC00092966 | EASTMAN 1 W GA US |
| GHCND:USC00082915 | FEDERAL POINT FL US |
| GHCND:USC00082944 | FERNANDINA BEACH FL US |
| GHCND:USC00093460 | FOLKSTON 3 SW GA US |
| GHCND:USW00012816 | GAINESVILLE REGIONAL AIRPORT FL US |
| GHCND:USC00083470 | GLEN ST MARY 1 W FL US |
| GHCND:USC00083956 | HIGH SPRINGS FL US |
| GHCND:USC00084289 | INVERNESS 3 SE FL US |
| GHCND:USC00084366 | JACKSONVILLE BEACH FL US |
| GHCND:USW00013889 | JACKSONVILLE INTERNATIONAL AIRPORT FL US |
| GHCND:USC00084731 | LAKE CITY 2 E FL US |
| GHCND:USC00085076 | LISBON FL US |
| GHCND:USC00085099 | LIVE OAK FL US |
| GHCND:USC00085539 | MAYO FL US |
| GHCND:USC00096087 | MOULTRIE 2 ESE GA US |
| GHCND:USC00086414 | OCALA FL US |
| GHCND:USC00086753 | PALATKA FL US |
| GHCND:USC00087025 | PERRY FL US |
| GHCND:USC00097201 | PRESTON GA US |
| GHCND:USW00003822 | SAVANNAH INTERNATIONAL AIRPORT GA US |
| GHCND:USC00087812 | ST AUGUSTINE FL US |
| GHCND:USC00088529 | STARKE FL US |
| GHCND:USW00093805 | TALLAHASSEE REGIONAL AIRPORT FL US |
| GHCND:USC00098703 | TIFTON GA US |
| GHCND:USC00089120 | USHER TOWER FL US |
| GHCND:USC00099186 | WAYCROSS 4 NE GA US |
| GHCND:USC00389469 | YEMASSEE SC US |

Rainfall was characterized on an annual basis by summing up the annual departures from the long-term averages of the respective years at each rainfall station (Table 4). The results indicate that the years 2000 and 2006 were generally the driest years in the period of 2000 through 2010. The years 2004 and 2005 were generally the wettest years. The years 2002 and 2008 were the most average years.

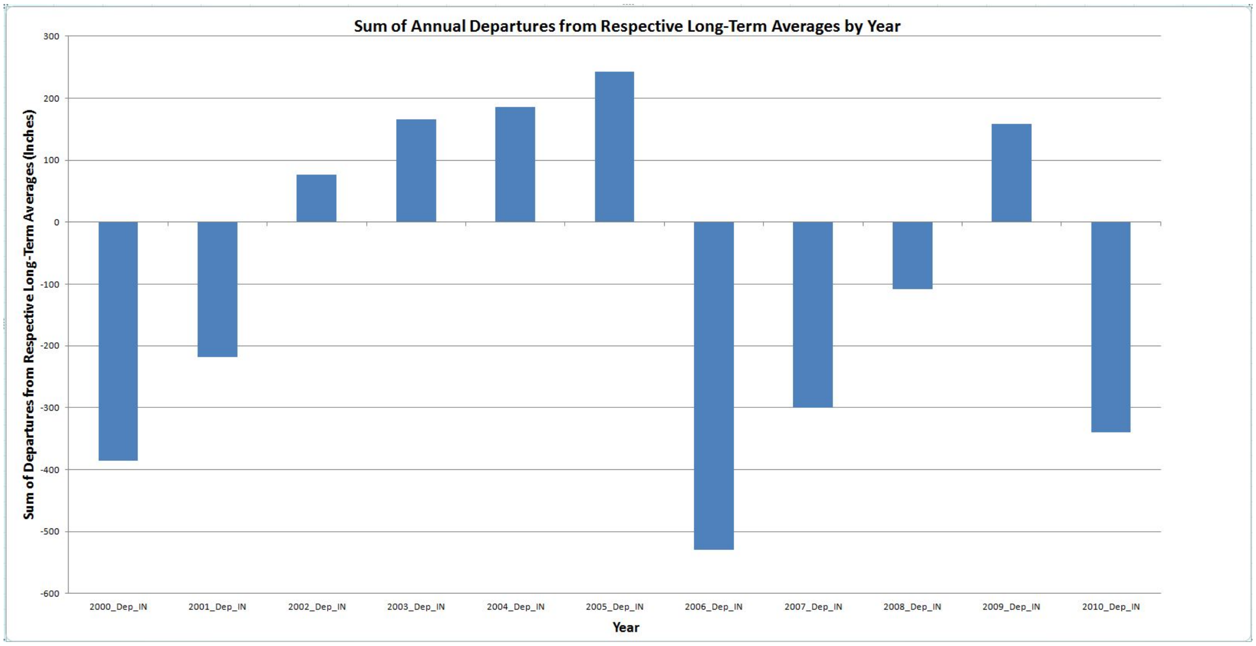


**Figure 18. Sums of Annual Departures from Respective Long-Term Averages by Year (Inches).**

Departures were determined relative to the long-term average rainfall amount of the year or month and rainfall gage in question. The long-term average amount was typically determined as the average of the annual totals of the period of record through the year 2010. However, long periods of missing data were present in some data sets, in some instances spanning periods of years. In such cases, the average was determined using data collected in the period immediately following the period of missing data through the year 2010. An example of a rainfall station in this category is Live Oak. At the Live Oak station, continuous reporting did not commence until 1953, though the full period of record for the Live Oak station stretches back to 1898. Hence, the annual and monthly long-term averages for the Live Oak station were based on the period of 1953 through 2010. Other details concerning the processing of the available rainfall data are outlined in Appendix C. A copy of the Excel spreadsheet used in the processing of the data are available on the SJRWMD FTP site, as noted in Appendix C.

The “memory” of all preceding rainfall events included in a cumulative departure analysis up to a given point in time is reflected in the value of the cumulative departure curve at that point in time. This aspect of the cumulative departure analysis makes relatively long-term rainfall patterns within a year more discernible.

The annual sums of the absolute values of the monthly cumulative departures of a given rainfall station are used herein as a relative measure of the extent that rainfall amounts spent above or below monthly long-term average levels within a given year. It is possible, for example, for a given year to have a relatively small annual departure but large positive and/or negative monthly departures occurring over successive months that more or less cancel each other.

Cumulative departures for each of the years in the period of 2000 through 2010 were determined on a monthly basis for each rainfall station (Table 4). To represent the year as a whole, the absolute values of the monthly cumulative departures were summed for all stations on a yearly basis (Figure 19). The closer a given sum is to 0 (i.e., "long-term average") the more average a given year is considered to be with regard to rainfall patterns within the year in question. Based on this approach, the years 2002 and 2008 are the "most average" rainfall years within the area of the proposed model domain in the period of 2000 through 2010 (Figure 19).

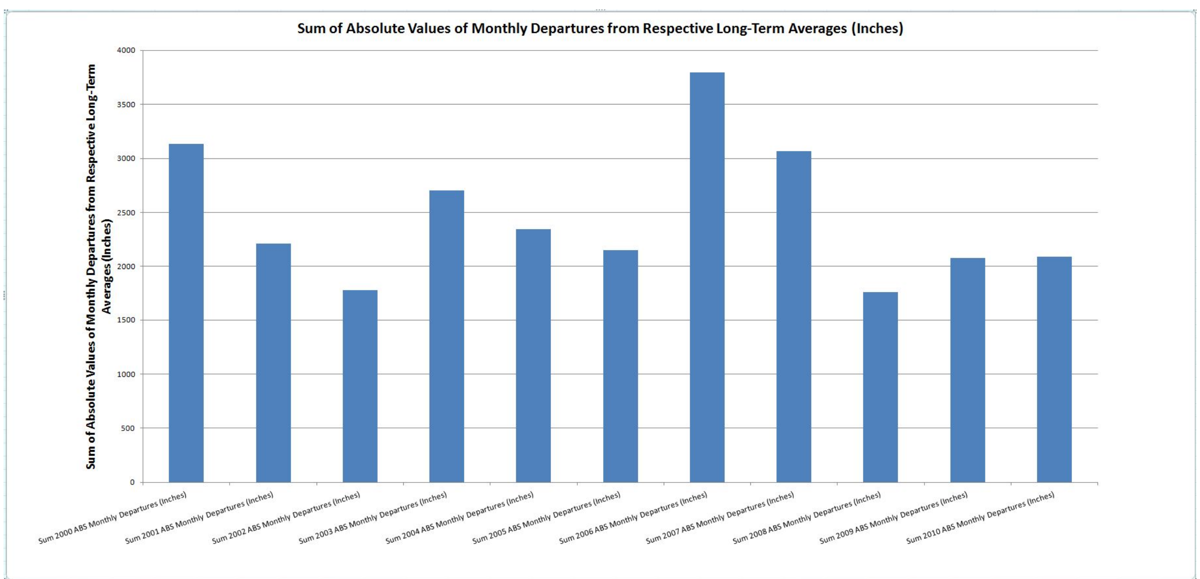


**Figure 19. Sum of the Absolute Values of the Monthly Cumulative Departures within the Proposed Model Domain by Year.**

# MODEL CODE AND APPROACH

## Model Code Selection

The model will be fully three-dimensional and limited to the simulation of freshwater flow in the FAS and overlying IAS and SAS. Calibration will be to both steady-state and transient conditions. MODFLOW 2005 (Harbaugh, 2005) is capable of handling these requirements. In addition, MODFLOW 2005 is public-domain software, is available for download from the internet at no cost to the downloader, and is recognized and used throughout the world. Therefore, the model code will be MODFLOW 2005 (Harbaugh, 2005).

## NFSEG Regional Groundwater Steady-State Flow Model Configuration Plan

### Steady-State Calibration Concepts

The NFSEG regional groundwater flow model will be developed in stages. The initial stage will consist of the development of a steady-state version of the model. The term "steady-state" means constant with respect to time. The steady-state period is one in which groundwater levels, as represented in well hydrographs, do not trend significantly either upwardly or downwardly. This is not to imply that water-level fluctuations do not occur in a steady-state period. Water-level fluctuations above and below the median are to be expected for any period. In a steady-state period, however, the fluctuations occur around a median water level that remains more or less constant with respect to time, as opposed to an increasing or decreasing median.

Two steady-state periods will be identified for use in the present model-calibration process. One will be a relatively dry period, and the other will be a relatively wet period. The differences in climatic conditions will help to test the "robustness" of the calibration, the measure of the ability to represent different climatic and/or pumping conditions using a given set of calibration-derived hydraulic parameters.

Steady-state calibration can and should be performed with respect to streamflow rates as well as groundwater levels. Including observations of observed streamflows is important in order to constrain the range of possible recharge rates and reduce the correlation between recharge and hydraulic conductivity during model calibration. The types of flow rates to which steady-state calibration is performed typically include stream base-flow rates and spring discharges. Stream base-flow rates can be estimated from stream-gage observations using base-flow separation techniques. Spring discharges can be estimated based on measurement of spring-run discharge and sometimes based on direct velocity measurements obtained at the spring orifice.

Selected Steady-State Calibration Periods

Based on the preceding analysis of water levels and rainfall, the “dry steady-state year” will be 2001, and the “wet steady-state year” will be 2009. Relatively stable water levels were generally prevalent within these two years throughout the potential model domain, stable water levels being indicative of steady-state conditions. At the same time, 2001 was relatively dry, while 2009 was relatively wet. In addition, the year 2001 simulated steady-state conditions will be used as initial conditions for transient simulations, which will represent the period of 2001 through 2010.

Representation of Aquifers and Semiconfining Units

The NFSEG regional groundwater flow model will be a fully three-dimensional groundwater flow model. In fully three-dimensional representation, semiconfining units are treated as aquifer layers. As a result of this type of representation, semiconfining units can be treated as sources of groundwater for wells, springs, and streams. In the NFSEG model, this type of representation will enable the simulation of spring discharge from the IAS. An example of an IAS spring is Wadesboro Springs in Clay County, Florida. This approach will also enable the simulation of well discharge from the IAS. Withdrawals from the IAS for domestic self-supply are relatively widespread in Bradford County, Florida. In Camden and Glynn counties, Georgia, the Brunswick aquifer system, which is part of the IAS, is a significant withdrawal source. This type of representation is not possible in the alternative approach, in which semiconfining units are represented merely as a leakance or VCONT layers. Hence, the fully three dimensional approach is more generalized and rigorous.

For transient simulations, the fully three-dimensional approach enables the assignment of semiconfining-unit storage properties. This can be important in areas of higher semiconfining-unit storage capacity, because higher values of semiconfining-unit storage properties can result in significant lag-time effects in regards to the vertical propagation of drawdown across a semiconfining unit. Higher storage capacity occurs in areas of greater semiconfining-unit thickness and/or clay content. This situation occurs in regards to the IAS of coastal northeast Florida and southeast Georgia.

Because the assignment of aquifer permeability and thickness properties are independent in the fully three-dimensional approach, regions in which a given semiconfining unit may function more like an aquifer or portion thereof than semiconfining unit can be more easily and accurately represented. This capability may be important in regards to the representation of the middle semiconfining unit of the FAS in areas where, in past conceptualization (e.g., Miller, 1986), the middle semiconfining unit was thought to be absent but, under the present conceptualization (L. Williams *et al.*, In Progress), the stratigraphic features that are used to define the middle semiconfining unit are thought to be present but of widely varying permeability.

Pinch-out of internal semiconfining units can be facilitated by the fully three-dimensional approach as well. In areas in which a given semiconfining unit is absent, a finite but relatively small thickness can be assigned to the representative model layer in question. The assigned vertical permeability, however, will be representative of the bounding aquifers rather than semiconfining-unit material. This approach is necessary because the grid cells in question will need to be active in order to allow the simulation of vertical leakage across the model layer in question. In most cases, the particular permeability values assigned will be determined through the calibration process, since precise estimates are not readily available.

<u>Surface Water Balance by HSPF– Boundary Conditions and Result Comparisons</u>

Surface water balance estimates to establish boundary conditions and comparisons for the NFSEG groundwater model will be determined by surface water models. The surface water models will use Hydrological Simulation Program—FORTRAN (HSPF; Bicknell et al., 1997) software. HSPF is a comprehensive, rainfall-runoff-water-quality model and will be used to represent surface-water basins of the NFSEG model domain, plus contributing watersheds as necessary.

An important objective of the HSPF models is that they be used to narrow and help quantify the expected range of plausible recharge rates over the model domain. Development of these rainfall-runoff models will be done in concert with the groundwater flow models to ensure that the recharge rates and groundwater outflows estimated by the rainfall-runoff models are consistent with the hydrogeology of a given area, with the results from obtained from the groundwater flow models, and with ancillary data.

<u>HSPF/BASINS</u>

The NFSEG active cells cover all or part of 45 USGS, HUC8 watersheds. An additional 15 HUC8 watersheds will be modeled to account for surface water flow into the 45 watersheds overlying the NFSEG active cells (Figure 20).

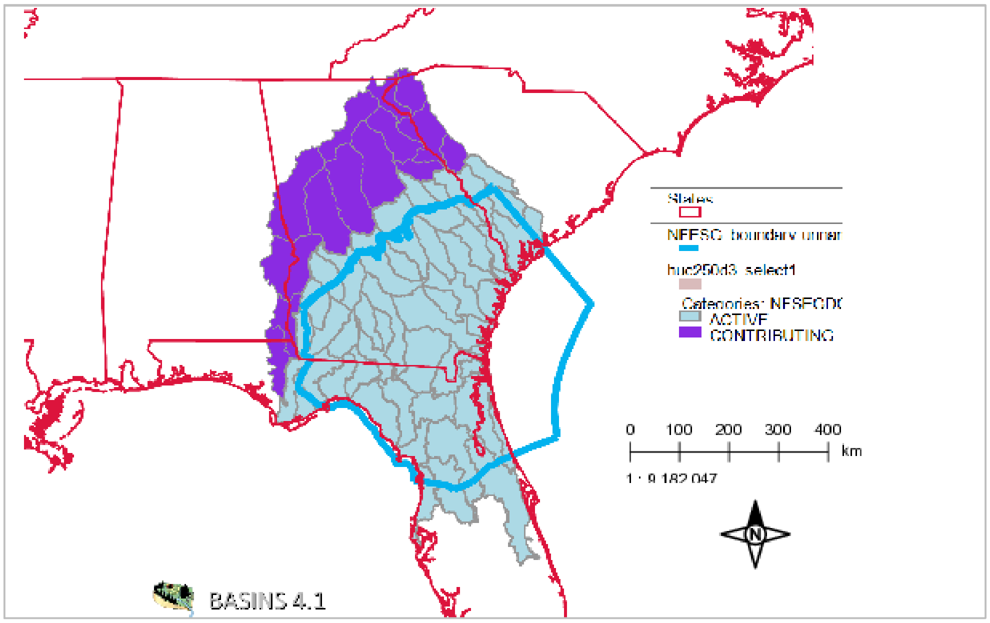


**Figure 20. USGS HUC8 watersheds within the active cells of the NFSEG groundwater model and contributing watersheds.**

The initial model setup will be developed using BASINS (Better Assessment Science Integrating point & Non-point Sources), ArcGIS, and TauDEM (watershed delineation). BASINS is a pre/post processor for HSPF developed for the USEPA. The land use in the model will be the National Land Cover Database 2006, and the reach and watershed characterization will use the National Hydrographic Database Plus (NHD Plus). Rainfall and potential evaporation (the evaporation from a shallow body of water) are the required meteorological inputs for HSPF and will be downloaded using standard BASINS tools for the meteorological stations in each watershed or developed as area-weighted estimates from Daymet or MODIS.

Some understanding of how HSPF views the world is necessary to establish where MODFLOW and HSPF overlap in the overall water balance. Figure 21 through Figure 23 illustrate the water storages and flows through the HSPF system for pervious and impervious land use elements.

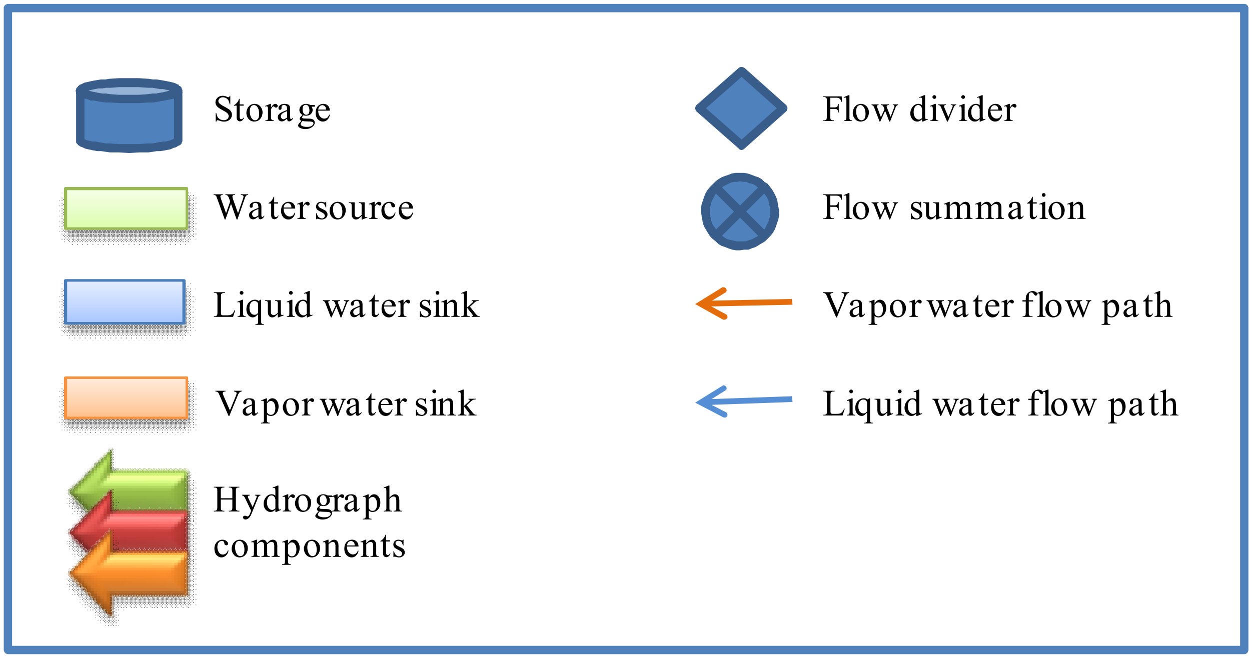

**Figure 21. Legend for HSPF model simulation graphics in**

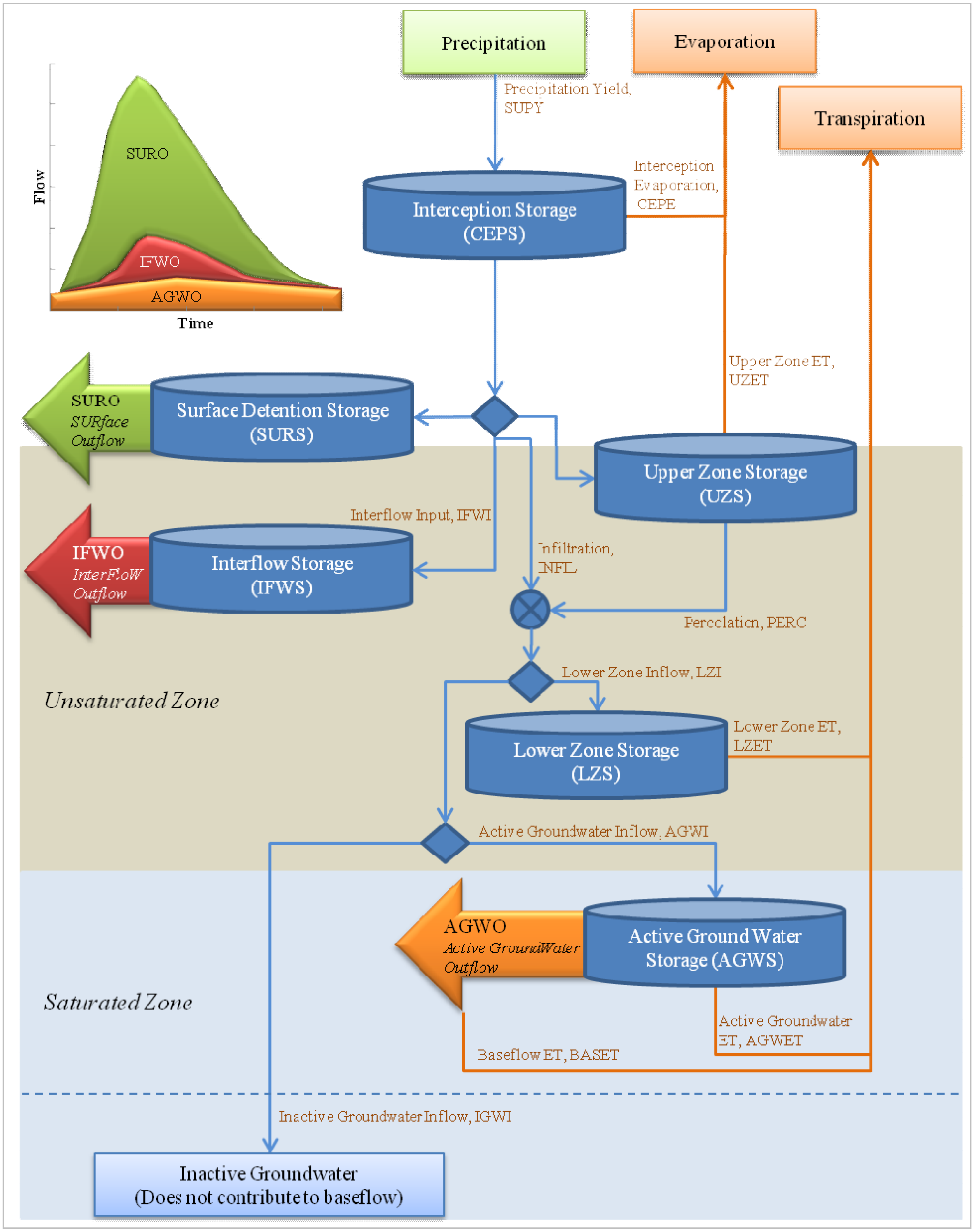


**Figure 22. Illustration of water storage and movement in the HSPF model pervious land element (PERLND).**

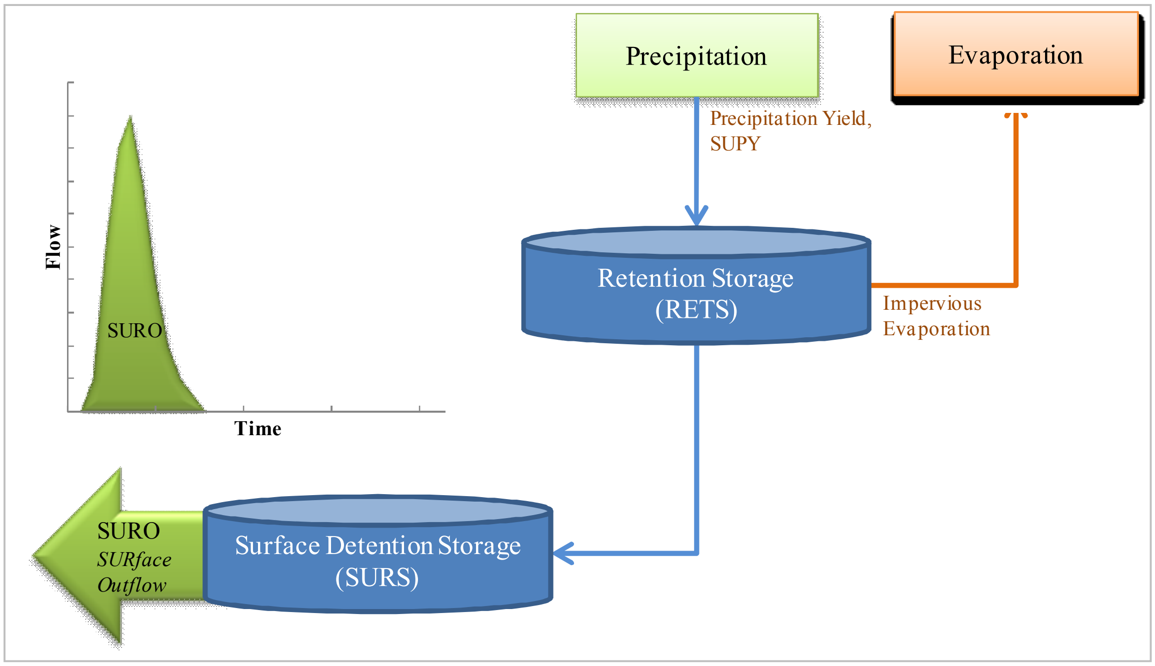


**Figure 23. Illustration of water storage and movement in the HSPF model impervious land element (IMPLND).**

In the steady-state version of the NFSEG groundwater flow model, the rate of evapotranspiration (ET) from the saturated zone will be estimated through use of the MODFLOW ET package. In the MODFLOW ET package, the rate of saturated ET varies linearly with the depth to the water table between a maximum value that occurs at the "ET surface" typically assumed to be land surface, and 0 feet/day (ft/day), which occurs at the "extinction depth." The extinction depth will be based on an approach presented by Shah *et al.* (2007). The maximum saturated ET rate to be utilized in the calculation of the saturated ET rate will be the potential ET rate minus the sum of the unsaturated ET components, which will be obtained from HSPF.

Table 5 lists the overlapping parts of the MODFLOW and HSPF water balances and the uses within each.

**Table 5. Connection between MODFLOW and HSPF variables.**

| **MODFLOW** | **HSPF Variables** (variable definitions below and in Figure 21 - Figure 23) | **Purpose** |
|---|---|---|
| Recharge to surficial | IGWI + AGWI | MODFLOW input |
| Recharge from surficial to next lower aquifer. If MODFLOW indicates discharge to surficial, then IGWI should be near zero. | IGWI | Comparison/calibration |
| Baseflow | AGWO | Comparison/calibration |
| Maximum Unsaturated ET | PERLND: Potential ET – CEPE – UZET – LZET | MODFLOW/ET package input |
| Saturated ET | AGWET + BASET | Comparison/calibration |

**where: IGWI: Inactive Groundwater Inflow**
**AGWI: Active Groundwater Inflow**
**AGWO: Active Groundwater Outflow**
**CEPE: Interception Evaporation**
**UZET: Upper Zone Evapotranspiration**
**LZET: Lower Zone Evapotranspiration**
**AGWET: Active Groundwater ET**
**BASET: Baseflow ET**
**PERLND: Pervious Land Element**

Inactive Groundwater Inflow(IGWI) is defined in the HSPF environment as the saturated groundwater component of the water balance that does not contribute to baseflow. It is always a loss out of the 'bottom' of the HSPF water balance. IGWI in terms of a representation in MODFLOW would be analogous to recharge from the surficial to the next lower aquifer.

*Irrigation*

Irrigation in HSPF can be included in two ways, imposed as an external time-series (analogous to adding additional precipitation), or using a crop demand algorithm based on the AFSIRS model. The irrigation demand time-series will be established by the SJRWMD Water Supply Planning group. HSPF additionally requires the acres of irrigated land broken down to as fine a spatial scale as possible in order to be included in the correct subwatershed.

*Water Sources*

Surface and groundwater supplies need to be split into the portion used for irrigation and what is returned to surface waters through a wastewater treatment plant. As part of this task, the locations of the surface and groundwater withdrawals and the wastewater plant discharges will be identified and their withdrawal and discharge rates compiled or estimated.

*Land Use*

The National Land Cover Database (NLCD) land use coverage is a convenient, consistent, nationwide land use coverage. It consists of the groups identified in the first column of Table 6. The initial parameter ranges used in the first cut model will be taken from previous models developed by the SJRWMD.

**Table 6. Preliminary mapping of current District HSPF land use groups to NLCD categories to define initial parameter ranges.**

| NLCD Land Use | Use Current HSPF Parameter Ranges From: | Notes |
|---|---|---|
| Water-Open | Water | |
| IceSnow-Perennial | (not applicable) | |
| Developed-Open Space | Open and barren land | |
| Developed-Low Intensity | Low density residential | |
| Developed-Medium Intensity | Medium density residential | |
| Developed-High Intensity | Industrial and commercial | |
| Barren Land | Open and barren land | |
| Unconsolidated Shore | (generic parameter ranges) | |
| Transitional | Forest or Forest regeneration | |
| Forest-Deciduous | Forest | |
| Forest-Evergreen | Forest | |
| Forest-Mixed | Forest | |
| Scrub-Dwarf | Rangeland | |
| Scrub-Scrub | Rangeland | |
| Grassland | Rangeland | |
| Agriculture-Pasture | Pasture | Divide into irrigated/non-irrigated |

| | | |
|---|---|---|
| Agriculture-Cultivated Crops | Agricultural general | Divide into irrigated/non-irrigated |
| Wetlands-Woody | Wetlands | |
| Wetlands-Palustrine Forested | Wetlands | |
| Wetlands-Palustrine Scrub | Wetlands | |
| Wetlands-Estuarine Forested | Wetlands | |
| Wetlands-Estuarine Scrub | Wetlands | |
| Wetlands-Emergent Herbaceous | Wetlands | |
| Wetlands-Palustrine Emergent | Wetlands | |
| Wetlands-Estuarine Emergent | Wetlands | |
| Aquatic Bed-Paustrine | Water | |
| Aquatic Bed-Estuarine | Water | |

*HSPF Data Requirements*

Table 7 lists the data requirements for HSPF.

**Table 7. HSPF data requirements.**

| Data | Source |
|---|---|
| Precipitation | National Land Data Assimilation System (NLDAS) |
| Evaporation | National Land Data Assimilation System (NLDAS) |
| Flow | Download from USGS National Water Information System (USGS-NWIS) |
| Irrigation time series | External time-series developed by SJRWMD Water Supply Planning and Georgia EPD |
| Irrigated acreage | SJRWMD Water Supply Planning and Georgia EPD |
| Surface water withdrawals | SJRWMD Water Supply Planning and Georgia EPD |
| Groundwater withdrawals | SJRWMD Water Supply Planning and Georgia EPD |
| Water treatment plant discharges | SJRWMD Water Supply Planning and Georgia EPD |
| Urban irrigation demand | SJRWMD Water Supply Planning and Georgia EPD |

*HSPF Calibration*

A version of PEST with parallel processing capabilities (Hunt, et al., 2010) will be used to assist in the calibration of the models. Weights between the different observation groups (daily, monthly, annual, frequency distribution, etc.) and between stations will be established by the modeler to develop a consistent calibration across the entire watershed. Regularization of parameters between watersheds using PEST is not planned, but a manual review and adjustment of parameter ranges will be made to ensure that adjacent watersheds have similar parameter values.

Calibration Process:

1. Data Collection: Gather hydrologic data from models developed in Georgia (i.e. surface water withdrawals, agricultural water demand, municipal wastewater reuse for urban irrigation, model parameters from existing HSPF models, etc.)
2. Facilitate collaborative workshops for the modelers to identify and solve problems and document the process.
3. Establish baseline models using BASINS, ArcGIS, and TauDEM. The models will likely have multiple calibration points within the overall watershed, but each watershed will have only one model.
4. Copy project directory with BASINS name (HUC8 name) and structure to the overall project directory..
5. Establish initial parameter ranges for each land use based upon parameter ranges used in previous SJRWMD models. See Table 6.
6. Develop the data for the irrigation module and add to models.
7. Apply PEST template script to convert to PEST project (to be written).
8. Run BeoPEST (SJRWMD parallel version of PEST).
9. Evaluate performance and adjust parameter ranges and objective function weights accordingly.
10. When MODFLOW results are available, compare overlapping water balance volumes.
11. Repeat steps 8 and 9 as many times as necessary to have a satisfactory calibration.

If time and processing resources are sufficient, a calibration may be accomplished by integration of the MODFLOW and HSPF models into a single model batch file called during a given BeoPEST calibration run.

After there is a model represented for every subwatershed, a script will be run to read water balance values for each land use out of the binary output files, multiply by the land use area in the area table (exported from ArcGIS) to establish an area-weighted depth in inches for all required surface water balance components for each MODFLOW cell.

<u>MODFLOW Representation of Streams, Lakes, and Oceans</u>

Streams and lakes will be represented in the model using the MODFLOW River Package. The waters of the Atlantic Ocean will be represented as equivalent fresh-water specified heads within aquifer layer 1 (i.e., the representation of the

SAS). The waters of the Gulf of Mexico will be represented as the equivalent fresh-water source heads of the GHB lateral boundary conditions along the representation of the Gulf coast portion of the model western lateral boundary.

Use of the River Package in regards to lakes will involve specification of median lake stage for the calibration period in question and the specification of a conductance value. Hence, lakes for which adequate stage information is not available will likely not be represented explicitly as lakes but, rather, as active grid cells of the representation of the SAS (model layer 1).

Rivers and streams will be represented using the river package also. The flowlines of river and streams will be obtained from the N H D (NHD; http://nhd.usgs.gov/ ). Stream reaches will be classified according to the Strahler number of the reach in question. Reach water-surface elevation will be interpolated between gauge sites, where gauge sites are available and surveyed. Base flows will be derived from gauged stream flows through a base-flow separation technique. Base flow will be an important calibration variable for constraining the range of possible recharge rates and reducing correlation between calibrated values of hydraulic conductivity and recharge.

Springs will be represented in the model using GHB conditions. The source head of the GHB used to represent a given spring will be the estimated spring-pool elevation. Spring discharge will be an important calibration variable also. Aquifers with known springs include the IAS and FAS. Seepage faces are concentrated in the SAS at steep heads. Steep heads within the model domain with significant discharge include ones located at Gold Head Branch State Park and the Ravine Gardens State Park in Clay and Putnam counties, Florida, respectively. Significant seepage faces can be represented using GHB conditions or or as river-package conditions, depending on the situation.

Representation of Sinks and Drainage Wells

A number points of direct inflow into the FAS are present within the potential study area. These include sinkholes and drainage wells. The major sinkholes in this regard include Alachua Sink, Haile Sink, and sinkholes in Orange Lake in Alachua County. Drainage wells are present at Lake Alice in Gainesville, Florida, and also in Ocala and Live Oak, Florida. Three wells are used to inject treated wastewater into the FAS at the Kanapaha waste-water treatment plant near Gainesville, Florida (Figure 24).

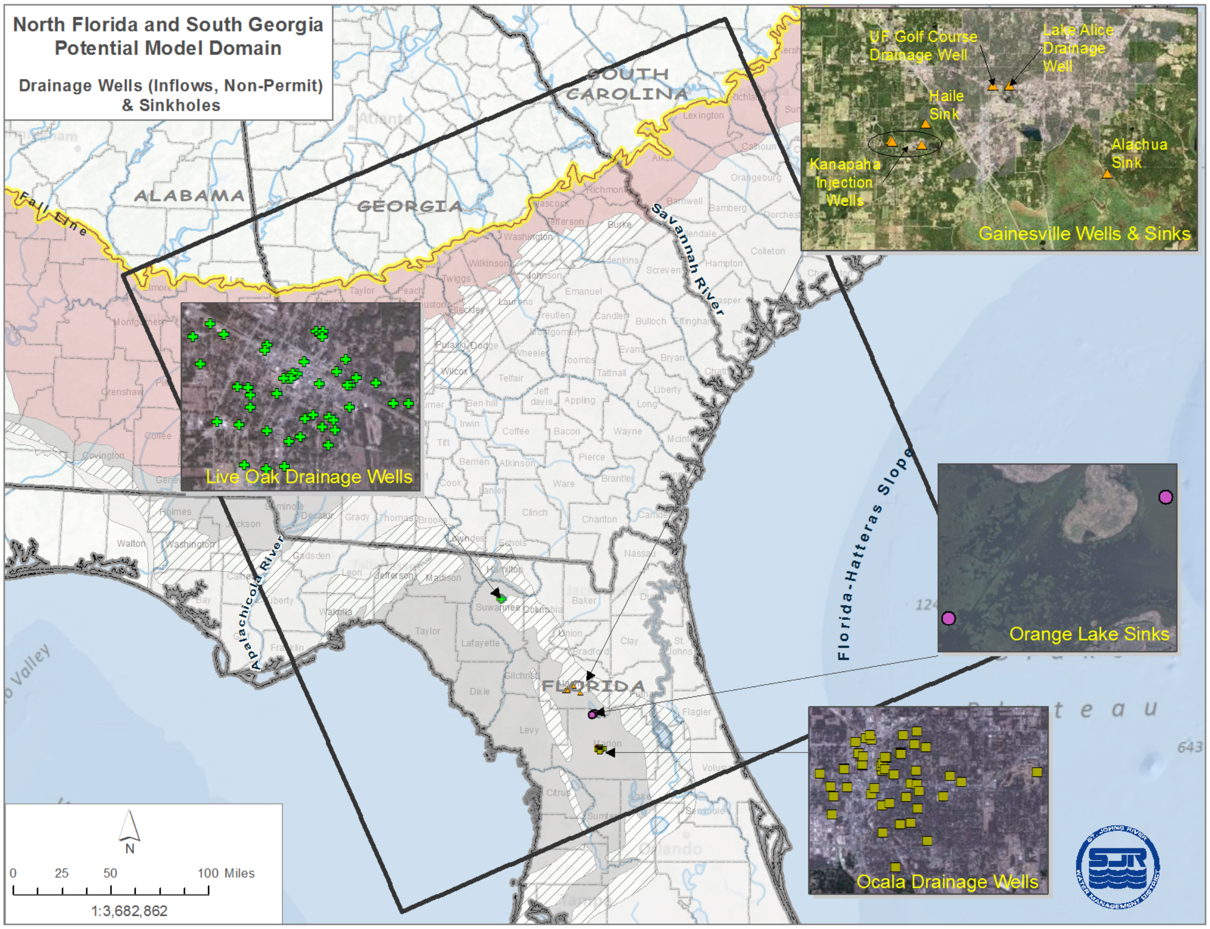


**Figure 24. Locations of Points of Direct Inflow in the Floridan Aquifer System.**

Two previous studies that have attempted to estimate influx rates at Alachua Sink, Haile Sink, and Lake Alice are by Phelps (1987) and Russo (In Progress). Estimates regarding Alachua Sink and Haile Sink from these two sources are in good agreement. The estimates of drainage-well influx at Lake Alice do not agree well, however, so some additional research will need to be performed in the case of Lake Alice. Flux rates into sinkholes at Orange Lake were estimated by Motz *et al.* (1998) and by Russo (In Progress). The estimate resulting from the study by Motz *et al.* (1998) is somewhat smaller than that of Russo (In Progress; 15.6 mgd vs. 25 mgd). However, based on the locations and numbers of the subject sinkholes as shown in the two reports, it is not clear at present that the same sets of sinkholes are being addressed. Likely as not, there are many sinkholes in the bed of Orange Lake, so, to some extent, the flux of water from the lake into the FAS will need to be treated as one of heightened IAS vertical conductivity. Some additional investigation will be performed to clarify the number of known sinkholes in Orange Lake and the associated influx rates.

Regarding the drainage-well complexes in the cities of Ocala and Live Oak, Florida, influx rates for these drainage wells apparently have not been determined. However, Kimrey & Fayard (1984) show the locations of the subject drainage wells and also provide estimates of the respective cumulative drainage-basin areas. Using these basin areas, the influx into the FAS via the drainage wells may be estimated roughly in each case as the product of the respective basin area and the difference in total precipitation within the calibration year and minimum evapotranspiration. These estimates will most likely represent the high end of the potential range, but, again, they may be the best attainable. The resulting estimate of total influx in each case will be distributed evenly amongst the respective complex of drainage wells. Additional work will be performed to determine if more recent information is available concerning the drainage-well complexes of Ocala and Live Oak, Florida.

Estimates of the influx rates of the injection wells at the Kanapaha waste-water treatment plant will be obtained from Gainesville Regional Utilities.

Porter Sink in the bed of Lake Jackson in Tallahassee, Florida, may be included as a point influx also. Porter Sink, being exceptionally large, drains the lake dry periodically and maintains it in that condition for extended periods (http://www.dep.state.fl.us/geology/geologictopics/jacksonsink.htm and http://en.wikipedia.org/wiki/Lake_Jackson_(Tallahassee,_Florida)). An estimate of the long-term average flux through the bottom of Lake Jackson is available in Bartel *et al.* (1992). More information concerning the influx to the FAS via Porter Sink will be sought.

Many other karstic features, sinks and rises for instance, are known to exist in the area of the Cody Scarp within the potential model domain. In cases of known features, an approach similar to that outlined above will be used in the model representation. Obviously, in cases in which the features in question are not known or cannot be characterized well with available data, they will be represented indirectly through adjustment of model parameters in the calibration process.

Sources of Initial Model Hydraulic Parameters

Initial estimates of horizontal and vertical hydraulic conductivity will obtained from existing groundwater flow models. These models include but are not necessarily limited to those of Bush & Johnston (1988), Motz *et al.* (1995), Motz & Dogan (2005), CDM, Inc. (2011), Payne *et al.* (2005), S. A. Williams (2006), Planert, (2007), and Russo (In Progress). Revision of another regional groundwater flow model of the SRWMD by Schneider *et al.* (2008) currently being performed by Intera, Inc., will be included as well, as will the results of a revision of the model of Russo (In Progress), also being performed by Intera, Inc.

In addition to the results of modeling studies, a review of the results of aquifer-performance tests of the Upper Floridan aquifer performed by Kuniansky *et al.* (2012) will be used to provide initial estimates of hydraulic conductivity of the Upper Floridan aquifer.

Calibration Strategies

The steady-state version of the NFSEG regional groundwater flow model will be calibrated initially through a manual, trial-and-error process of minimizing the difference between observed flows and groundwater levels and their simulated equivalents. The manual calibration will be used to help obtain a more detailed conceptualization of the groundwater flow system. The manually calibrated version of the steady-state model will subjected to testing to ensure soundness in the model design and initial calibration. The testing will include a sensitivity analysis. Sensitivity analysis is important because the results indicate the relative degree of influence of various model parameters. Once the process of manual calibration and testing is concluded, the model will be subjected to automated calibration using PEST (Doherty, 2010). PEST is an inverse simulation tool that will enable further refinement of the steady-state calibration and more sophisticated sensitivity analysis.

The steady-state version of the groundwater flow model will be calibrated to dry-year (2001) conditions first followed by calibration to wetter-than-normal conditions in 2009. Both calibrations will be performed manually initially and then with PEST. The results of the dry-year (2001) steady-state simulation will be used as initial conditions in the transient calibration process. Model testing will include simulation to different pumping scenarios, including predictive scenarios or hypothetical scenarios, assuming the availability of projected or hypothetical pumping data.

## Calibration Statistics

The degree of calibration is typically measured by the degree to which various simulated aquifer responses match corresponding observed or estimated values, the primary one being aquifer water levels. Others include spring flows, which are measured directly, and stream baseflows, which are often estimated from observed streamflows (and sometimes from analyses of streamflow and water-quality data) but may be measured directly during low-flow conditions. The differences between observed and corresponding simulated values are called residuals. The objective of the calibration is to minimize the residuals while representing the groundwater flow system in a manner that is generally consistent with known aquifer-system characteristics.

Water-level residuals are determined based on water levels obtained from observation wells. Generally, the number of observation wells in the Upper Floridan aquifer is greater than the number in the SAS and much greater than the number in the Lower Floridan aquifer. This, along with other factors, usually results in a better, more reliable calibration of the layer(s) representing the Upper Floridan aquifer.

Water levels will be calibrated in the both the steady-state and transient calibrations with the following calibration objectives (Sepulveda *et al.*, 2012):

**Table 8. Calibration Goals for Steady-State and Transient Calibration of the NFSEG Regional Groundwater Flow Model (after Sepulveda *et al.*, 2012).**

| Statistical Criterion | Proposed Target Percent |
|---|---|
| -5 feet < Mean Residual < 5 feet | 80% |
| -2.5 feet < Mean Residual < 2.5 feet | 50% |
| Mean Absolute Residual < 5 feet | 80% |
| Mean Absolute Residual < 2.5 feet | 50% |
| Root Mean Square of Errors < 5 feet | 80% |

Water levels in the Floridan aquifer in areas north of the Gulf Trough are on the order of 100 to 300 feet, NAVD88, whereas south of it they tend to be on the order of tens of feet, NAVD88. This means that the absolute residual can be higher in the area north of the Gulf Trough while, relatively speaking (as a percent of aquifer water level), still being within an acceptable range. This suggests the need, potentially at least, to partition the model domain into at least two subregions for purposes of calculating water-level residuals, one being the area more or less north of the Gulf Trough and the other being the area south of the Gulf Trough. This approach will enable relaxation of water-level residual requirements in the area north of the Gulf Trough.

Regarding spring discharges, the objective will be to have the root-mean square of error within 10 percent of the measured flows for spring flows larger than or equal to 10 cubic feet per second (cfs) and within 20 percent for smaller springs (Sepulveda *et al.*, 2012). For baseflows, the objective will be to have the root-mean square of error within 20 percent for all baseflows.

In addition to water levels and flow rates, comparison of calibration-derived hydraulic parameters such as horizontal and vertical hydraulic conductivity to aquifer performance-test (APT) results will be assessed as well. The comparisons, however, will likely be more qualitative than quantitative due to inherent problems of comparing APT-derived values to large-scale representations of aquifer characteristics. Such problems arise from disparities between the actual groundwater flow system and the ideal groundwater flow system for which the equations of APTs are derived.

It should be emphasized that the objectives stated above are goals, not hard-and-fast requirements. The actual calibration process will proceed to an adequate, feasible extent. In some cases, the objectives stated above may not be attainable, because of inadequate data or other peculiar circumstances.

### Possible Revision of the Steady-State Model

The preceding discussion is subject to revision depending on the outcome of the steady-state model calibration and testing processes. This statement applies to all aspects of the model design and conceptualization, including the extent of the proposed model domain, the model-layering scheme, and the grid discretization scheme. Factors that could lead to re-conceptualization include issues of numerical stability and model runtimes.

## NFSEG Transient Groundwater Flow Model Configuration Plan

### Purpose

The primary purpose of the transient calibration is the further refinement of the steady-state calibration results for purposes of improved model predictions, whether steady-state or transient in nature. In effect, the transient calibration is a measure of the model's ability to reproduce observed water levels and flow rates under new and variable hydrologic conditions (i.e., the periods of changing water levels and flow rates represented in the transient calibration). The transient calibration will result in estimates of aquifer storage coefficients, which cannot be determined as a result of steady-state calibration.

### Transient Calibration Period

The period of 2002-2010 will be used as the transient calibration period. Simulated steady-state conditions in 2001 will be used as the initial conditions for the transient simulation period.

### Temporal Discretization of the Transient Model

The transient version of the NFSEG regional groundwater flow model will be calibrated through use of monthly stress periods. Monthly stress periods are reasonable given that commercial/industrial pumping data are usually available only as monthly totals. Agricultural withdrawal rates can probably be estimated for a smaller timeframe, but knowledge of the factors on which such estimates are based probably is not available to a level of precision that merits less than a monthly estimate. The same can be said in regards to recharge estimates. Monthly stress periods are consistent with the regional scope of the model as well.

### Model Configuration and Calibration Strategies

The initial estimates of the aquifer and semiconfining-unit hydraulic parameters in the transient version of the NFSEG groundwater flow model will be the values resulting from the steady-state calibration process. Initial monthly recharge rates in addition to pumping rates will need to be supplied to the model. The initial monthly recharge rates will be obtained from HSPF models. As stated previously in regard to the steady-state annual recharge estimates, the monthly recharge amounts will not be precise and thus will be subject to additional refinement in transient calibration process. Precipitation amounts will also be delineated on a monthly basis. Median monthly base flows and spring discharges will be delineated also to enable comparison to corresponding model-simulated values.

Transient Calibration Objectives

Water-level and flow residuals in the transient calibration will be determined on a monthly basis within the transient calibration period. When the flow and water-level observation data are not available at a daily time step, residuals will be computed as the difference between the monthly median observed values and corresponding simulated monthly values (otherwise monthly mean values will be used). Calibration statistics will be determined for each well based on the complete set of residuals for the well in question. Calibration objectives will be same as those of the steady-state calibration (Table 8).

Transient Lateral Boundary Conditions

The source heads of the GHB conditions used to represent flux across the model southern and eastern lateral boundaries will be updated on a monthly basis. The source heads of the GHBs used to represent the flux from the FAS into the Gulf of Mexico along the Gulf coast will be held constant with time, as they will be used to represent mean sea level. Similarly, the offshore area of the Atlantic Ocean in model layer 1 will be represented with constant equivalent fresh-water heads. The aquifer water levels assigned to aquifer layer 5 (Pearl River Aquifer) along the northern lateral boundary will be updated monthly. All other lateral boundary conditions will be no-flow boundary conditions, so there will be no need to update water levels in those cases. They will remain unchanged for all transient time steps.

PEST Calibration and Uncertainty Analysis

Initial calibration of the transient model will be performed manually. The inverse calibration tool PEST (Doherty, 2010) will be used to refine and complete the calibration process. PEST will be used as well to perform a detailed sensitivity analysis. If predictive simulations are performed as part of the model-development process, then PEST will be used to perform a detailed uncertainty analysis.

## EXPECTED MODEL CAPABILITIES AND LIMITATIONS

As stated previously, the NFSEG groundwater flow model will be regional in nature. Thus, the primary function of the model will be the reasonable representation of pumping-induced drawdown across relatively large distances, e.g., the effects of pumping in southeast Georgia on locations within the SRWMD or vice versa, as well as changes in flows from regional stresses. In order to fulfill this objective reliably, the model should be calibrated and configured in a manner that is consistent with generally accepted standards. The model will provide a framework for the development of sub-regional groundwater flow models of areas of critical concern, as identified in the NFSEG charter. The model will be used to import regional-scale drawdowns to the lateral boundaries of the subregional groundwater flow models as well. Therefore, the quality of the model calibration within and in the vicinity of the SRWMD and SJRMWD portions of the model domain will be high, given data limitations, particularly within the areas of critical concern. The Georgia portion of the model will be calibrated to the highest possible degree, as well. But calibration quality in the Georgia portions of the model domain may be limited by the additional restrictions on data availability of that area, particularly water-use data.

The regional nature of the model will result in limitations. The ability of the model estimate drawdown will be limited by the model grid-cell size. Obviously, drawdowns over areas completely contained in one or a few grid cells will be limited due to the averaging effect that occurs over such small areas. Also, the model will be limited in its ability to assess the interaction of groundwater and surface-water processes. Sub-regional or local-scale models are more appropriate for such assessments. Finally, the primary objective of the model will be to to simulate groundwater flow and levels within the Upper Floridan aquifer of the FAS and groundwater discharge from the Upper Floridan aquifer to streams that intersect this aquifer. Representation of groundwater flows and levels in the SAS is more difficult due to a relative lack of data for representation of the SAS. Therefore, the simulations determined by the model for the FAS will be superior to those determined for the SAS.

## BIBLIOGRAPHY

Barker, R. A. & Pernik, M. (1994) Regional Hydrology and Simulation of Deep Ground-Water Flow in the Southeastern Coastal Plain Aquifer System in Mississippi, Alabama, Georgia, and South Carolina (U.S. Geological Survey Professional Paper No. 1410-C). U.S. Geological Survey. Retrieved from http://pubs.er.usgs.gov/publication/pp1410C

Bartel, R. L., Macmillan, T. L. & Ard, F. B. (1992) Lake Jackson Regional Stormwater Retrofit Plan (Northwest Florida Water Management District Water Resources Special Report No. 9201). Northwest Florida Water Management District. Retrieved from http://www.nwfwmd.state.fl.us/pubs/lakejackson/Lake%20Jackson%20Regional%20Stormwater%20Retrofit%20Plan%20WRSP%2092-1-Final.pdf

Bicknell, B. R., Imhoff, J. C., Kittle, J. L., Donigian, A. S., Jr. & Johanson, R. C. (1997) Hydrological Simulation Program--FORTRAN: User's manual for version 11 ( No. EPA/600/R-97/080), 755. Athens, GA: U.S. Environmental Protection Agency. Retrieved from http://hspf.com/pub/hspf/HSPF12.2Manual.zip

Bush, P. W. & Johnston, R. H. (1988) Ground-water hydraulics, regional flow, and ground-water development of the Floridan aquifer system in Florida and in parts of Georgia, South Carolina, and Alabama (U.S. Geological Survey Professional Paper No. 1403-C). U.S. Geological Survey. Retrieved from http://pubs.er.usgs.gov/publication/pp1403C

CDM, Inc. (2011) Groundwater Flow Modeling of the Coastal Plain Aquifer System of Georgia; Georgia State-Wide Groundwater Resources Assessment (Report by CDM, Inc., to Environmental Protection Division, Georgia Department of Natural Resources). CDM, Inc.

Countryman, R. A. & Stewart, M. A. (1997) Geophysical delineation of the position of the saltwater interface in the Lower Suwannee River Basin: Final contract report for Suwannee River Water Management District and U.S. Geological Survey (Contract Report), 538.

Doherty, J. (2010) PEST, Model-independent parameter estimation--User Manual, 5th Edition with Minor Revisions. Watermark Numerical Computing.

Harbaugh, A. W. (2005) MODFLOW-2005 : the U.S. Geological Survey modular ground-water model--the ground-water flow process (U.S. Geological Survey Techniques and Methods No. 6-A16). U.S. Geological Survey. Retrieved from http://pubs.usgs.gov/tm/2005/tm6A16/

Kimrey, J. O. & Fayard, L. D. (1984) Geohydrologic reconnaissance of drainage wells in Florida (U.S. Geological Survey Water-Resources Investigations

Report No. 84-4021). U.S. Geological Survey. Retrieved from http://pubs.usgs.gov/wri/1984/4021/report.pdf

Kinnaman, S. L. & Dixon, J. F. (2011) Potentiometric Surface of the Upper Floridan Aquifer in Florida and parts of Georgia, South Carolina, and Alabama, May-June 2010. U.S. Geological Survey Scientific Investigations Map 3182, U.S. Geological Survey.

Krause, R. E. & Randolph, R. B. (1989) Hydrology of the Floridan Aquifer System in Southeast Georgia and Adjacent Parts of Florida and South Carolina (U.S. Geological Survey Professional Paper No. 1403-D). U.S. Geological Survey. Retrieved from http://pubs.er.usgs.gov/publication/pp1403D

Kuniansky, E., Bellino, J. C. & Dixon, J. F. (2012) Transmissivity of the Upper Floridan aquifer in Florida and parts of Georgia, South Carolina, and Alabama. U.S. Geological Survey Scientific Investigations Map 3204, U.S. Geological Survey. Retrieved from http://pubs.usgs.gov/sim/3204/

Miller, J. A. (1986) Hydrogeologic Framework of the Floridan Aquifer System in Florida and in Parts of Georgia, South Carolina, and Alabama (U.S. Geological Survey Professional Paper No. 1403-B). U.S. Geological Survey. Retrieved from http://pubs.er.usgs.gov/publication/pp1403B

Motz, L. H., Beddow, W. D., II, Caprara, M. R., Gay, J. D. & Sheaffer, S. M. (1995) North-Central Florida Regional Ground-Water Investigation and Flow Model (Final Report) (St. Johns River Water Management District Special Publication). SJ95-SP7. St. Johns River Water Management District. Retrieved from http://www.sjrwmd.com/technicalreports/pdfs/SP/SJ95-SP7.pdf

Motz, L. H. & Dogan, A. (2005) North-Central Florida Active Water-Table Regional Groundwater Flow Model (St. Johns River Water Management District Special Publication No. SJ2005-SP16). Palatka, Florida: St. Johns River Water Management District. Retrieved from http://floridaswater.com/technicalreports/pdfs/SP/SJ2005-SP16.pdf

Motz, L. H., Spangler, D. P., Strazimiri, D. L. & Moffor, G. (1998) An Impact Analysis of the Ground Water and Geological Effects of Potential Control of The Sinkhole Discharge at Heagy-Burry Park, Orange Lake, Florida (St. Johns River Water Management District Special Publication No. SJ98-SP3).

Palatka, Florida: St. Johns River Water Management District. Retrieved from http://floridaswater.com/technicalreports/pdfs/SP/SJ98-SP3.pdf

Payne, D. F., Rumman, M. A. & Clarke, J. S. (2005) Simulation of Ground-Water Flow in Coastal Georgia and Adjacent Parts of South Carolina and Florida-Predevelopment, 1980, and 2000 (U.S. Geological Survey Scientific Investigations Report No. 2005-5089). U.S. Geological Survey. Retrieved from http://pubs.water.usgs.gov/sir2005-5089/

Phelps, G. G. (1987) Effects of surface runoff and treated wastewater recharge on quality of water in the Floridan aquifer system, Gainesville Area, Alachua County, Florida (U.S. Geological Survey Water-Resources Investigations Report No. 87-4099). U.S. Geological Survey. Retrieved from http://pubs.usgs.gov/wri/1987/4099/report.pdf

Planert, M. (2007) Simulation of Regional Ground-Water Flow in the Suwannee River Basin, Northern Florida and Southern Georgia (U.S. Geological Survey Scientific Investigations Report No. 2007-5031). U.S. Geological Survey. Retrieved from http://pubs.usgs.gov/sir/2007/5031/

Russo, V. (In Progress) Northeast Florida Groundwater Flow Model – Version 3. St. Johns River Water Management District.

Schneider, J. W., Ph.D., Upchurch, S. B., Ph.D., P.G., Chen, J., P.G. & Cain, C. (2008) Simulation of Groundwater Flow in North Florida and South-Central Georgia. SDII, Inc.

Sepulveda, N., Tiedeman, C. R., O'Reilly, A. M., Davis, J. B. & Burger, P. (2012) Groundwater Flow and Water Budget in the Surficial and Floridan Aquifer Systems in East-Central Florida (U.S. Geological Survey Scientific Investigations Report No. 2012-5161). U.S. Geological Survey. Retrieved from http://pubs.usgs.gov/sir/2012/5161/pdf/2012-5161.pdf

Shah, N., Nachabe, M. & Ross, M. (2007) Extinction Depth and Evapotranspiration from Ground Water under Selected Land Covers. *Ground Water* **45**(3), 329–338.

Williams, L., Davis, J. & Boniol, D. (In Progress) Hydrogeologic Horizons of the Floridan Aquifer System. St. Johns River Water Management District.

Williams, S. A. (2006) Simulation of the Effects of Groundwater Withdrawals from the Floridan Aquifer System in Volusia County and Vicinity (St. Johns River Water Management District Technical Publication No. SJ2006-4). St. Johns River Water Management District. Retrieved from http://www.sjrwmd.com/technicalreports/pdfs/TP/SJ2006-4.pdf

# APPENDIX A: HYDROGRAPHS USED IN ANALYSIS OF WATER LEVELS

## Well Hydrographs Included in Cluster and Principal-Component Analyses

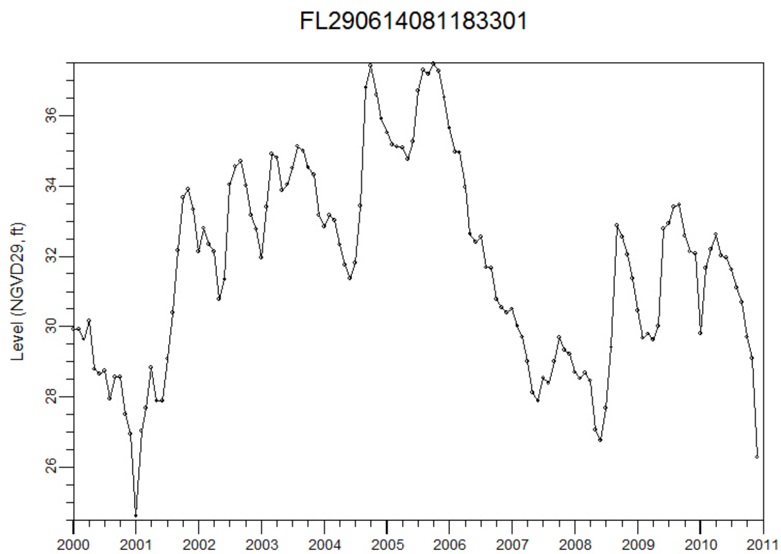


**Figure 25. Hydrograph of Well FL290614081183301 (Site 1; Cluster 1).**

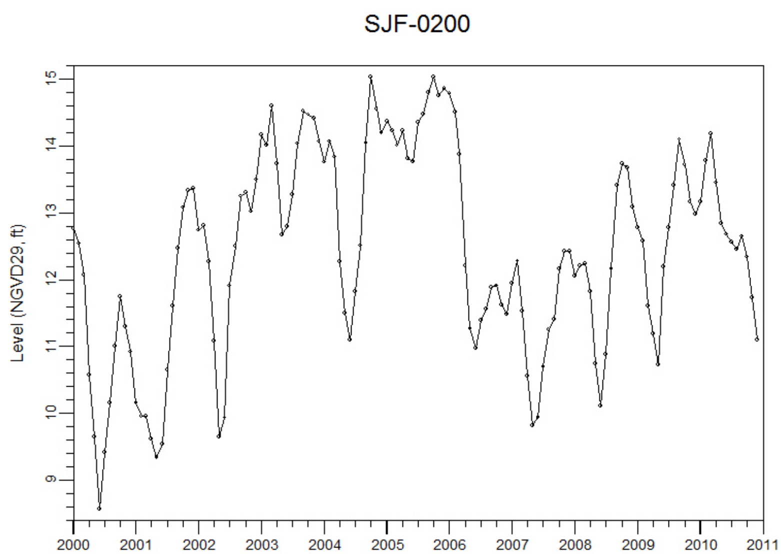


**Figure 26. Hydrograph of Well SJF-0200 (Site 2; Cluster 1).**

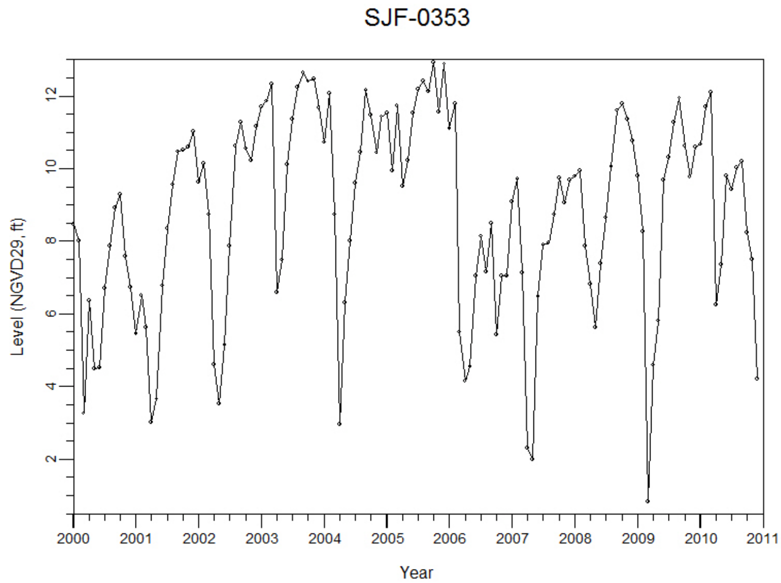


**Figure 27. Hydrograph of Well SJF-0353 (Site 3; Cluster 1).**

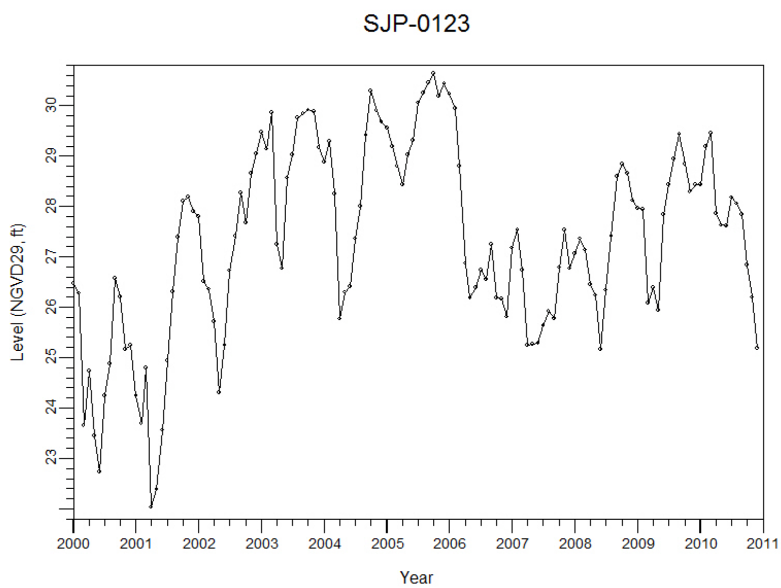


**Figure 28. Hydrograph of Well SJP-0123 (Site 4; Cluster 1).**

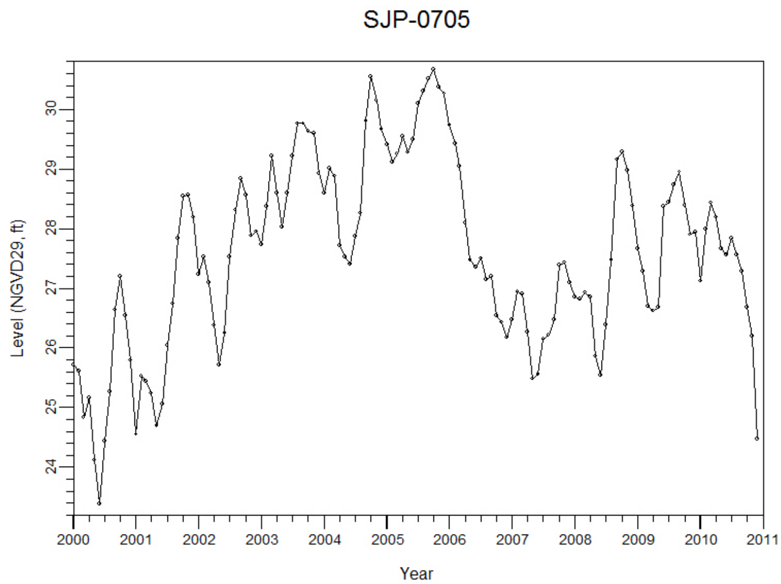


**Figure 29. Hydrograph of Well SJP-0705 (Site 5; Cluster 1).**

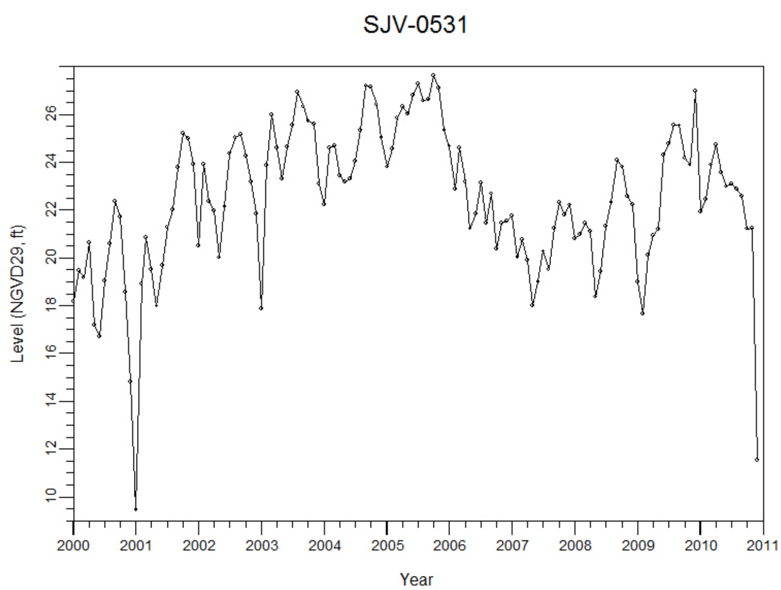


**Figure 30. Hydrograph of Well SJV-0531 (Site 6; Cluster 1).**

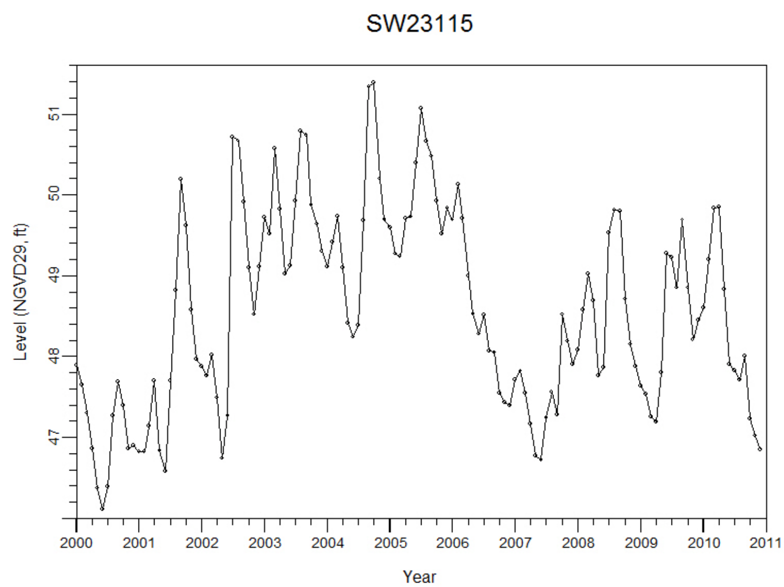


**Figure 31. Hydrograph of Well SW23115 (Site 7; Cluster 1).**

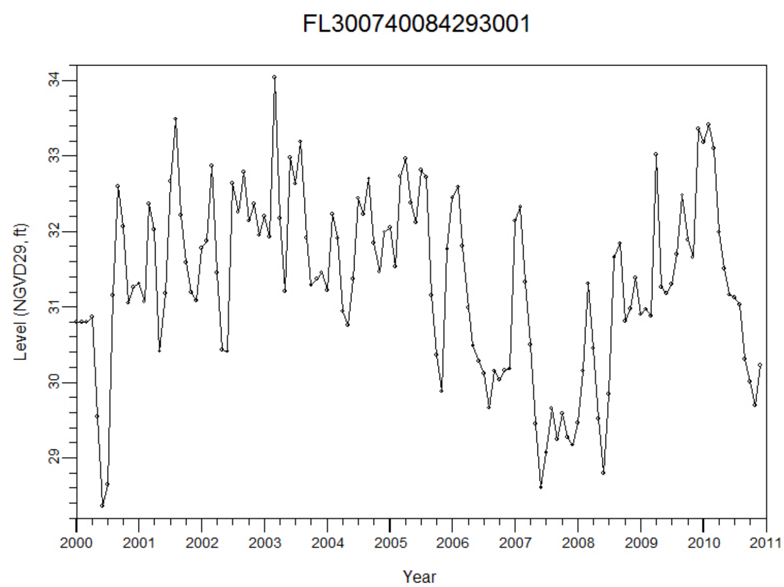


**Figure 32. Hydrograph of Well FL300740084293001 (Site 8; Cluster 2).**

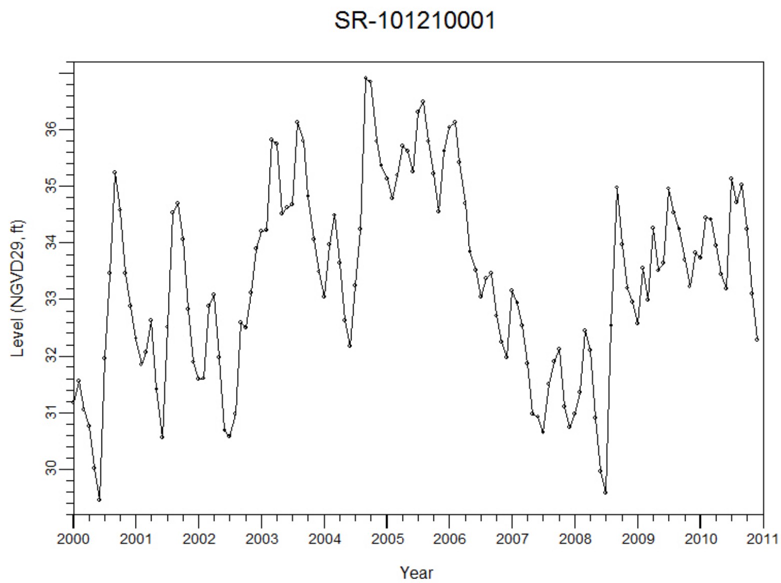


**Figure 33. Hydrograph of Well SR-101210001(Site 9; Cluster 2).**

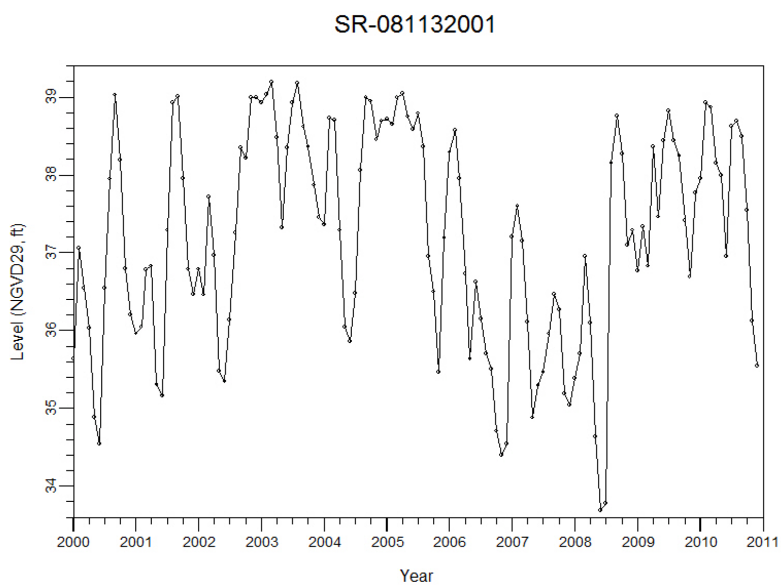


**Figure 34. Hydrograph of Well SR-081132001 (Site 10; Cluster 2).**

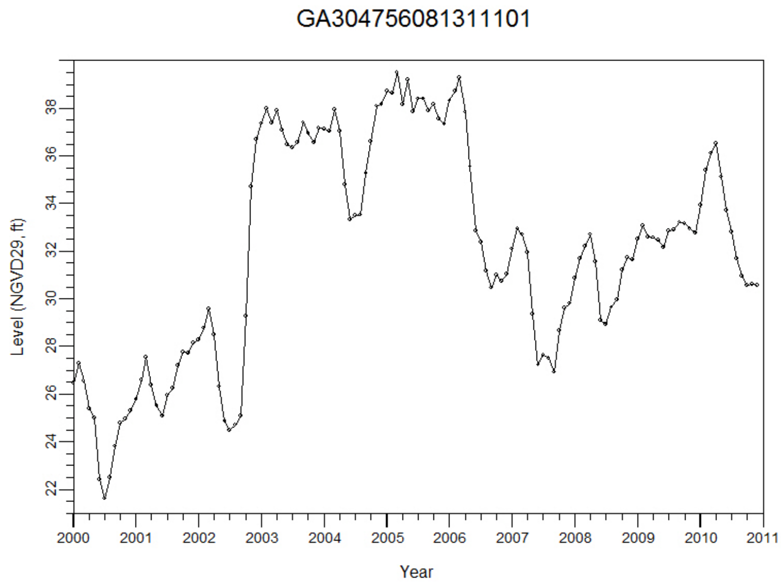


**Figure 35. Hydrograph of Well GA304756081311101 (Site 11; Cluster 3).**

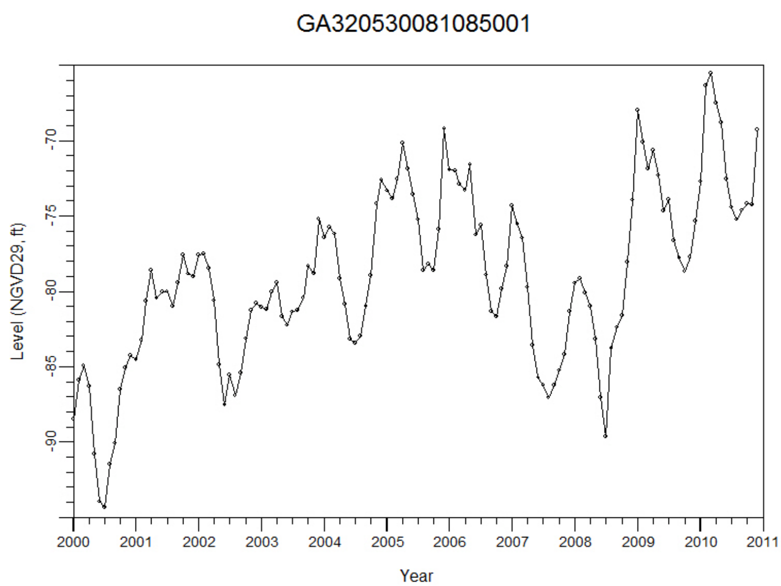


**Figure 36. Hydrograph of Well GA320530081085001 (Site 12; Cluster 3).**

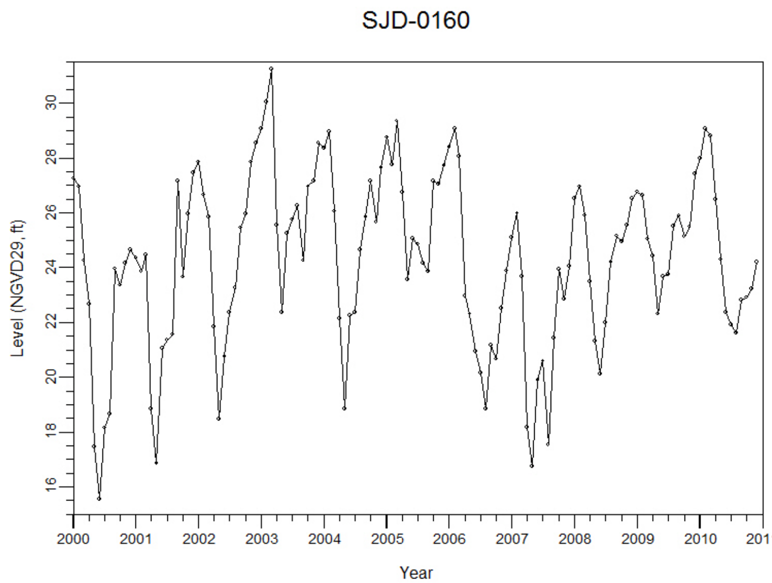


**Figure 37. Hydrograph of Well SJD-0160 (Site 13; Cluster 3).**

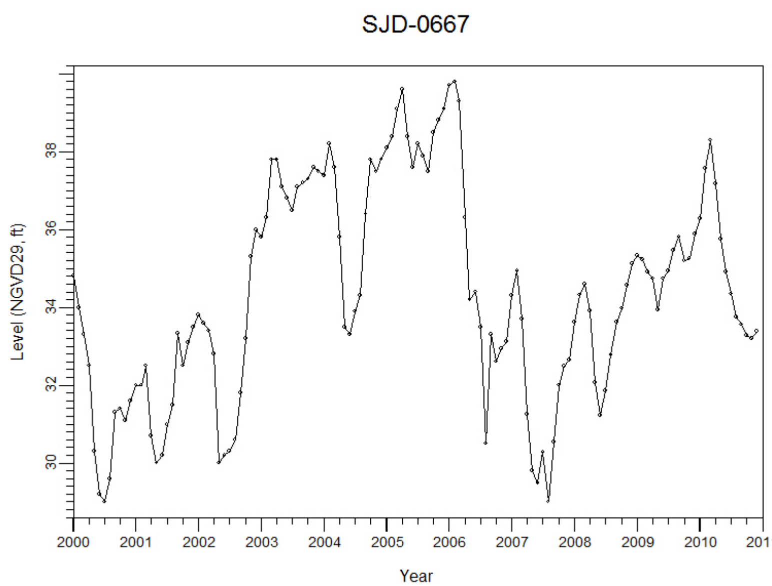


**Figure 38. Hydrograph of Well SJD-0667 (Site 14; Cluster 3).**

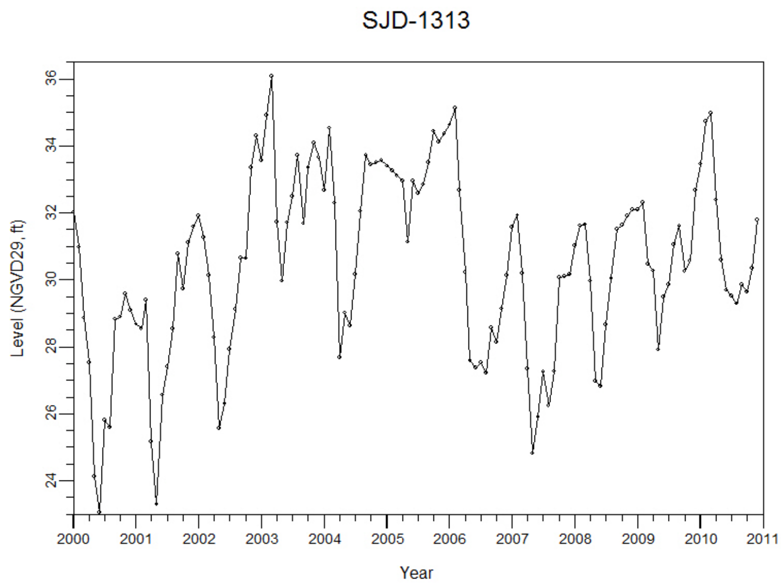


**Figure 39. Hydrograph of Well SJD-1313 (Site 15; Cluster 3).**

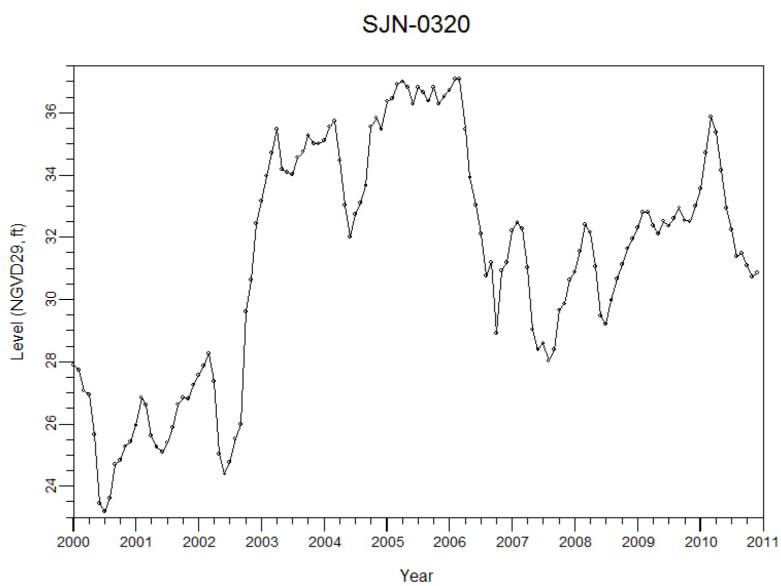


**Figure 40. Hydrograph of Well SJN-0320 (Site 16; Cluster 3).**

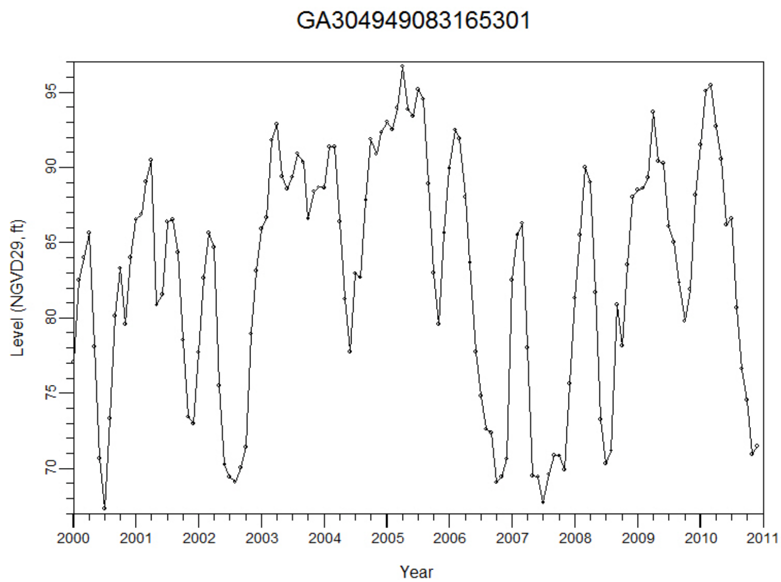


**Figure 41. Hydrograph of Well GA304949083165301 (Site 17; Cluster 4).**

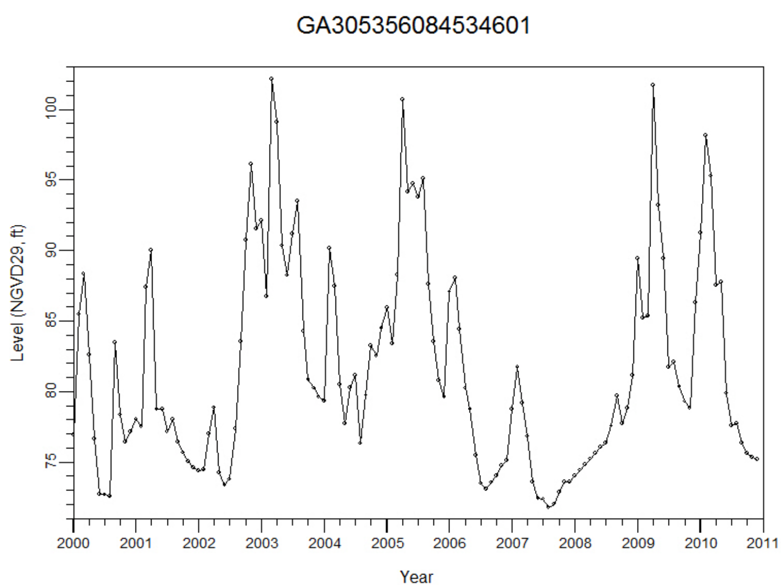


**Figure 42. Hydrograph of Well GA305356084534601 (Site 18; Cluster 4).**

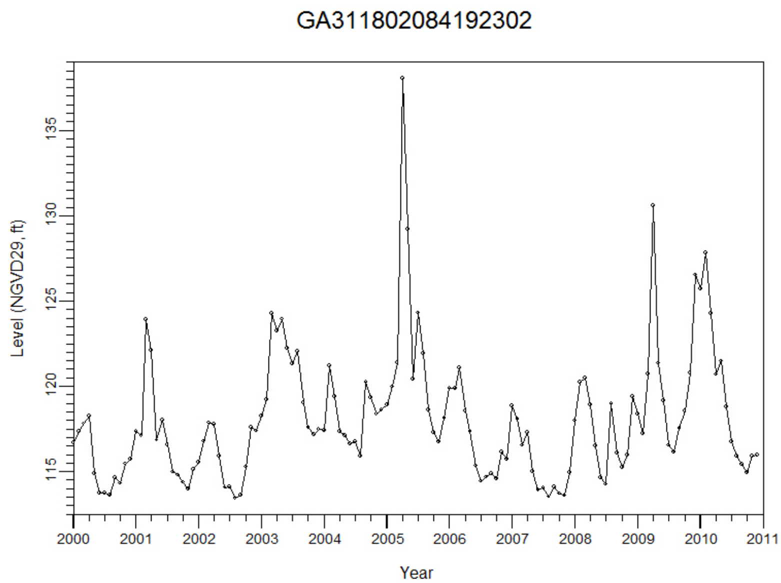


**Figure 43. Hydrograph of Well GA311802084192302 (Site 19; Cluster 4).**

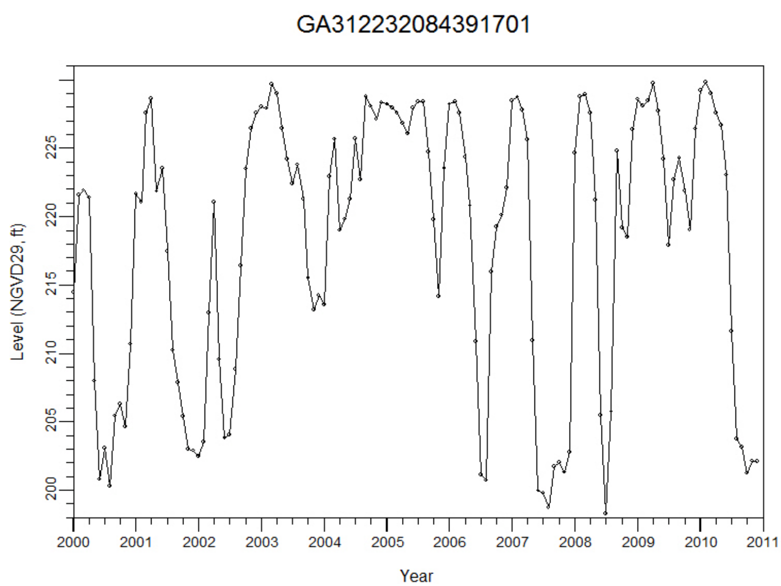


**Figure 44. Hydrograph of Well GA312232084391701 (Site 20; Cluster 4).**

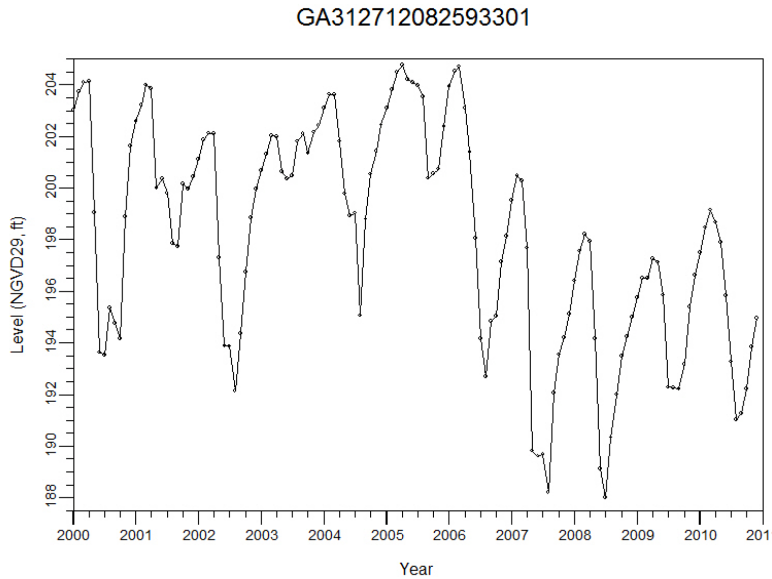


**Figure 45. Hydrograph of Well GA312712082593301 (Site 21; Cluster 4).**

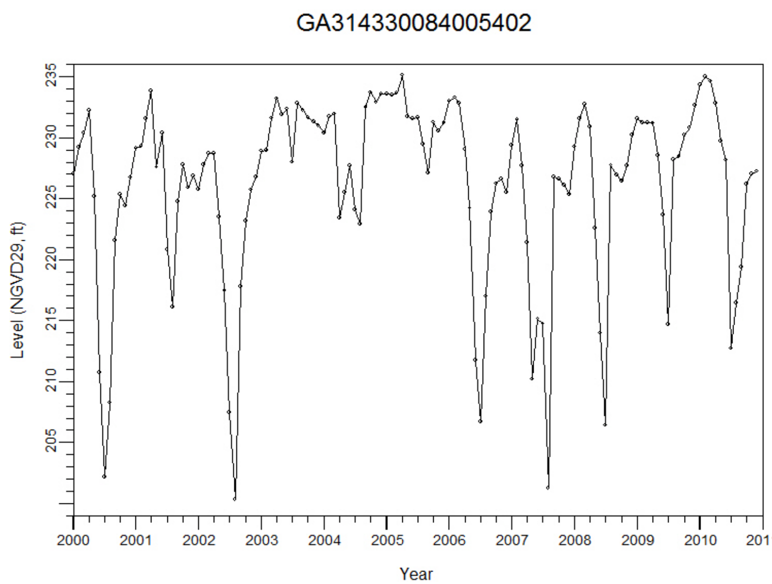


**Figure 46. Hydrograph of Well GA314330084005402 (Site 22; Cluster 4).**

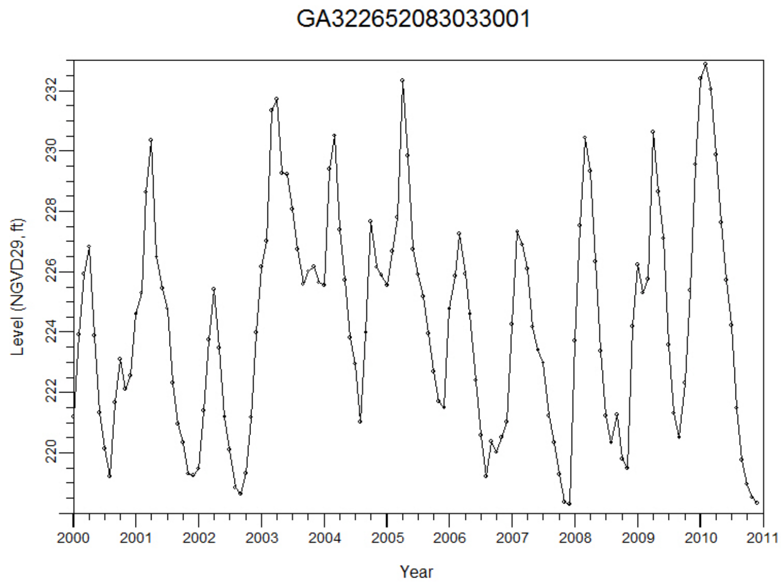


**Figure 47. Hydrograph of Well GA322652083033001 (Site 23; Cluster 4).**

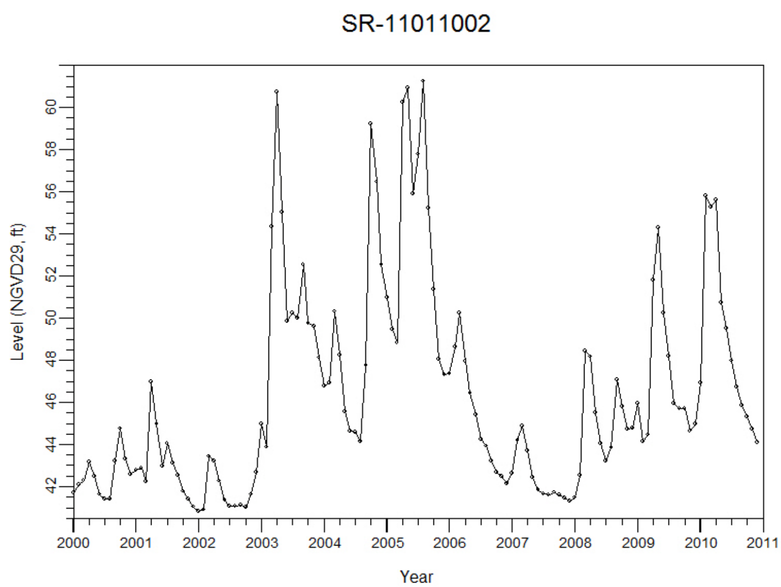


**Figure 48. Hydrograph of Well SR-011011002 (Site 24; Cluster 5).**

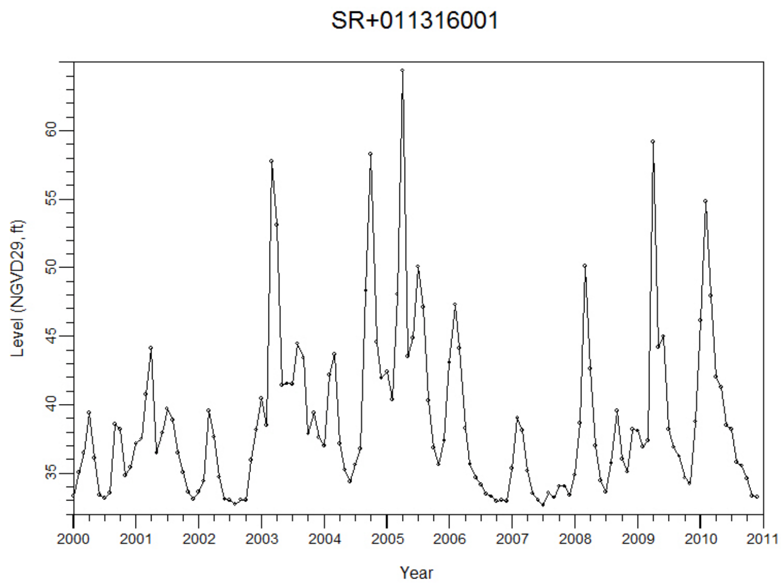


**Figure 49. Hydrograph of Well SR+011316001 (Site 25; Cluster 5)**

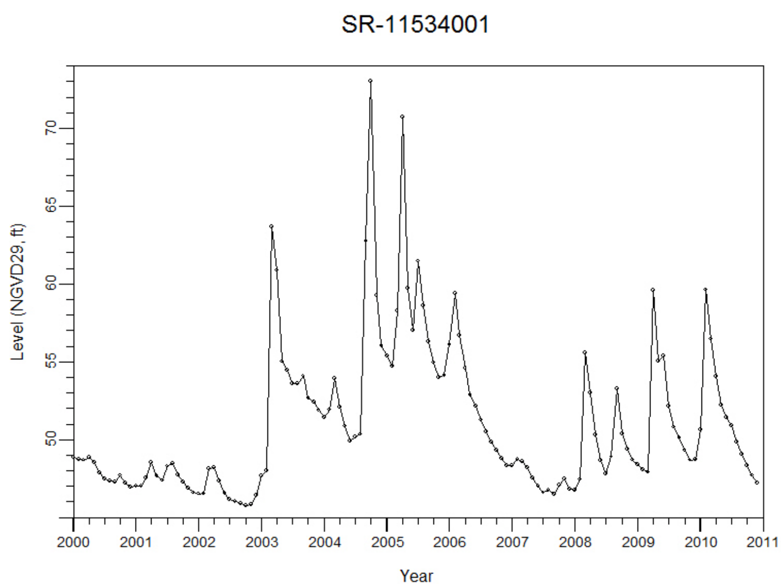


**Figure 50. Hydrograph of Well SR-011534001( Site 26; Cluster 5).**

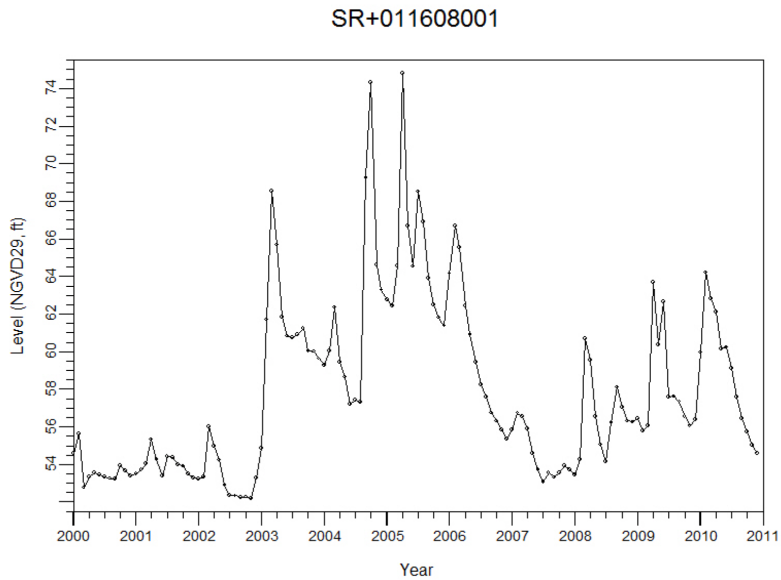


**Figure 51. Hydrograph of Well SR+011608001 (Site 27; Cluster 5).**

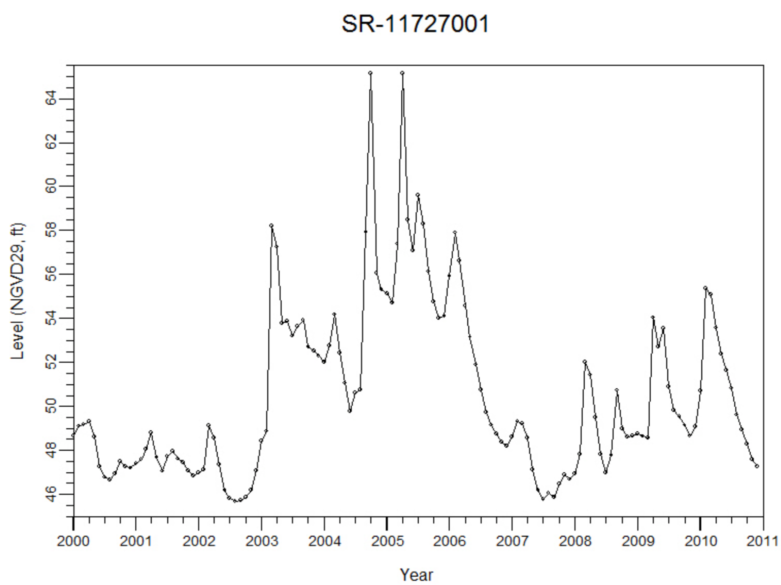


**Figure 52. Hydrograph of Well SR-011727001 (Site 28; Cluster 5).**

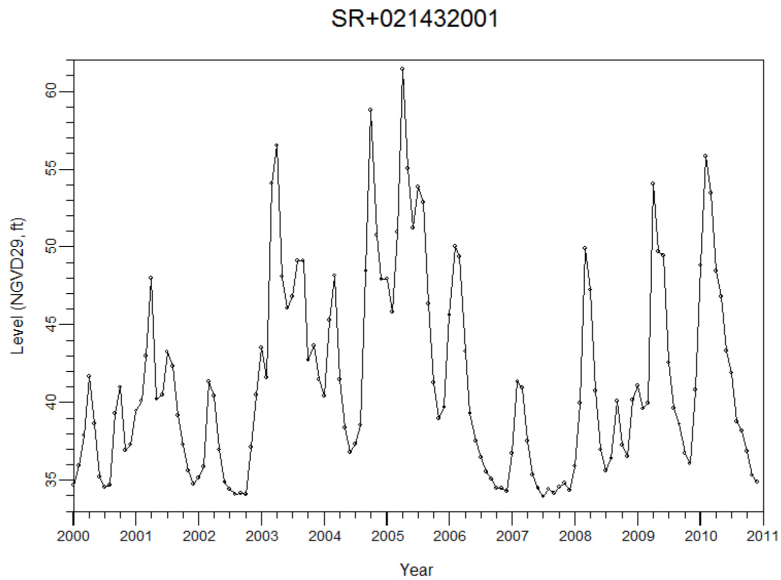


**Figure 53. Hydrograph of Well SR+021432001 (Site 29; Cluster 5).**

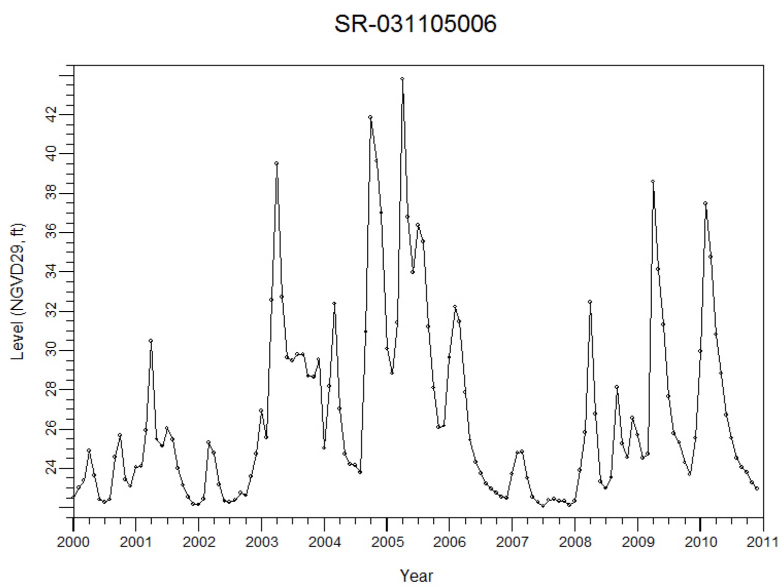


**Figure 54. Hydrograph of Well SR-031105006 (Site 30; Cluster 5).**

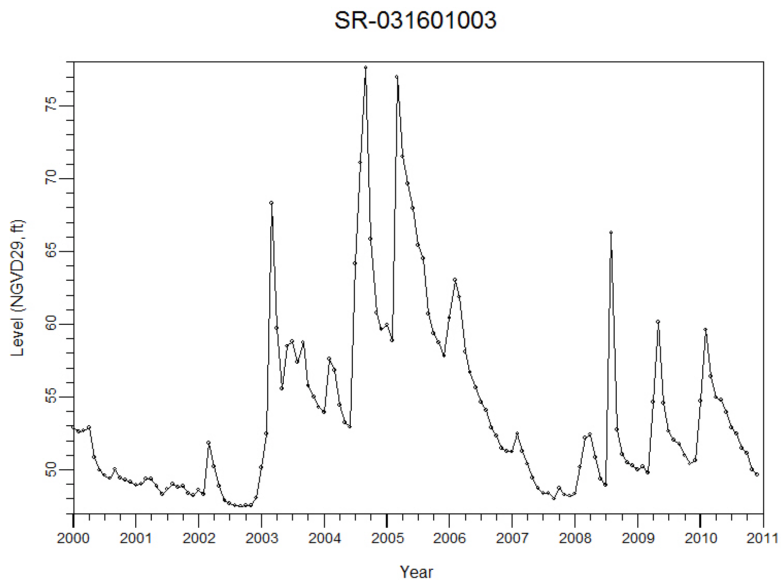


**Figure 55. Hydrograph of Well SR-031601003 (Site 31; Cluster 5).**

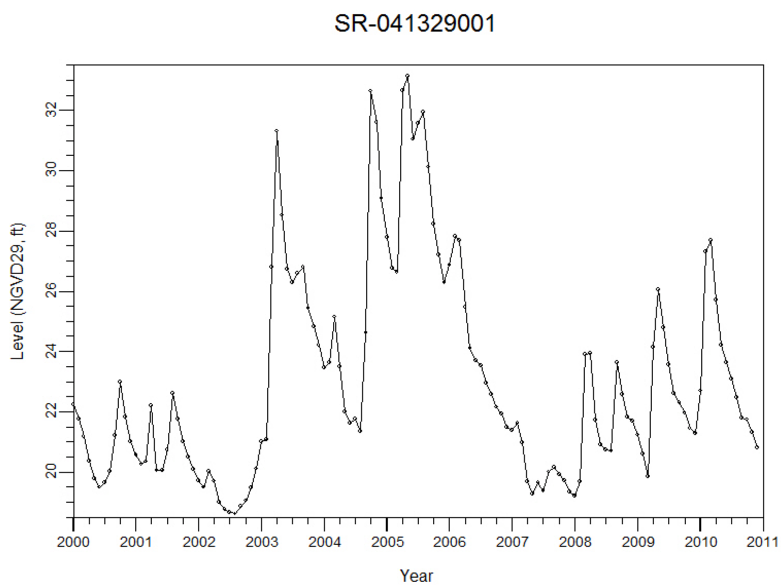


**Figure 56. Hydrograph of Well SR-041329001 (Site 32; Cluster 5).**

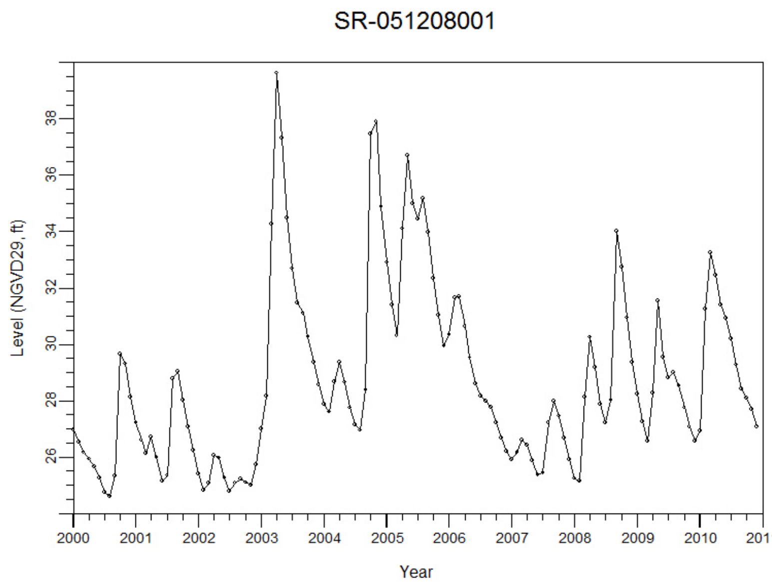


**Figure 57. Hydrograph of Well SR-051208001 (Site 33; Cluster 5).**

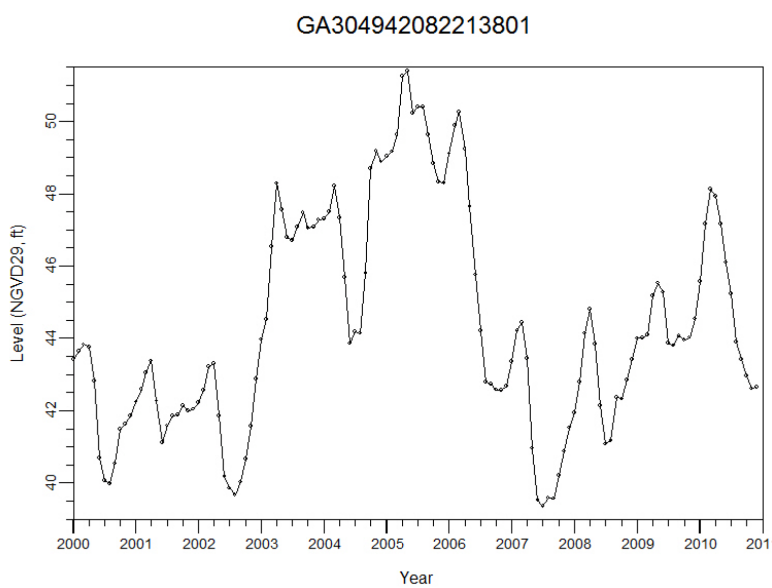


**Figure 58. Hydrograph of Well GA304942082213801 (Site 34; Cluster 6).**

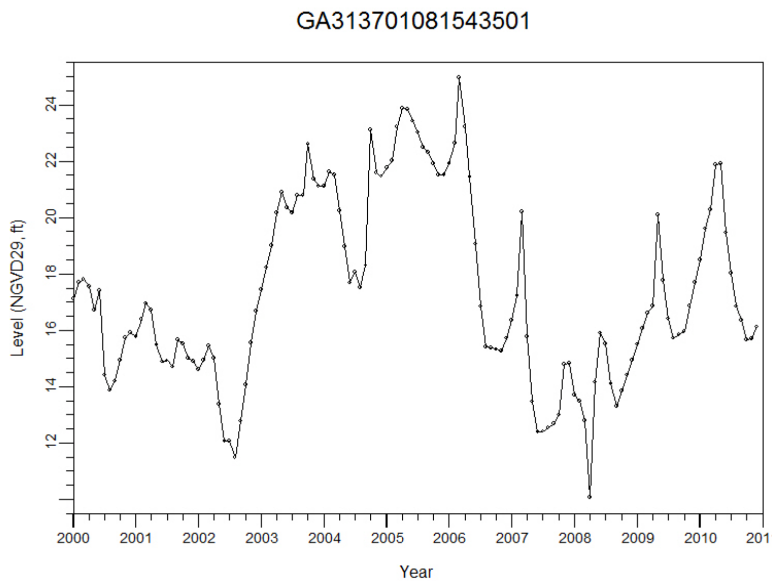


**Figure 59. Hydrograph of Well GA313701081543501 (Site 35; Cluster 6).**

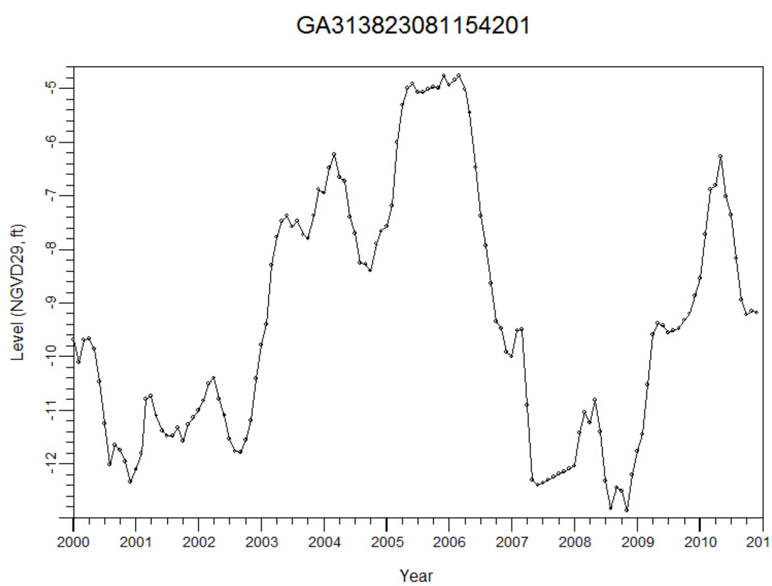


**Figure 60. Hydrograph of Well GA313823081154201 (Site 36; Cluster 6).**

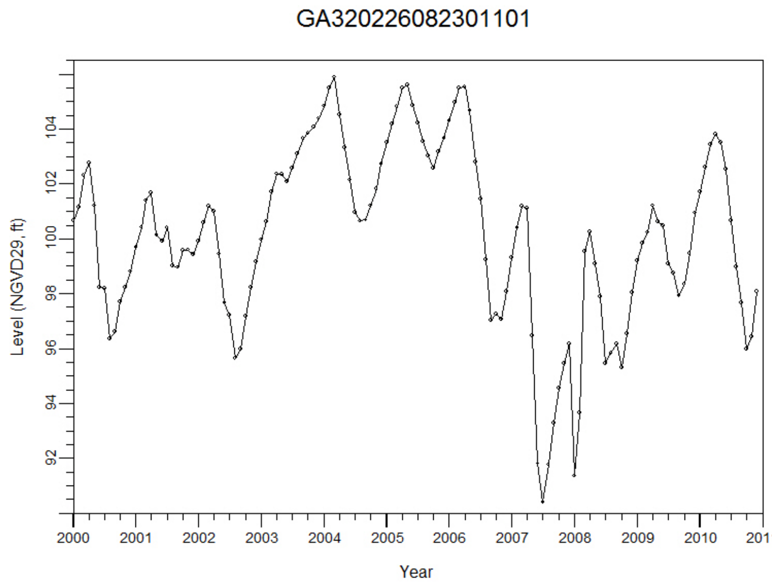


**Figure 61. Hydrograph of Well GA320226082301101 (Site 37; Cluster 6).**

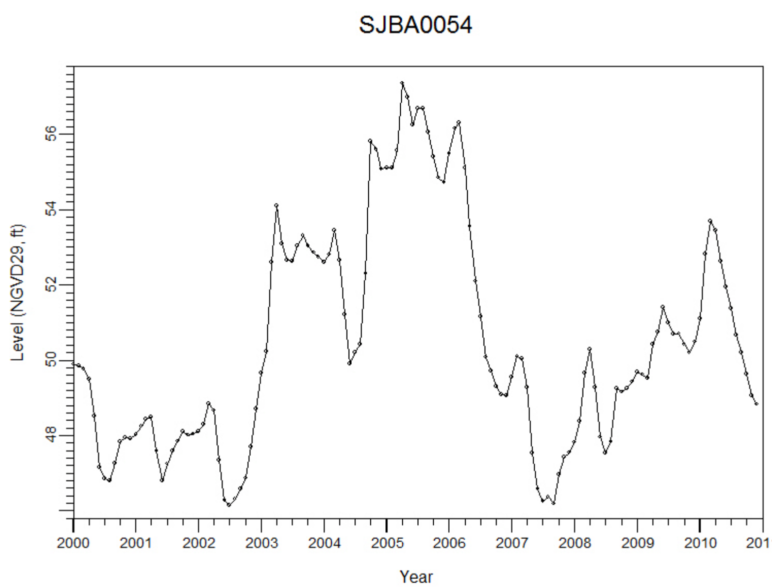


**Figure 62. Hydrograph of Well SJBA0054 (Site 38; Cluster 6).**

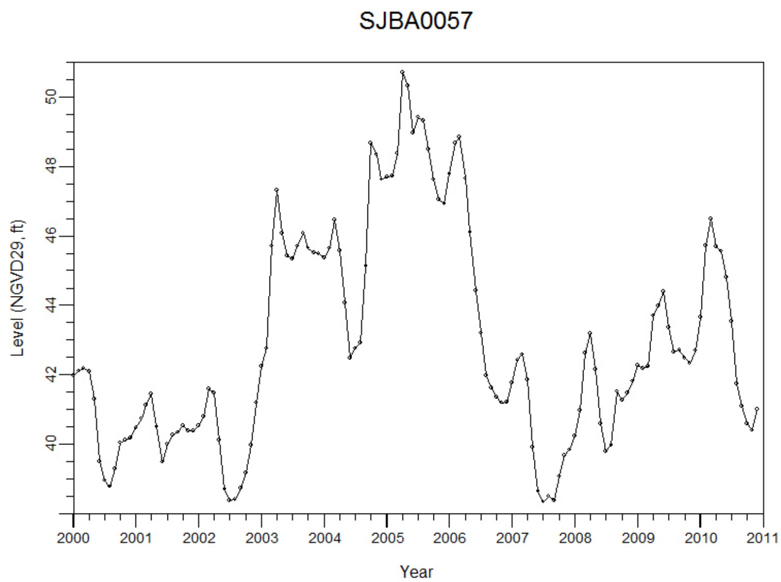


**Figure 63. Hydrograph of Well SJBA0057 (Site 39; Cluster 6).**

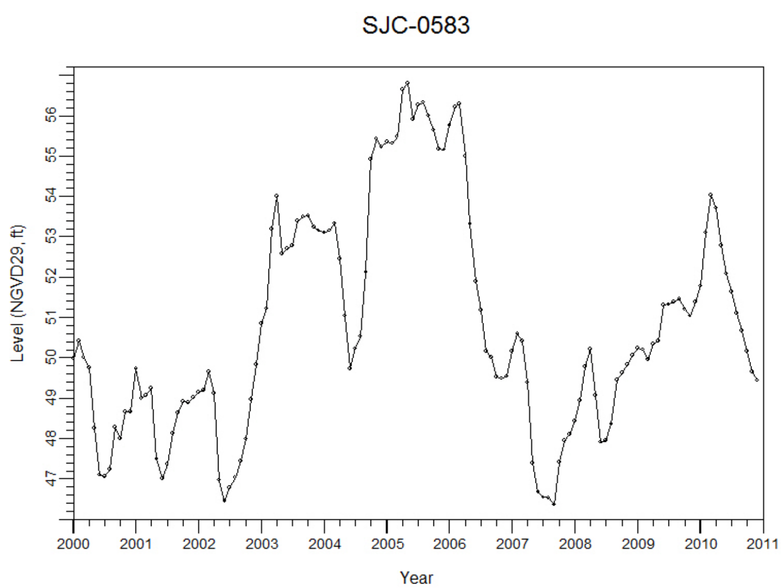


**Figure 64. Hydrograph of Well SJC-0583 (Site 40; Cluster 6).**

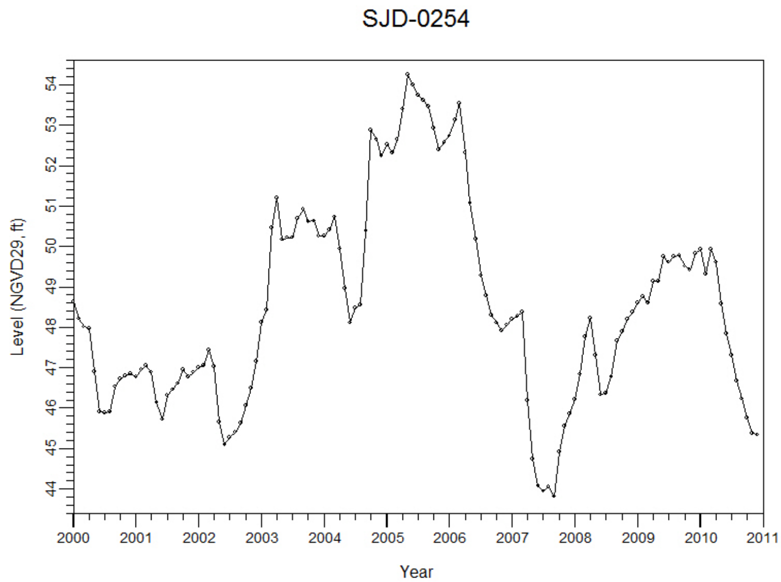


**Figure 65. Hydrograph of Well SJD-0254 (Site 41; Cluster 6).**

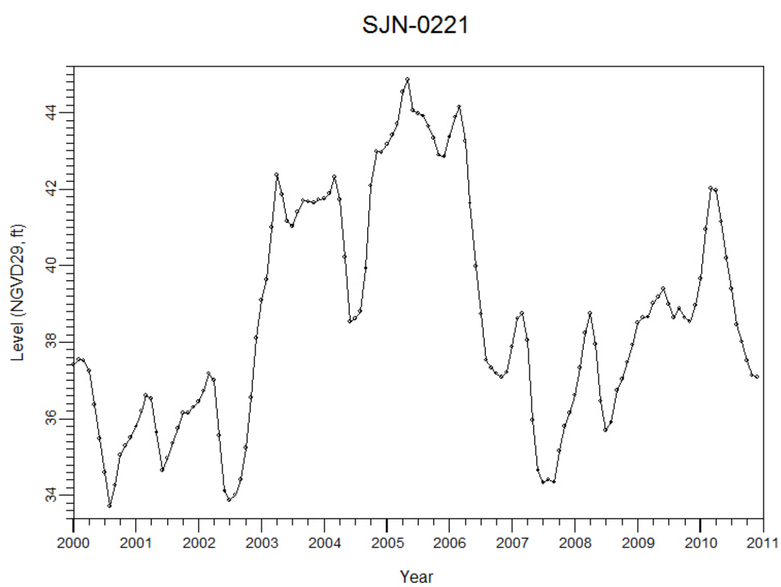


**Figure 66. Hydrograph of Well SJN-0221 (Site 42; Cluster 6).**

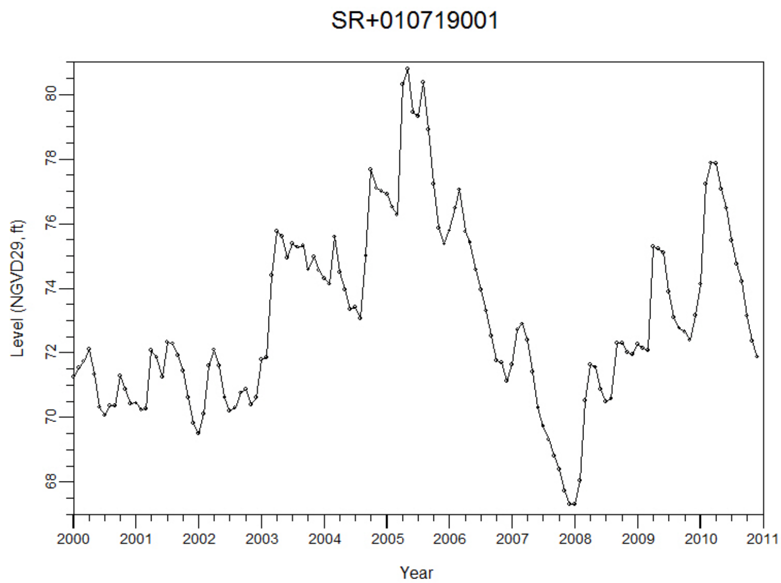


**Figure 67. Hydrograph of Well SR+010719001 (Site 43; Cluster 6).**

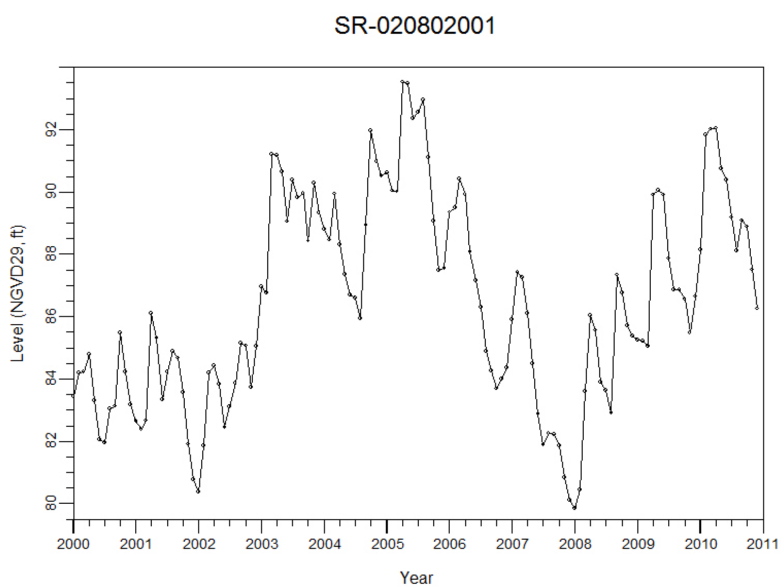


**Figure 68. Hydrograph of Well SR-020802001 (Site 44; Cluster 6).**

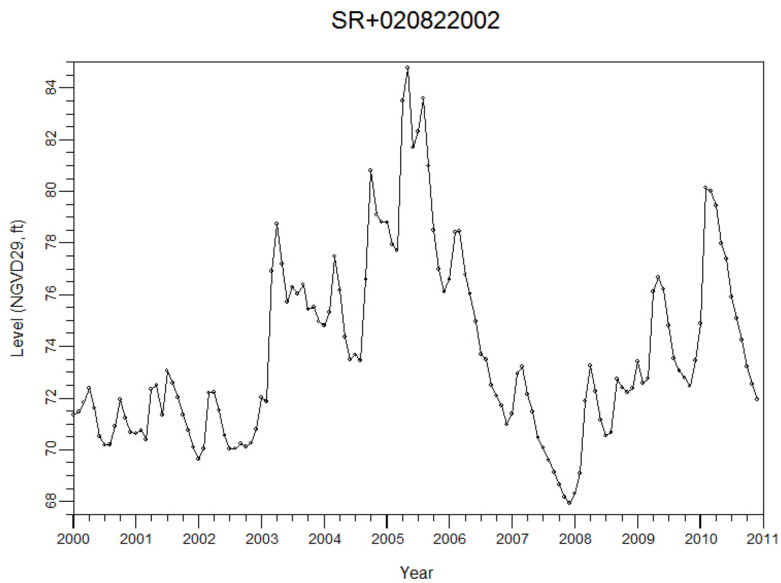


**Figure 69. Hydrograph of Well SR+020822002 (Site 45; Cluster 6).**

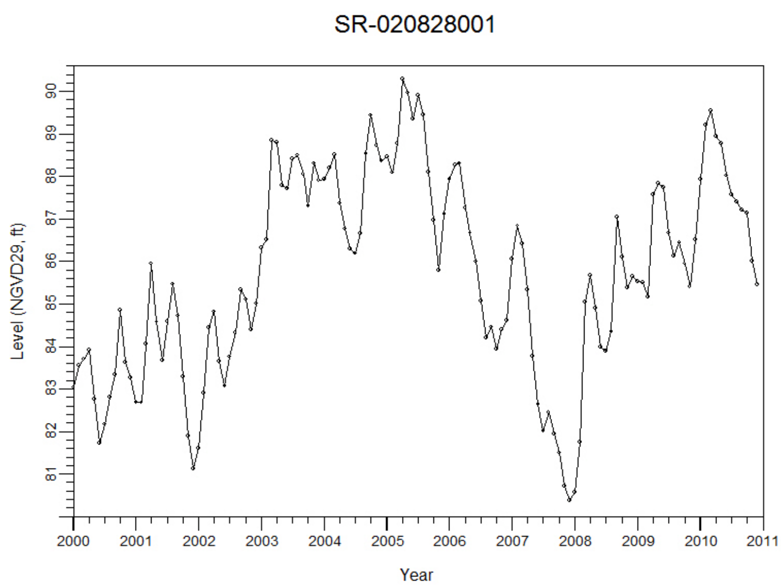


**Figure 70. Hydrograph of Well SR-020828001 (Site 46; Cluster 6).**

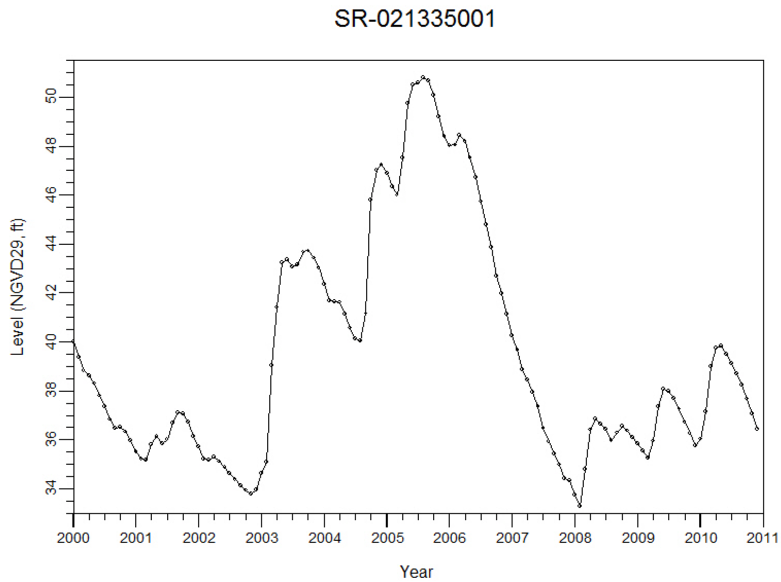


**Figure 71. Hydrograph of Well SR-021335001 (Site 47; Cluster 6).**

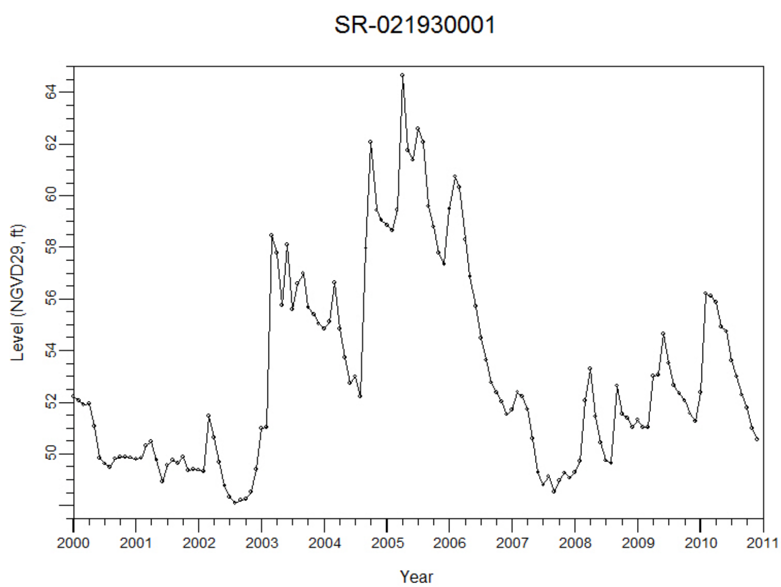


**Figure 72. Hydrograph of Well SR-021930001 (Site 48; Cluster 6)**

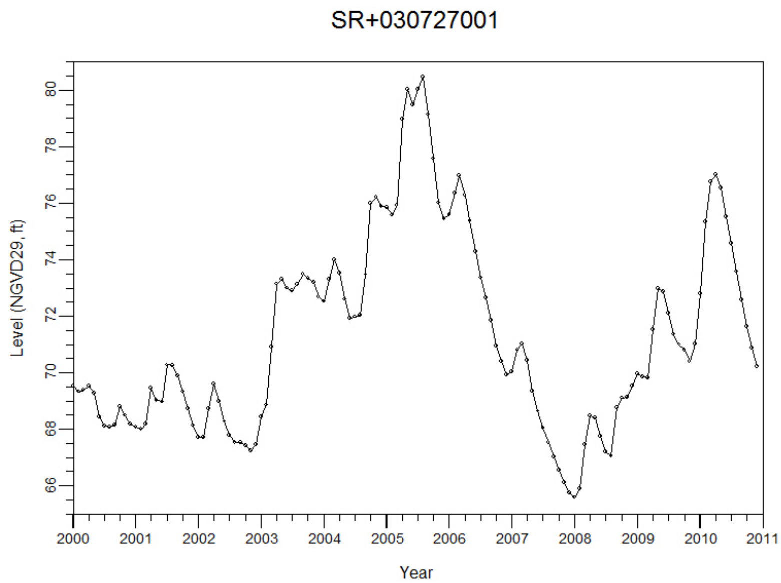


**Figure 73. Hydrograph of Well SR+030727001 (Site 49; Cluster 6).**

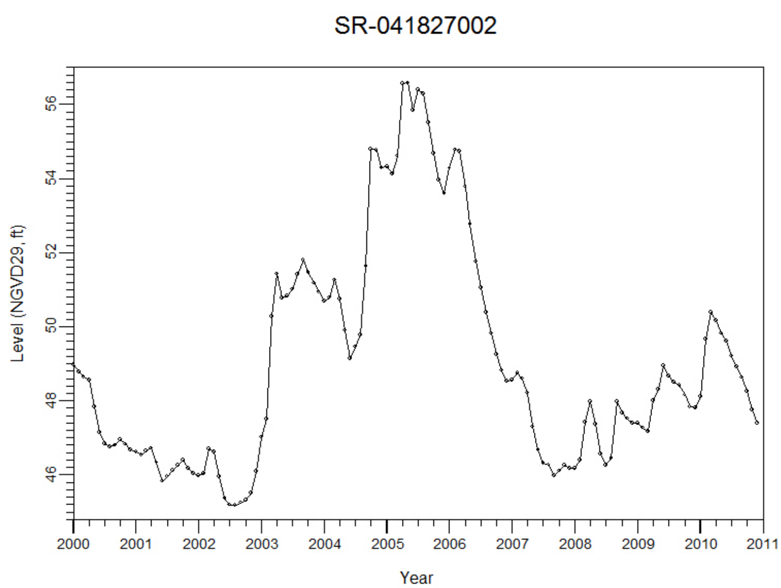


**Figure 74. Hydrograph of Well SR-041827002 (Site 50; Cluster 6).**

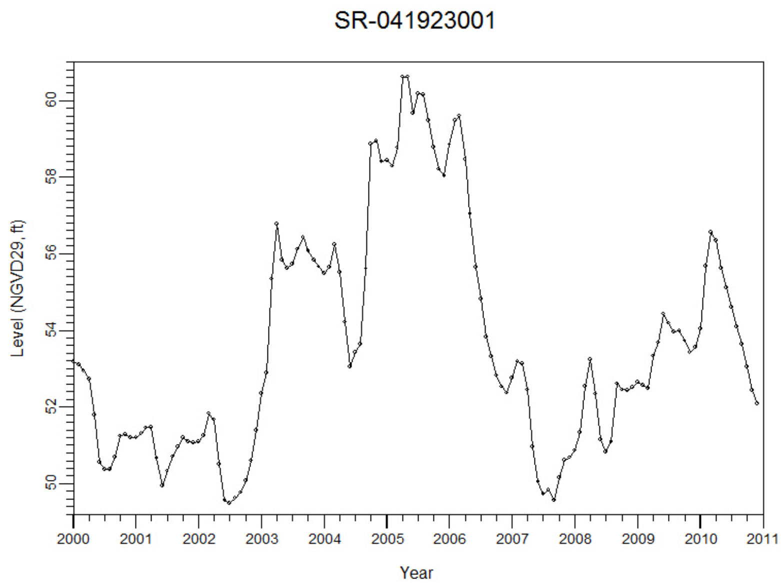


**Figure 75. Hydrograph of Well SR-041923001 (Site 51; Cluster 6).**

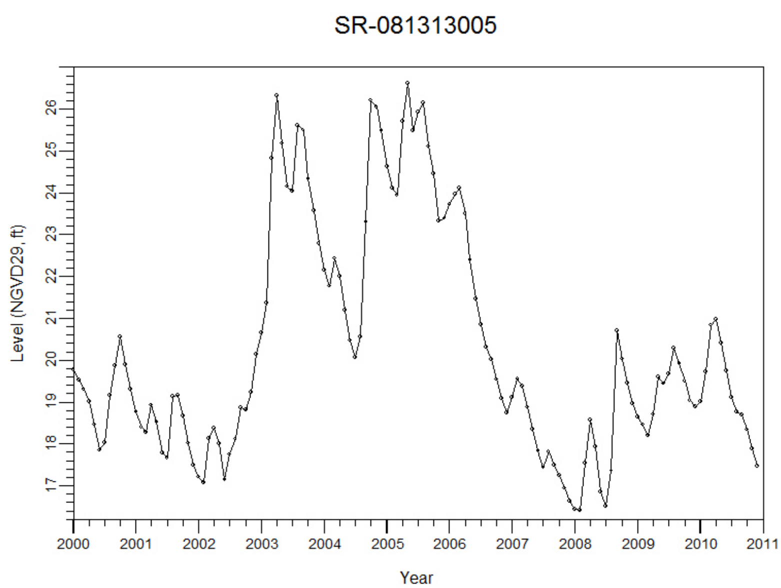


**Figure 76. Hydrograph of Well SR-081313005 (Site 52; Cluster 6).**

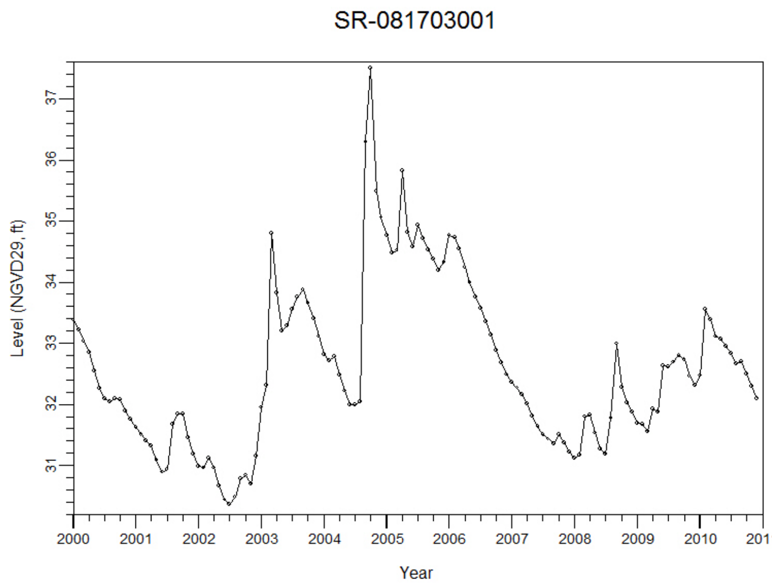


**Figure 77. Hydrograph of Well SR-081703001 (Site 53; Cluster 6).**

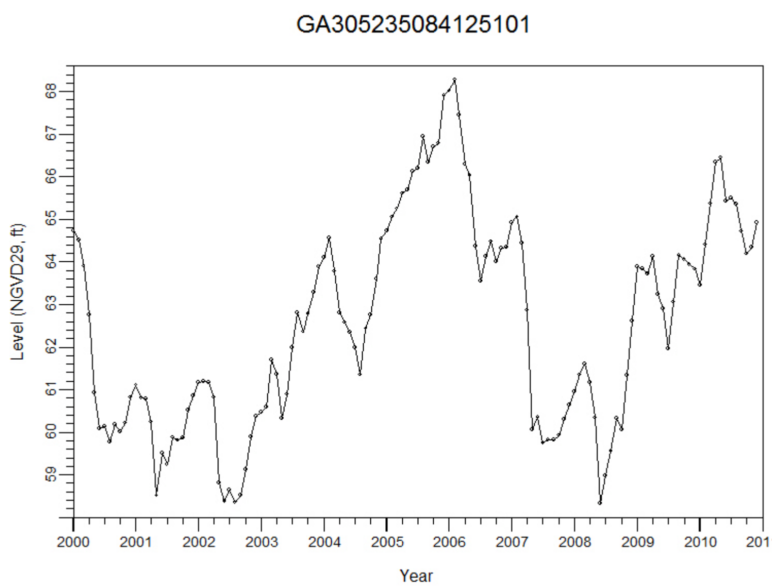


**Figure 78. Hydrograph of Well GA305235084125101 (Site 54; Cluster 7).**

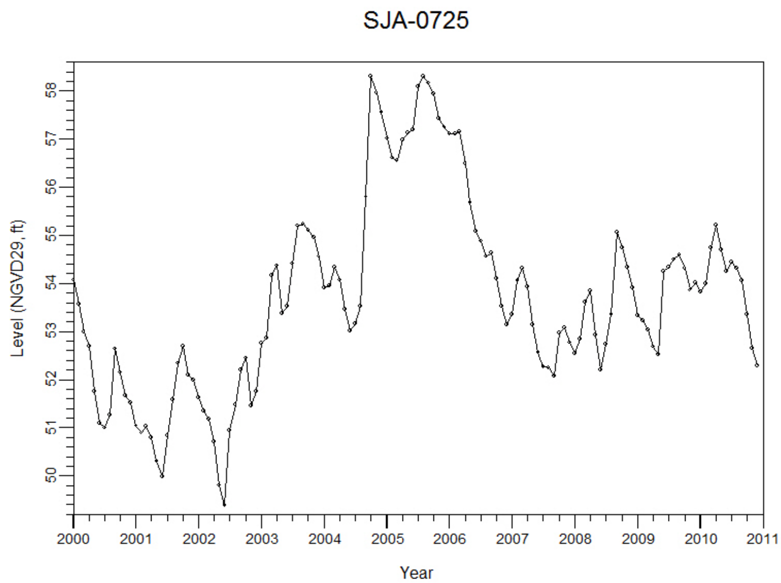


**Figure 79. Hydrograph of Well SJA-0725 (Site 55; Cluster 7).**

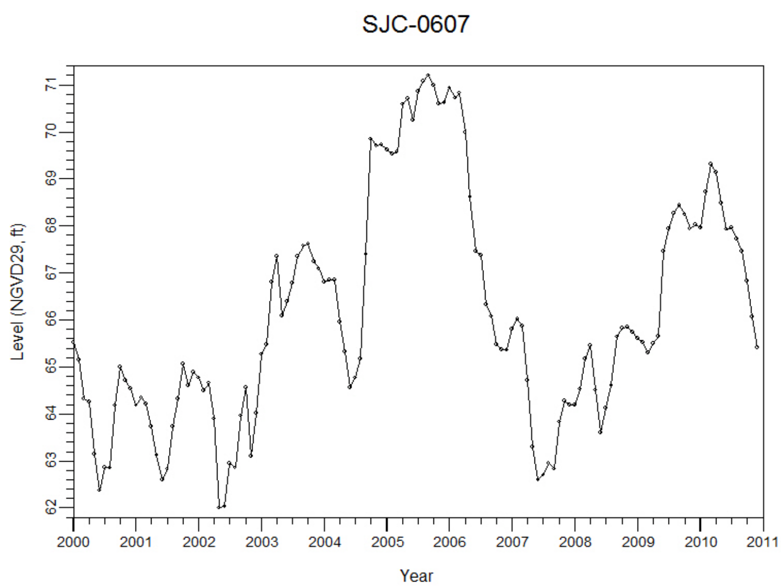


**Figure 80. Hydrograph of Well SJC-0607 (Site 56; Cluster 7).**

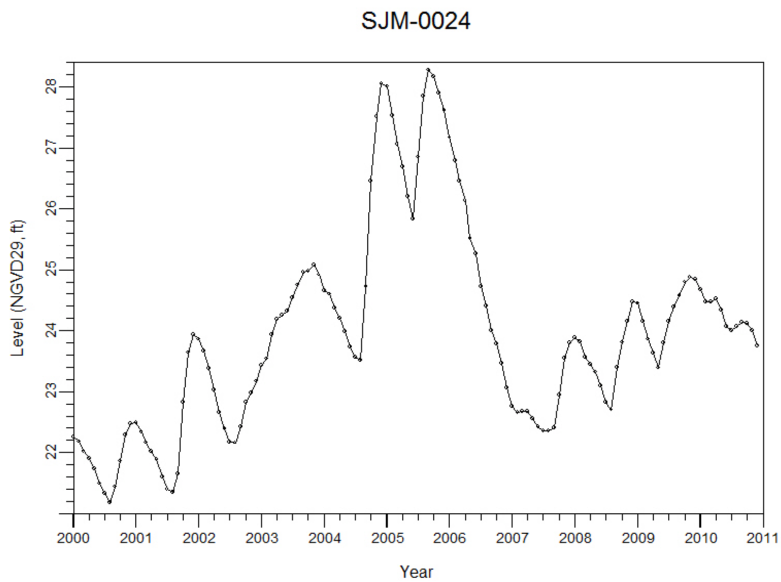


**Figure 81. Hydrograph of Well SJM-0024 (Site 57; Cluster 7).**

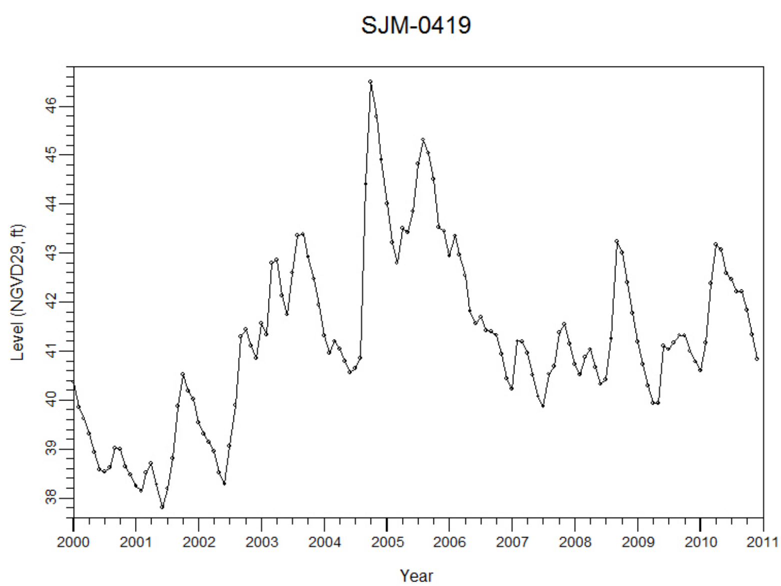


**Figure 82. Hydrograph of Well SJM-0419 (Site 59; Cluster 7).**

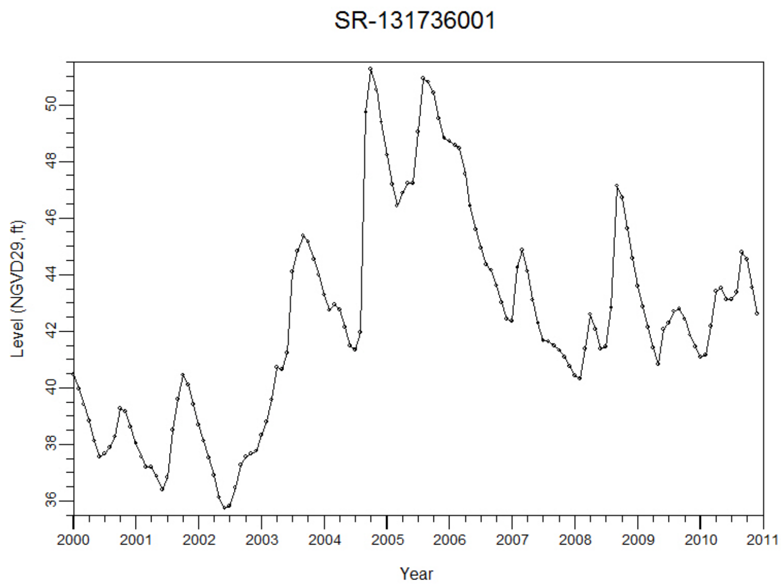


**Figure 83. Hydrograph of Well SR-131736001 (Site 60; Cluster 7).**

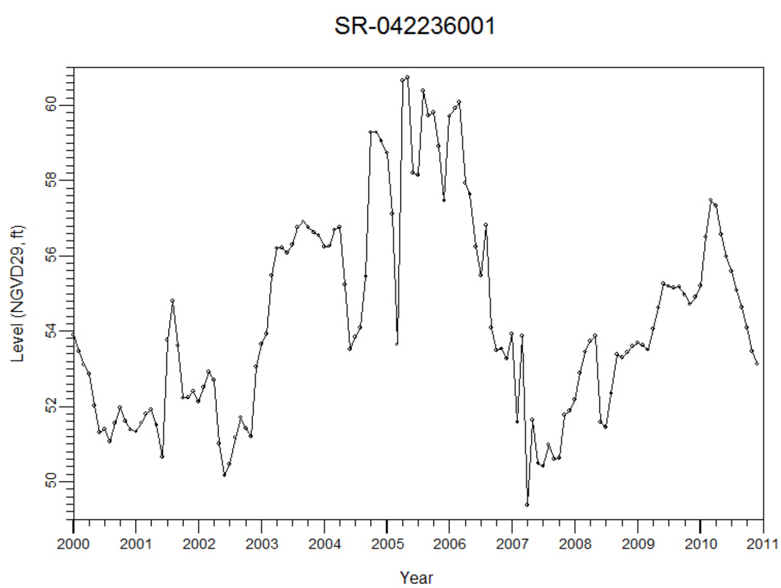


**Figure 84. Hydrograph of Well SR-042236001 (Site 61; Cluster 7).**

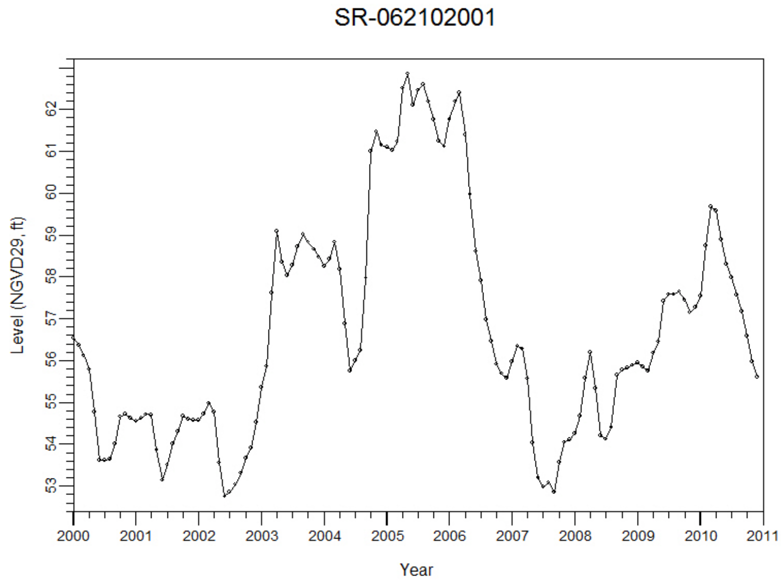


**Figure 85. Hydrograph of Well SR-062102001 (Site 62; Cluster 7).**

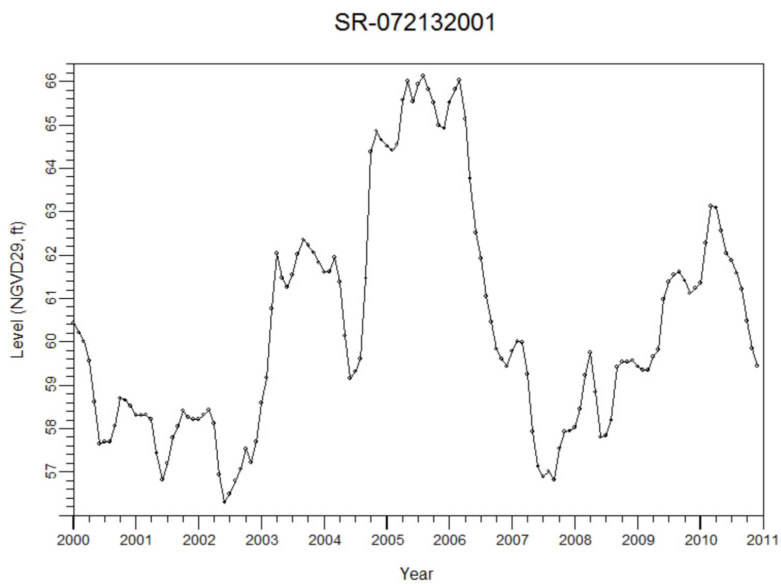


**Figure 86. Hydrograph of Well SR-072132001 (Site 63; Cluster 7).**

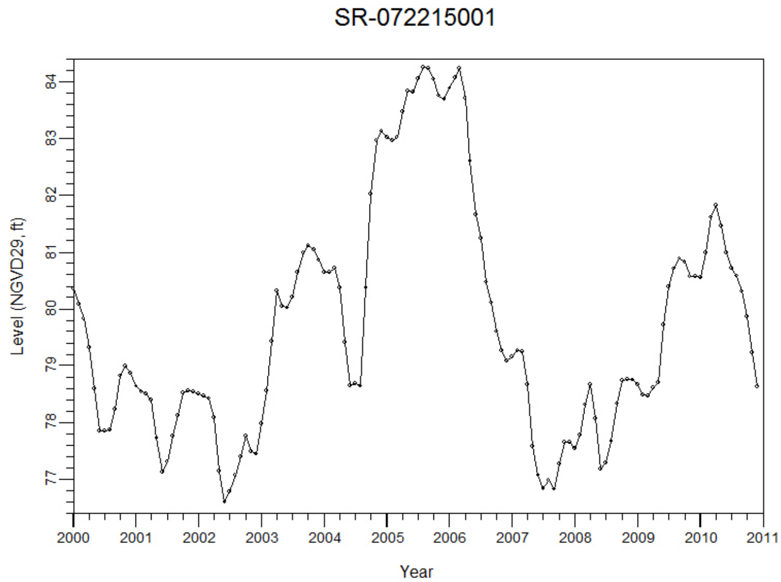


**Figure 87. Hydrograph of Well SR-072215001 (Site 64; Cluster 7).**

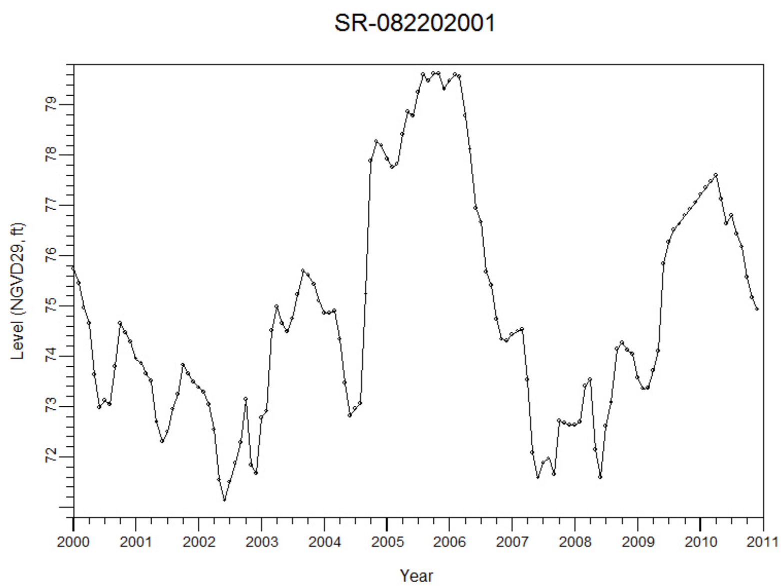


**Figure 88. Hydrograph of Well SR-082202001 (Site 65; Cluster 7).**

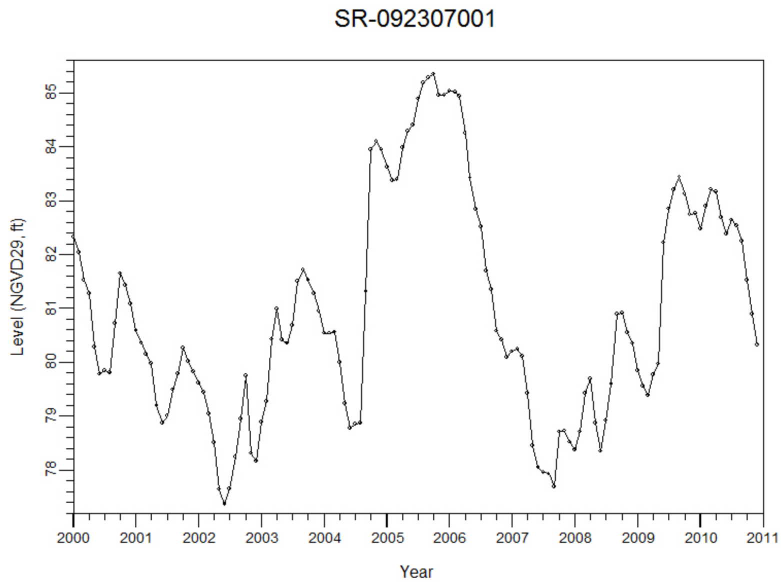


**Figure 89. Hydrograph of Well SR-092307001 (Site 66; Cluster 7).**

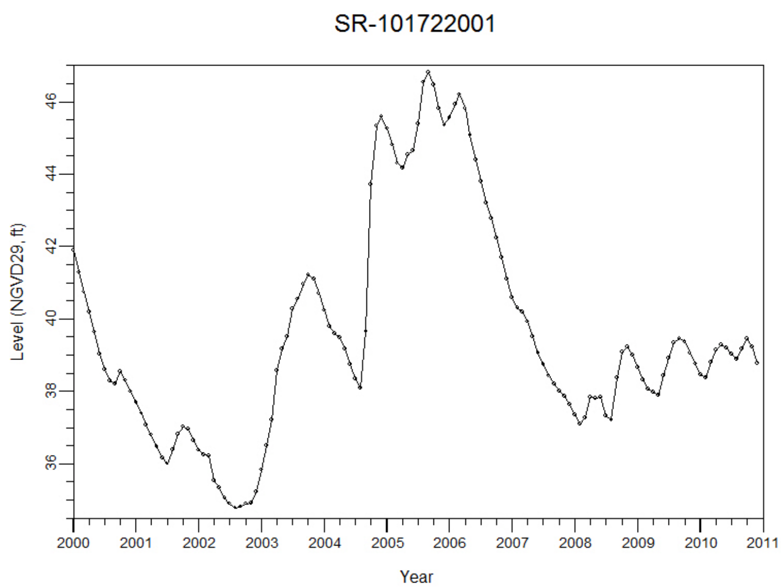


**Figure 90. Hydrograph of Well SR-101722001 (Site 67; Cluster 8).**

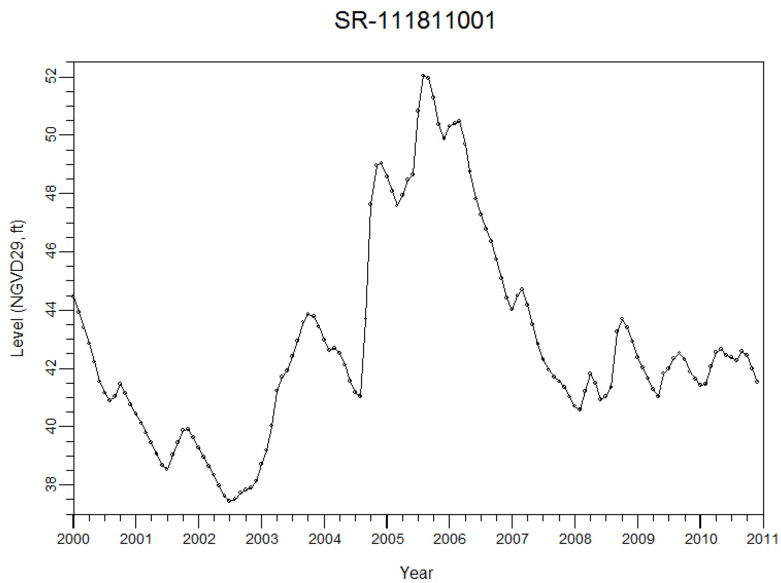


**Figure 91. Hydrograph of Well SR-111811001 (Site 68; Cluster 8).**

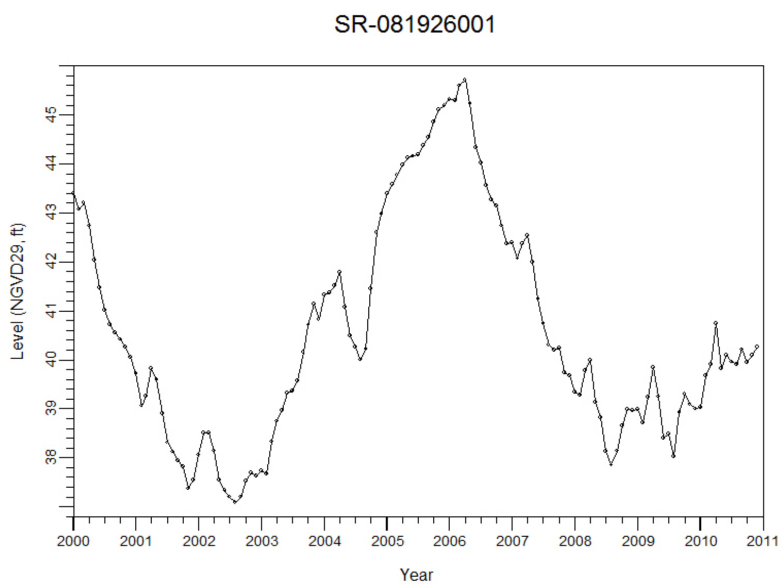


**Figure 92. Hydrograph of Well SR-081926001 (Site 69; Cluster 8).**

# APPENDIX B: SURFICIAL AQUIFER SYSTEM WELL HYDROGRAPHS

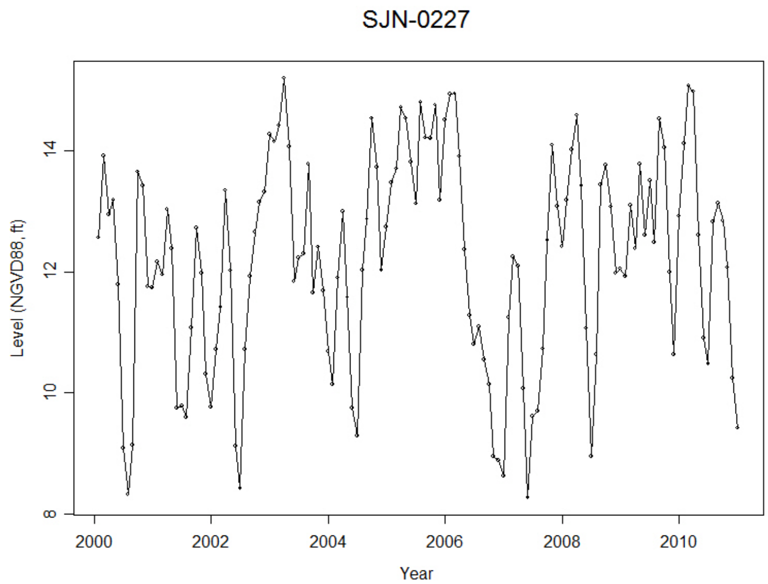


**Figure 93. Hydrograph of Well SJN-0227 (Site 1).**

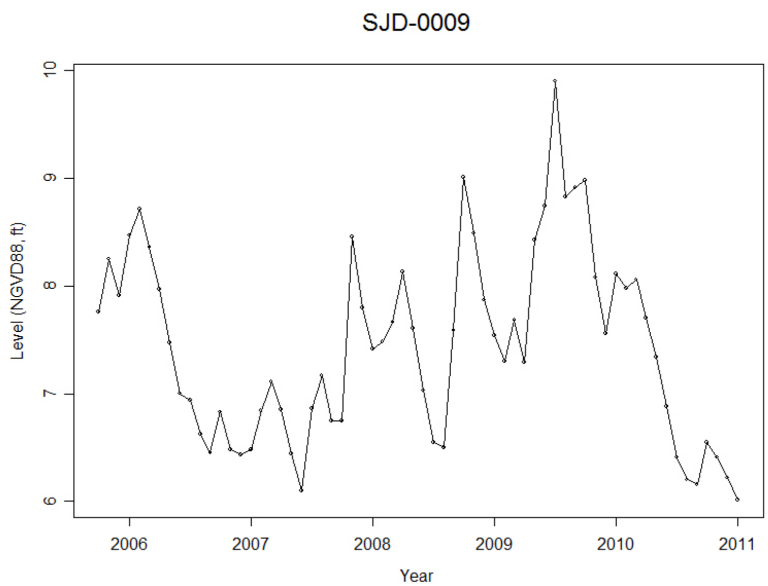


**Figure 94. Hydrograph of Well SJD-0009 (Site 2).**

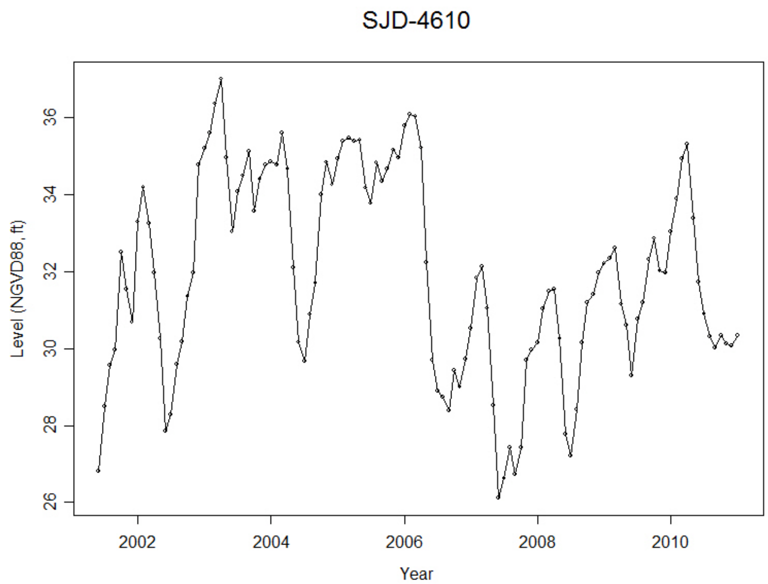


**Figure 95. Hydrograph of Well SJD-4610 (Site 3).**

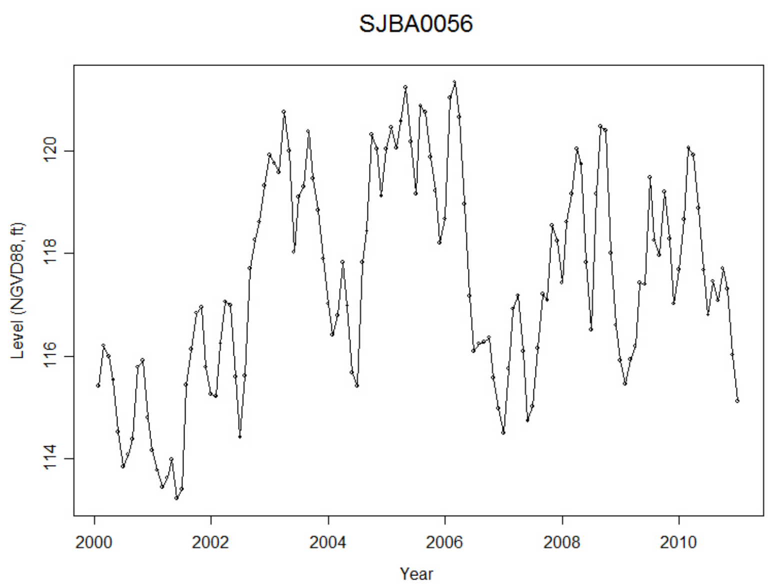


**Figure 96. Hydrograph of Well SJBA0056 (Site 4).**

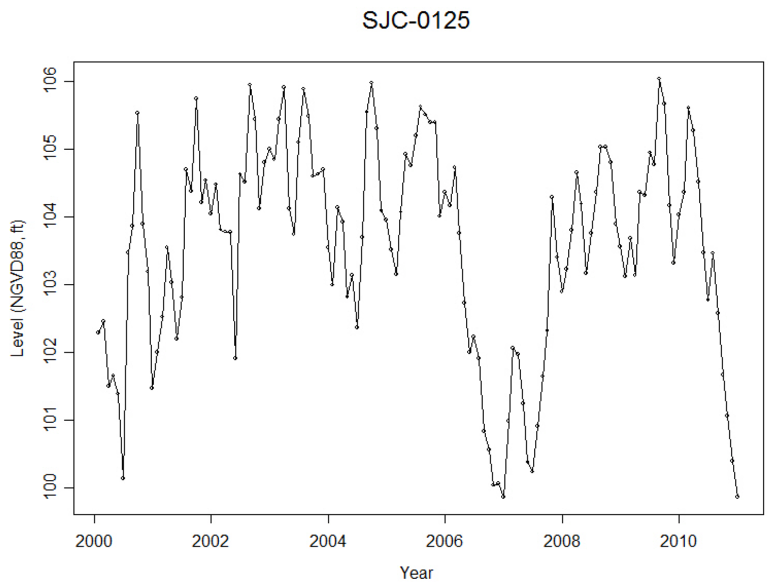


**Figure 97. Hydrograph of Well SJC-0125 (Site 5).**

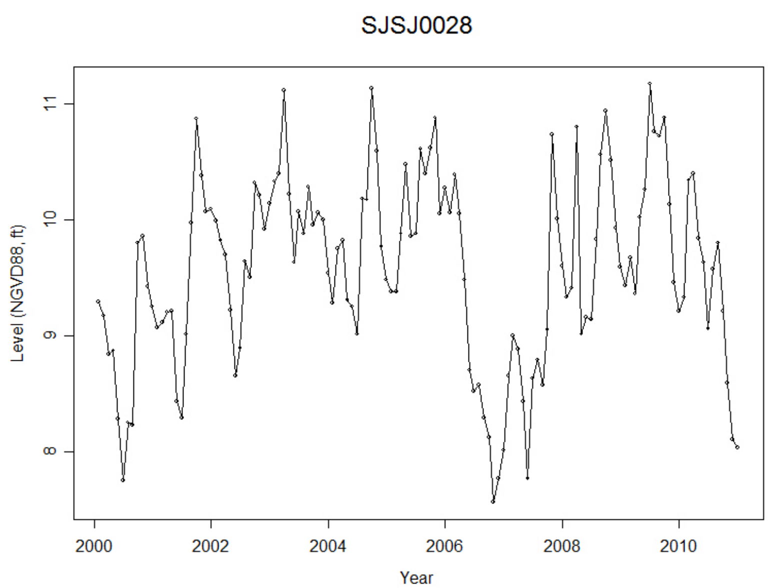


**Figure 98. Hydrograph of Well SJSJ0028 (Site 6).**

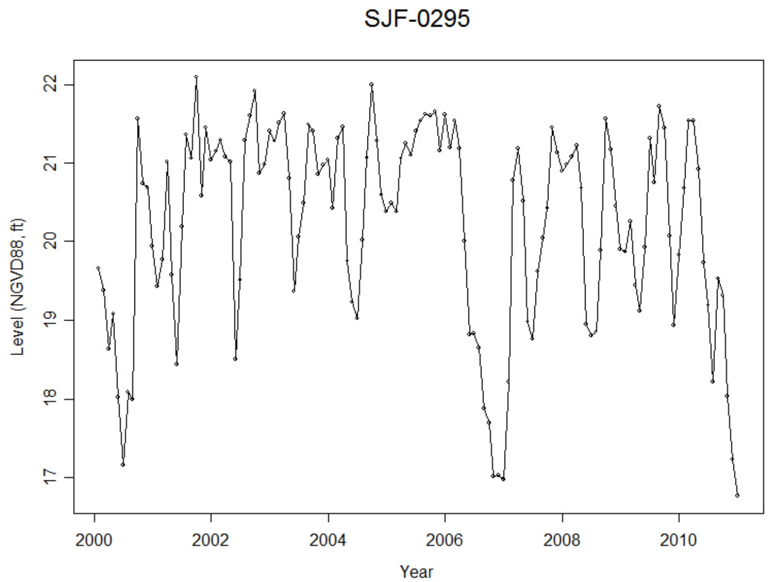


**Figure 99. Hydrograph of Well SJF-0295 (Site 7).**

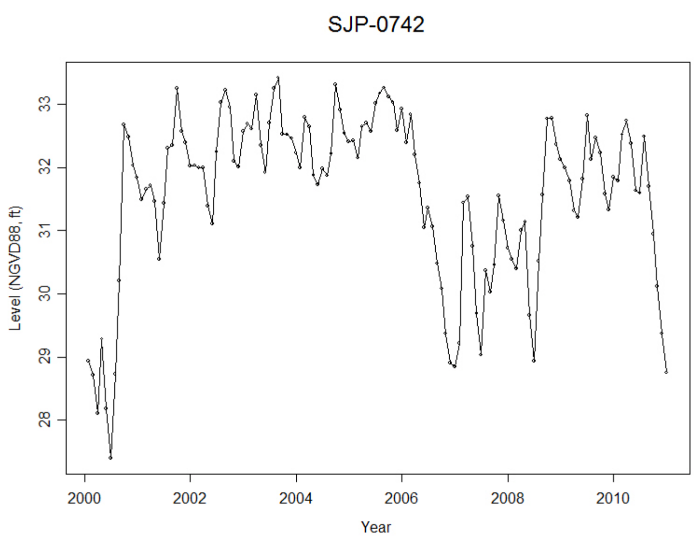


**Figure 100. Hydrograph of Well SJP-0742 (Site 8).**

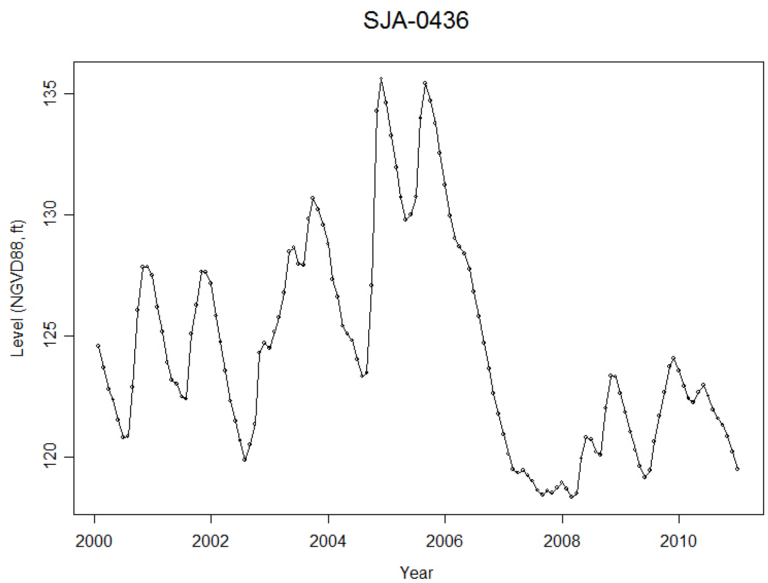


**Figure 101. Hydrograph of Well SJA-0436 (Site 9).**

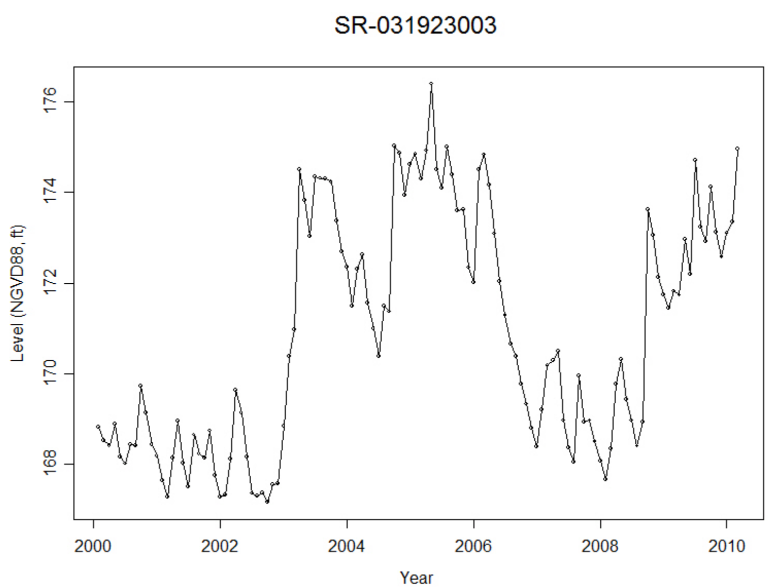


**Figure 102. Hydrograph of Well SR-031923003 (Site 10).**

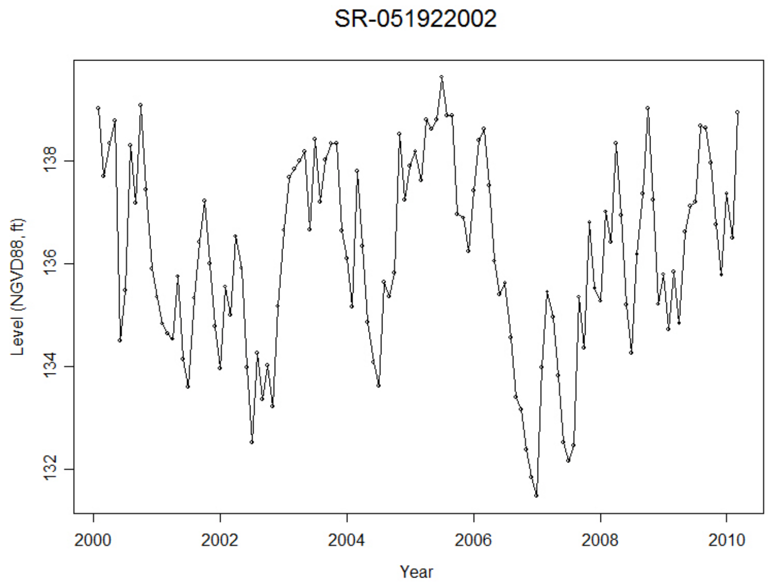


**Figure 103. Hydrograph of Well SR-051922002 (Site 11).**

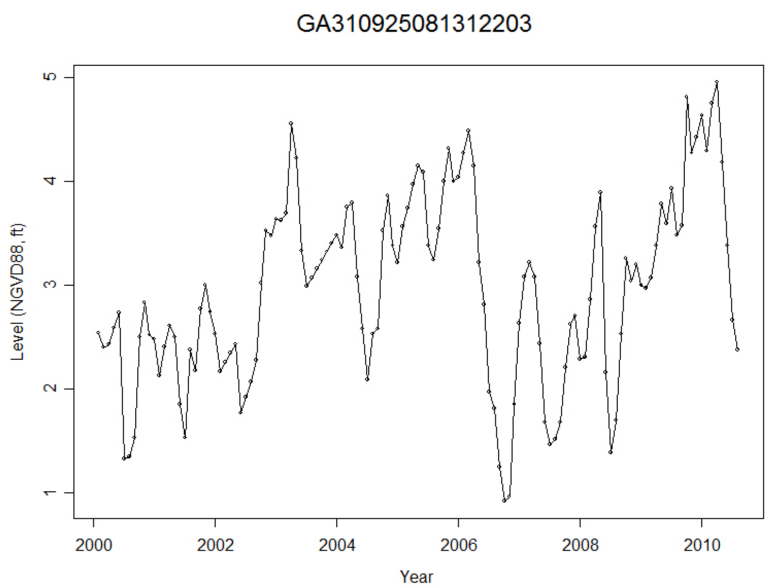


**Figure 104. Hydrograph of Well GA310925081312203 (Site 12).**

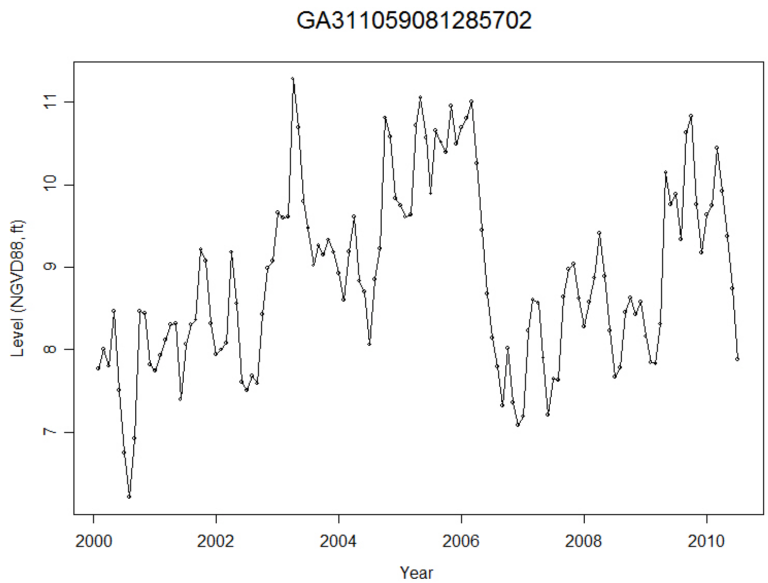


**Figure 105. Hydrograph of Well GA311059081285702 (Site 13).**

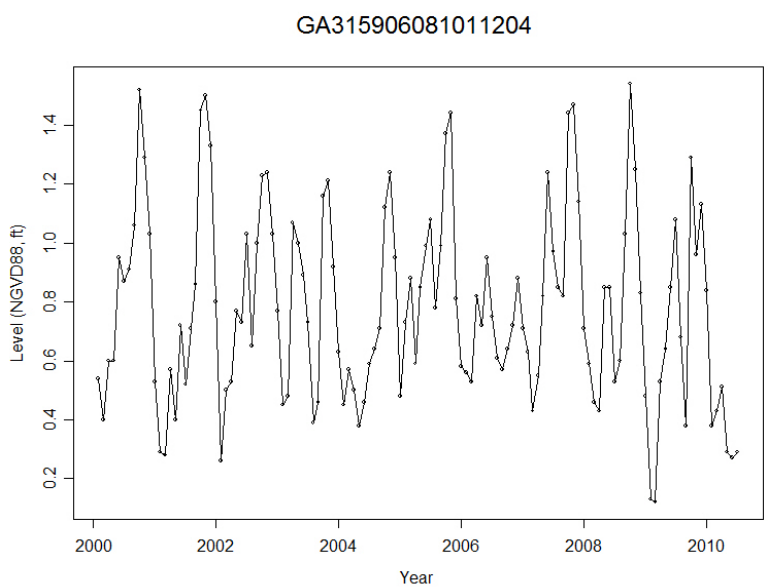


**Figure 106. Hydrograph of Well GA315906081011204 (Site 14).**

GA315950081161201

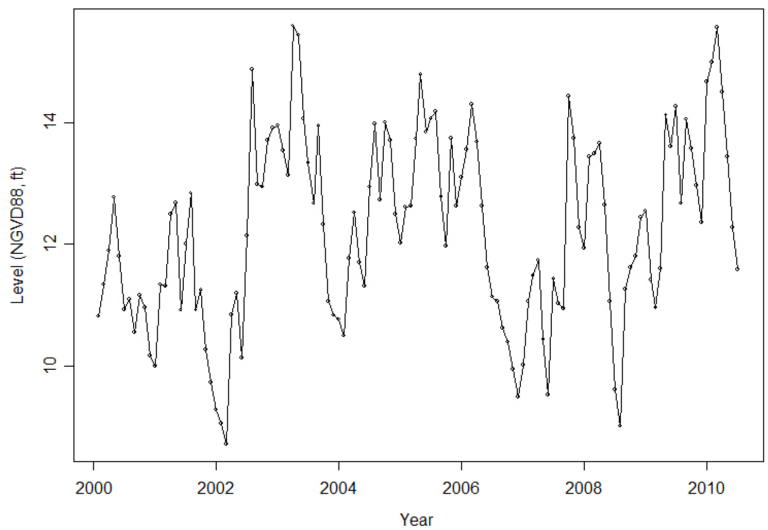


**Figure 107. Hydrograph of Well GA315950081161201 (Site 15).**

GA320127080511205

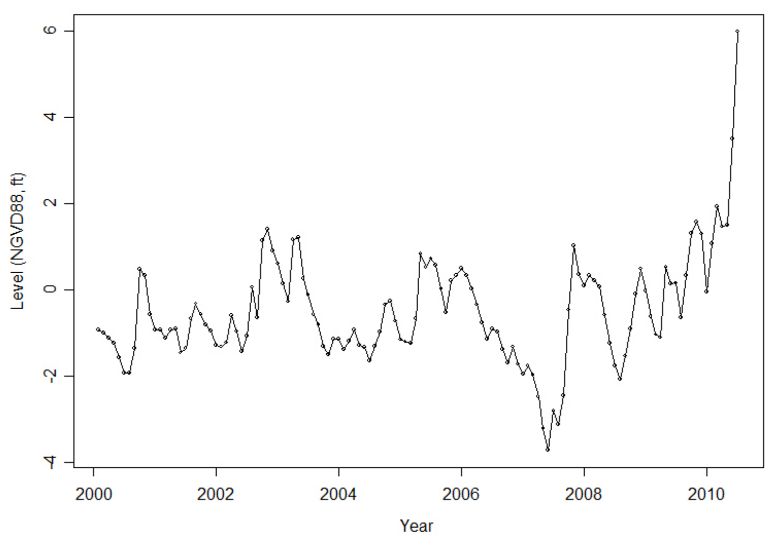


**Figure 108. Hydrograph of Well GA320127080511205 (Site 16).**

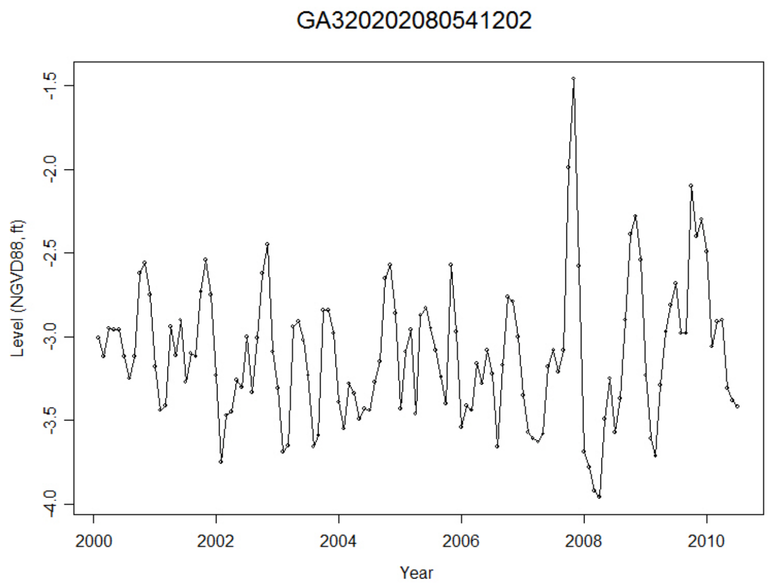


**Figure 109. Hydrograph of Well GA320202080541202 (Site 17).**

# APPENDIX C: ADDITIONAL DESCRIPTION OF RAINFALL ANALYSIS

## Approximation of Missing NOAA Monthly Values

Table 3 in the main body of the text lists the rainfall stations from which data were obtained for use in the analysis of rainfall within the proposed model domain, the data being in the form of monthly rainfall totals. The data sets fall within two categories: those obtained from David Clapp, a hydrologist with the SJRWMD who analyzes rainfall within and nearby the SJRWMD, and those obtained in “raw” format from NOAA. The data obtained from David Clapp were processed using the SJRWMD methodology for approximating and filling in missing monthly values. The NOAA data, being in raw format, contained missing values also, and a methodology was applied by the author for approximating and filling in the missing monthly values. However, the approach used by the author is presumed to be simpler and less rigorous than that used by David Clapp. The method used by the author will be described herein.

Data obtained from David Clapp represent the following stations:

**Table 9. Rainfall Stations for which Data were Obtained from D. Clapp, Hydrologist, SJRWMD**

| STATION | NAME |
|---|---|
| GHCND:USW00013878 | BRUNSWICK MALCOLM MCKINNON AIRPORT GA |
| GHCND:USC00081978 | CRESCENT CITY FL US |
| GHCND:USW00012834 | DAYTONA BEACH INTERNATIONAL AIRPORT FL US |
| GHCND:USC00082229 | DELAND 1 SSE FL US |
| GHCND:USC00082915 | FEDERAL POINT FL US |
| GHCND:USC00093460 | FOLKSTON 3 SW GA US |
| GHCND:USW00012816 | GAINESVILLE REGIONAL AIRPORT FL US |
| GHCND:USC00083470 | GLEN ST MARY 1 W FL US |
| GHCND:USC00083956 | HIGH SPRINGS FL US |
| GHCND:USC00084289 | INVERNESS 3 SE FL US |
| GHCND:USC00084366 | JACKSONVILLE BEACH FL US |
| GHCND:USW00013889 | JACKSONVILLE INTERNATIONAL AIRPORT FL US |
| GHCND:USC00084731 | LAKE CITY 2 E FL US |
| GHCND:USC00085076 | LISBON FL US |
| GHCND:USC00086414 | OCALA FL US |
| GHCND:USC00086753 | PALATKA FL US |
| GHCND:USC00087812 | ST AUGUSTINE FL US |
| GHCND:USC00088529 | STARKE FL US |
| GHCND:USC00089120 | USHER TOWER FL US |
| GHCND:USC00099186 | WAYCROSS 4 NE GA US |

Data obtained from NOAA in raw form represent the following stations:

**Table 10. Rainfall Stations for Which Data were Obtained Directly from NOAA**

| STATION | NAME |
|---|---|
| GHCND:USC00090140 | ALBANY 3 SE GA US |
| GHCND:USW00013870 | ALMA BACON CO AIRPORT GA US |
| GHCND:USW00012832 | APALACHICOLA AIRPORT FL US |
| GHCND:USC00091266 | BROOKLET 1 W GA US |
| GHCND:USC00091500 | CAMILLA 3 SE GA US |
| GHCND:USC00092266 | CORDELE GA US |
| GHCND:USC00092450 | CUTHBERT GA US |
| GHCND:USC00092783 | DOUGLAS GA US |
| GHCND:USC00092966 | EASTMAN 1 W GA US |
| GHCND:USC00085099 | LIVE OAK FL US |
| GHCND:USC00085539 | MAYO FL US |
| GHCND:USC00096087 | MOULTRIE 2 ESE GA US |
| GHCND:USC00087025 | PERRY FL US |
| GHCND:USC00097201 | PRESTON GA US |
| GHCND:USW00003822 | SAVANNAH INTERNATIONAL AIRPORT GA US |
| GHCND:USW00093805 | TALLAHASSEE REGIONAL AIRPORT FL US |
| GHCND:USC00098703 | TIFTON GA US |
| GHCND:USC00389469 | YEMASSEE SC US |

As stated previously, rainfall data obtained from NOAA were in raw format, meaning that missing monthly values were not supplied by NOAA. NOAA stations missing more than 3 monthly values in the period of 2000 through 2010 were not used in the analysis. This is the reason that a gap in the distribution of rainfall stations used in the analysis occurs in the area of the Florida-Georgia state line (Figure 17), as all stations in that area were deemed as missing an excessive number of monthly values in the period of 2000 through 2010. Stations missing monthly values in the period of 2000 through 2010 but used anyway are as follows: Alma Bacon (1 value); Douglas (1 value); Eastman (1 value); Preston (2 values); Tifton (1 value); and Yemassee (3 values).

In order to use these stations, a method for filling in the missing values had to be devised, and this included all missing values to be used in the determination of the long-term average of the month or year and station in question, not just those occurring in the period of 2000 through 2010. The approach used was to substitute an average rainfall amount of the month and station in question calculated for the *entire* period of record through the year 2010. This means that the average was based on the entire set of values of the month and gage in question, regardless of missing values in the cases of particular years within the period of record through 2010. Hence, missing monthly values were ignored in the calculation of the average value.

Once an average value was substituted in the place of a missing value of a given month, station, and year, it was thereafter treated as the actual monthly value of the month, station, and year in question. This means that it was used in the determination of the long-term monthly average through the year 2010 of the month and station in question. It was also used in the determination of the yearly total of the year in question and in the determination of the long-term annual average of the station in question. The long-term monthly average of a given month and station, so derived, was used, in turn, in the determination of the monthly-departure calculations of all monthly values of the month and station in question. Likewise, the long-term annual average of the station, so derived, was used in the determination of all annual departures of that station.

Successive periods of data were missing from the periods of record of some stations. An example of this is the period of 1912 through 1945 in the Cuthbert data set. In such cases, the long-term average calculation was based on the period comprised of the year immediately following the block of missing data through 2010. In the case of the Cutherbert data set, the long-term monthly averages were based on the monthly values of the years 1946 through 2010.

### Determination of Annual Departures from the Long-Term Average

Once the monthly and annual long-term averages were determined for each of the pertinent years in the record of a given station, the departures of each year's rainfall total from the yearly long-term average and each month's total from the monthly long-term average of the month and gage in question could be determined. To characterize the results on a region-wide basis, the totals of the annual departures of all stations included in the analysis were summed on a yearly basis and plotted in bar-chart format (Figure 18).

### Determination of the Sums of the Absolute Values of the Monthly Cumulative Departures

As stated in the main body of the report, cumulative-departure curves were calculated for each year in the period of 2000 through 2010 for all of the stations included in the analysis on a monthly basis. The cumulative-departure curves were used to assess the degree to which periods within each of the years were removed from "normal." To calculate the cumulative-departure curves, a monthly departure from the corresponding monthly mean first had to be determined for each of the months of each of the years of each of the stations included in the analysis. These departures were then summed successively to calculate the cumulative-departure curve of the year and station in question.

The monthly values that comprise the cumulative-departure curves are, in general, comprised of both negative and positive values. To prevent cancelling, the absolute values of the monthly values were obtained prior to summing the monthly values. The absolute values were summed for the year and station in question. Higher values are assumed to be indicative of a greater degree of eccentricity in the sub-year rainfall patterns that comprised the year in question. The totals of all stations were determined on a yearly basis in order to characterize the level of eccentricity by year (Figure 19).

**Spreadsheet Location**

Rather than provide a single example of the calculations that went into the rainfall analysis, the entire spreadsheet containing all rainfall data and the calculations used in the analysis has been made available at the following location on the SJRWMD FTP site:

ftp://ftp.sjrwmd.com/gwp/NFSEG_RAINFALL_ANALYSIS_SPREADSHEET/NFSEG_Rainfall_Analysis_10-23-2012_B.xlsx